JAERI-M
84-132

A THROUGH CALCULATION OF 1,100 MWe PWR LARGE BREAK LOCA BY THYDE-P1 EM MODEL

July 1984

Masayuki KANAZAWA, Yoshiro ASAHI and
Masashi HIRANO

日 本 原 子 力 研 究 所
Japan Atomic Energy Research Institute

JAERI-M レポートは，日本原子力研究所が不定期に公刊している研究報告書です。
入手の問合わせは，日本原子力研究所技術情報部情報資料課（〒319-11茨城県那珂郡東海村）あて，お申しこしください。なお，このほかに財団法人原子力弘済会資料センター（〒319-11 茨城県那珂郡東海村日本原子力研究所内）で複写による実費頒布をおこなっております。

JAERI-M reports are issued irregularly.
Inquiries about availability of the reports should be addressed to Information Section, Division of Technical Information, Japan Atomic Energy Research Institute, Tokai-mura, Naka-gun, Ibaraki-ken 319-11, Japan.

編集兼発行　日本原子力研究所
印　　刷　いばらき印刷㈱

JAERI-M 84-132

A through calculation of 1,100 MWe PWR large break LOCA by THYDE-P1 EM model

(Sample Calculation Run 80)

Masayuki KANAZAWA, Yoshiro ASAHI and Masashi HIRANO

Department of Reactor Safety Evaluation, Tokai Research Establishment, JAERI

(Received June 28, 1984)

THYDE-P1 is a code to analyze both the blowdown and refill-reflood phases of loss-of-coolant accidents (LOCAs) of pressurized water reactors (PWRs). Up to now, THYDE-P1 has been applied to various experiment analyses, which show its high capability to analyze LOCAs as a best estimate (BE) calculation code.

In this report, evaluation model (EM) calculation method, especialy in the blowdown and refill phases, is established equivalently to WREM/J2 which is regarded as appropriate for an EM calculation code, and the results of them are compared and discussed. The present calculation was the first executed by THYDE-P1-EM, and was performed as Sample Calculation Run 80 which was a part of a series of THYDE-P sample calculations. The calculation was carried out from the LOCA initiation till 400 seconds for a guillotine break at the cold leg of a commercial 1,100 MWe PWR plant. The calculated results agreed well to that of the WREM/J2 code.

Keywords : THYDE-P1 Code, Large Break, LOCA, PWR, Evaluation Model, WREM/J2, Blowdown, Refill, Reflood

THYDE－P1コード評価計算モデルによる1,100 MWe PWR大破断冷却材喪失事故の一貫計算（サンプル計算RUN 80）

日本原子力研究所東海研究所安全解析部
金澤 昌之・朝日 義郎・平野 雅司

（1984年6月28日受理）

THYDE－P1は，加圧水型原子炉の冷却材喪失事故におけるブローダウン，再浸水，再冠水過程を一貫して解析するコードである。従来，同コードは種々の実験解析に適用され，最適評価（BE）計算コードとして，その高い解析性能が示されてきた。

本報告では，同コードのブローダウン，再浸水期の計算に対し，評価計算（EM）コードとして妥当とされているWREM／J2と同等の計算手法を確立し，それにより実施した最初の評価計算の結果を，WREM／J2と比較検討した。本計算は，一連のTHYDE－P1サンプル計算のうち，RUN 80として行なったものである。計算は，1,100 MWeクラスの商用加圧水型原子力発電プラントの，コールドレグ，ギロチン破断による冷却材喪失事故（LOCA）を，400秒まで解析した。計算結果は，WREM／J2によるものと，良い一致が見られた。

Contents

目　次

List of Figures

List of Figures (continued)

List of Figures (continued)

List of Tables

1. Introduction

THYDE-P1 [1)-3)] is a computer code to analyse transient thermal-hydraulic responses of a pressurized water reactor (PWR) plant to a postulated loss-of-coolant accident (LOCA). Up to now, THYDE-P1 has been applied to various experiment analyses [3)-10)], which show its high capability to analyse LOCAs as a Best-Estimate (BE) calculation code. The THYDE-P1 interim version SV02L03 had been released through NEA DATA BANK in April 1982.

On the other hand THYDE-P1 had been designed to be used as an Evaluation Model (EM) calculation code. But no EM calculation had been executed.

The main features of the present EM calculation by THYDE-P1/EM are ;

a. heat generation rate of the fission products is multiplied by a factor of 1.2
b. operation time to be used for the calculation of actinide decay is infinity
c. saturated water is injected into lower plenum (L.P.) during reflooding phase, and
d. no ECC water is injected from the End of Bypass (EOBP) to the start of the Lower Plenum injection (LPinj).
e. no rewetting during blowdown

(item d is characteristic of THYDE-P1-EM calculation:see subsection 2.1.5.)

Now the heat slab model had been included in the latest version SV03L02, so that THYDE-P1 is equipped with almost all of the models needed in EM calculation.

In this report the result of the first through EM calculation, Sample Calculation Run 80, will be presented for a typical 4-loop PWR plant via the latest version of THYDE-P1, SV03L02, with some tentative modifications. The major models and assumptions applied in this calculation are summarized as follows :

a. Through EM calculation complied with the "Safety Evaluation Guideline for the performance of ECCS of

LWRs" [11]

b. Two core channels with a single cross flow

c. Single downcomer noding calculation

d. Double-ended guillotine break at cold leg

e. Pump coast down just after rupture

f. Discharge coefficient 0.6 for Moody correlation

g. FLECHT HTC correlation in reflooding phase

Among these items, a. and g. must have been implemented or developed, so that the focal points of the present work are ;

a. development of a series of valve operations in accordance with EM logic for ECC bypassing through downcomer top and

b. implementation of the FLECHT [12),13] correlation in the code .

The input data were made based on those used in the Sample Calculation Run 21 [10] , which had been provided as the Base Input for THYDE-P1 Published Version. And the heat slab data were added based on RELAP4/EM sample problem [14] because the geometrical data were almost identical with those used in it.

2. Code modification

The details of the models and methods used in the THYDE-P1 code are presented in Refs. 1) to 3) and some modifications made in the published version, SV02L03, are described in Refs. 4) to 10).

By EM logic, we define the special logic in use for WREM/J2 [19),20)] with respect to ECCS analysis. It seems that there are some paradoxical treatments in the EM logic used in WREM/J2. But it is hoped that such treatments make it possible to assure conservatism.

In establishing a through THYDE-P1-EM calculation, it was thought to be the most important that the calculation should be executed in a logic similar to that of the WREM/J2 code so that a conservatism equivalent to that of WREM/J2 could be assured.

The main objective of this work is to establish an EM logic in THYDE-P1 as closely to that of WREM/J2 as possible.

The present calculation, Sample Calculation Run 80, was performed by the latest version, SV03L02, with the code modifications to execute an EM calculation which will be summarized in this section. Among them the main items are ;

a. EM logic for ECC bypassing through the downcomer top
b. application of the FLECHT correlation
c. break flow model, and
d. two phase multiplier.

2.1. EM logic for ECC bypassing through downcomer top.

In this subsection the comparison between the present THYDE-P1-EM ECC downcomer bypassing model and that in WREM/J2 will be made along with the explanation of the modifications adopted in THYDE-P1-EM.

The main items of the THYDE-P1-EM ECC downcomer bypassing model are ;

a. estimation of the mass flow rate from the accumulator (ACC),
b. changing the ECC injection point by a series of

simplified valve operations,

c. estimation of the time at which ECC L.P. injection starts, and

d. removal of the liquid water from the loop.

2.1.1. Comparison between THYDE-P1 calculation scheme and that of WREM/J2

The WREM/J2 code package is composed of several codes. They are RELAP4/EM-BLOWDOWN, RELAP4-FLOOD, RELAP4-HOTCHANNEL, TOODEE-2, CONTEMPT-LT, etc., each of which calculates some special features of LOCA. For example, RELAP4-HOTCHANNEL executes only thermal calculation in core during blowdown phase.

The relationship of constitutive codes in the WREM/J2 code package is shown in fig. 2-1. compared with THYDE-P1. As shown in it, thermal-hydraulic calculation is executed by RELAP4/EM and RELAP4-FLOOD, and thermal calculation in core is done by RELAP4-HOTCHANNEL, RELAP4-FLOOD and TOODEE-2. As THYDE-P1 has no models for the hottest pin calculation and container pressure calculation, it is impossible to compare the results to those of TOODEE-2 and CONTEMPT-LT.

2.1.2. Estimation of mass flow rate from ACC

In the WREM/J2 code, the history of the ACC injection is calculated by the RELAP4/EM calculation, and its result is used in the RELAP4-FLOOD calculation as input data.

In the THYDE-P1-EM model, ECC injection stops for a while after EOBP and restarts (see subsection 2.1.3.) under the assumption that all the injection should be made to the lower plenum. So a scheme is needed to estimate the ACC mass flow rate during the hypothetical second injection period. Thus the following equation was used :

$$W_{ACC} = C \cdot A \sqrt{2\rho (P_{ACC} - P_{CL})/k} \qquad (2-1)$$

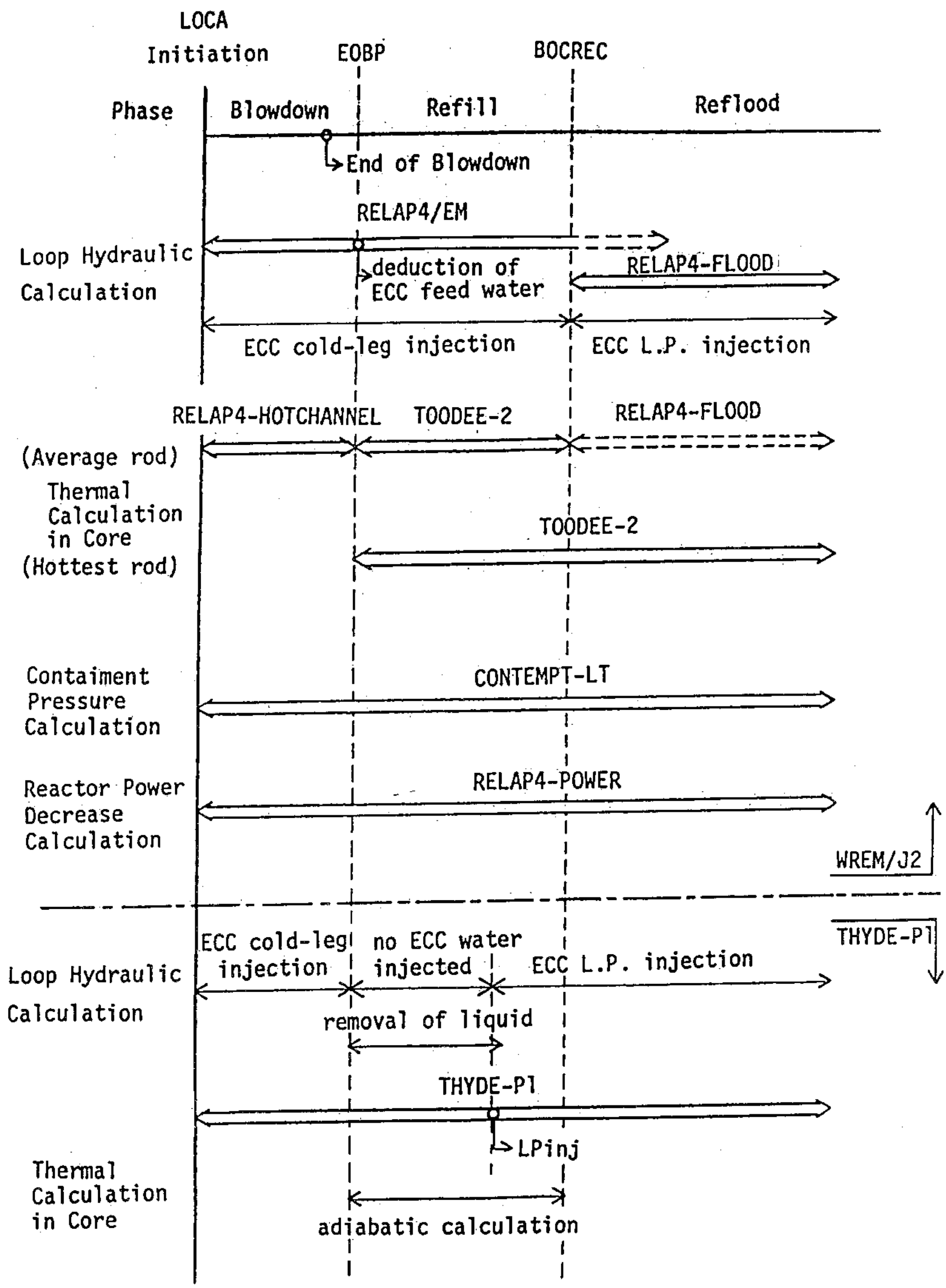

Fig. 2-1 Relationship of constitutive codes in the WREM/J2 code package

A : cross section of ACC linkage duct

P_{ACC} : pressure of ACC

P_{CL} : pressure of cold leg in the intact loop

k : loss coefficient

C : adjusting factor to assure $W_{ACC(T=T_{eobp}-\varepsilon)} = W_{ACC(T=T_{eobp}+\varepsilon)}$

2.1.3. Change of ECC injection point by a series of simplified valve operations

In the WREM/J2 code, ECC feed water is directly injected into lower plenum (L.P.) in the reflood calculation, though it is to be injected into cold leg during blowdown phase (see fig. 2-2). In order to adopt this scheme in THYDE-P1-EM, we assume that

a. ECC cold-leg injection stops at end of downcomer bypass (EOBP) and,

b. ECC L.P. injection starts at few seconds after EOBP. (see subsection 2.1.4.)

Tentatively, we implemented this scheme by the simplified valve model to be explained next. In the future version of THYDE-P1, these operations will be executed automatically by the THYDE-P1 valve model.

In order to facilitate item a., EOBP was considered to be one of the signals to trigger to cut off the ACC injection and pumped injection (PI). For item b., starting L.P.injection, the mass equation (f_1 equation) at L.P. was changed as ;

$$f_1 = G^A - G^E - L\frac{\bar{\rho}-\bar{\rho}_{old}}{\Delta T} + \frac{W}{A} \qquad (2-2)$$

W : mass flow rate of the ECC feed water (kg/sec)

A : cross section of L.P. (m^2)

where the part of W contributed by ACC injection is given by Eq. (2-1).

According to the RELAP-FLOOD calculation, the enthalpy of L.P. injection water was assumed to be h_{fs} . Because subcooled water injection could trigger abnormal condensation.

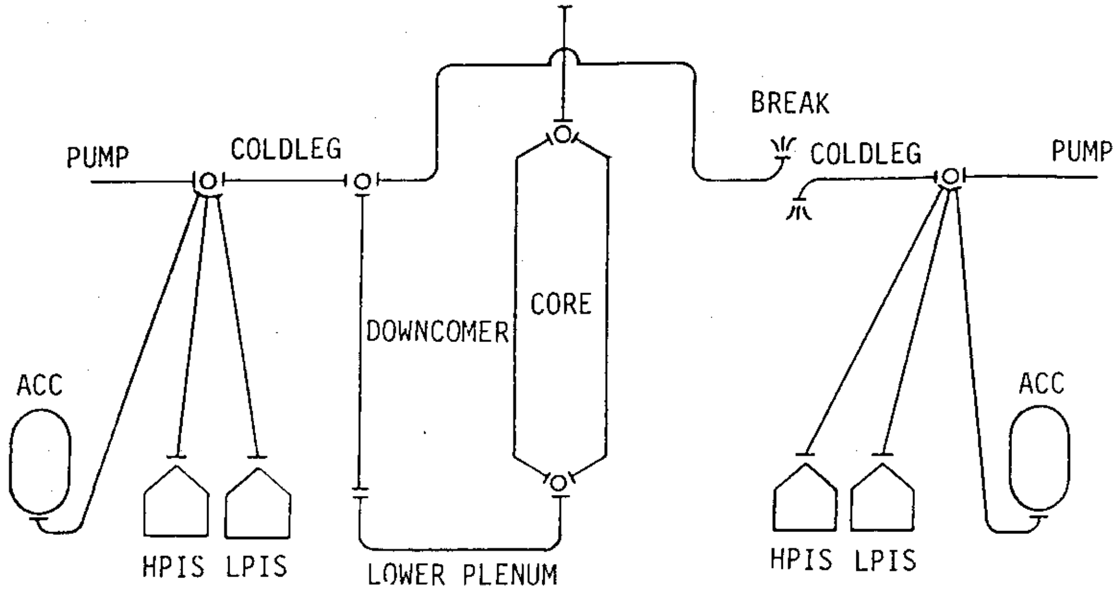

a. Before BOCREC

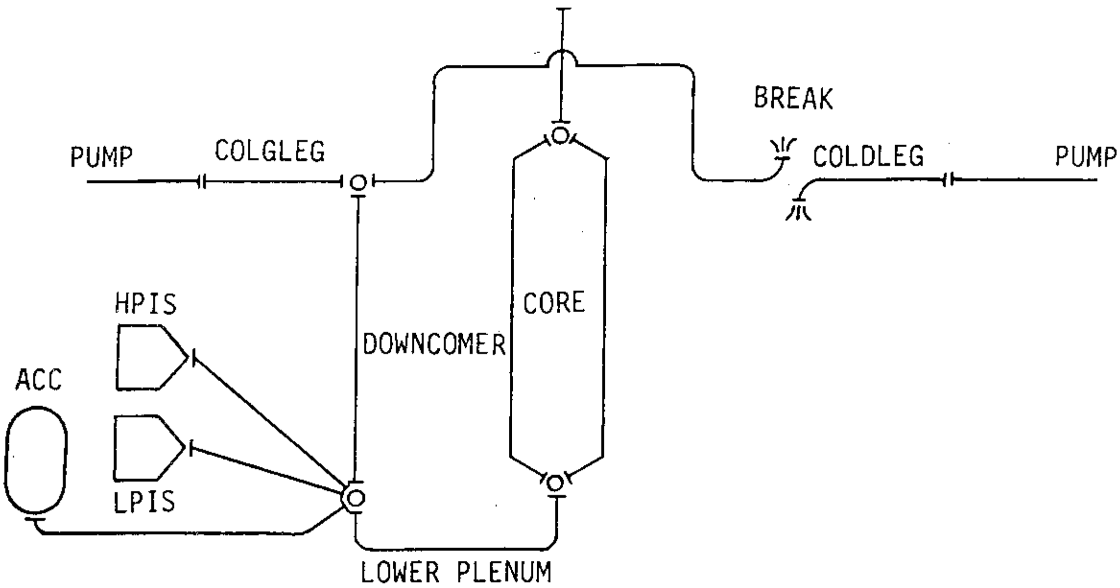

b. After BOCREC

fig. 2-2 Nodalization for ECC Injection Used in WREM/J2

Following WREM/J2, the perfect phase separation model at L.P. was presumed to avoid the fact that flow carries out the water from L.P. to the core and quenching begins at very early stage. The perfect phase separation model means that the enthalpy and the density of outlet flow from L.P. are assumed to be

h_{gs} and ρ_{gs} when $1.0 > x > 0.0$

$\bar{h}$ and $\bar{\rho}$ when $x \geqq 1.0$ or $x \leqq 0.0$

2.1.4. Estimation of ECC L.P. injection start time

According to the WREM/J2 code, L.P. injection start time was evaluated as follows ;

$$T_{LPinj} = T_{EOBP} + \Delta T_{fill} + \Delta T_{fall} \qquad (2-3)$$

ΔT_{fill} = time needed to fill the cold leg volume

ΔT_{fall} = time needed to fall down the downcomer

2.1.5. Removal of liquid water from loop

In the WREM/J2 code, the total mass of ECC water, which has been injected before EOBP, is deducted successively from water in the L.P., the downcomer and the cold legs when EOBP is detected. If the result is negative (usually it is negative indeed), the enthalpy of those nodes are set to h_{gs} . Furthermore the system condition is changed more severely in starting RELAP-FLOOD calculation; i.e. the qualities of all nodes except L.P. and downcomer are assumed as 1.0 or higher.

In order to introduce this algorithm into THYDE-P1, a scheme to expel the water is conceived such that heat is given to the nodes where it is subcooled or saturated, until it becomes superheated. In this method, it takes only a short while to do so, and since the core is insulated during refill phase in the calculation, it does not disturb the result such as the cladding surface temperature at all.

2.2. Application of FLECHT correlation

In the reflooding phase, only FLECHT heat transfer coefficient (HTC) correlation was adopted, and the carry over rate fraction (CRF) was not implemented. If we include the CRF correlation in THYDE-P1, we have to discard one of the conservation equations in THYDE-P1. In other words, we can obtain CRF itself in the THYDE-P1 calculation without a correlation for it. It means that we gave priority to the check of the FLECHT HTC correlation and the history of the fuel and cladding temperature.

With regard to quenching, the main difference between THYDE-P1 and WREM/J2 is that the latter uses the notion of water level and CRF correlation to evaluate the quenching parameters, but the former does not, and solves physical equation strictly even at the core nodes.

2.2.1. Decision of quenching node

In the THYDE-P1 code, there is no notion of water level. So the criteria for a node to be regarded as being quenched were set to be the following conditions ;

a. all the lower nodes have been quenched,

b. the cladding surface temperature must be below the Henry's quench temperature [15] , and

c. the coolant of that node must contain liquid water.

2.2.2. HTC of the quenching node

To evaluate the HTC of the quenching node , an interpolation by the quality x was used in accordance with WREM ;

$$HTC = 50 + 950(1-x)^3 \qquad (Btu/ft^2/hr/{}^\circ F) \qquad (2-4)$$

where $0.0 \leqq x \leqq 1.0$

2.3. Break flow model

In THYDE-P1, the slightly modified Zaloudek [16] equation and the Moody [17] correlation were connected smoothly at what is called the "transition quality" $x = 0.02$. In the present calculation the discharge coefficient C_d for the Moody correlation was set as $C_d^{sat} = 0.6$ by an input. In order not to underestimate the break flow, it was recommended [11] to use a different C_d value for the Zaloudek equation in EM calculations, which was set as $C_d^{sub} = 0.91$.

Consequently the following equations was adopted.

for $x \leqq 0.0$;

$$G_M = C_d^{sub} \cdot \sqrt{2\rho\,(P-C_2 P_{sat})} \qquad (2-5)$$

for $0.0 < x < 0.02$;

$$G_M = \eta\, G_{M(x=0.0)} + (1-\eta) G_{M(x=0.02)} \qquad (2-6)$$

for $0.02 \leqq x$;

$$G_M = C_d^{sat} \cdot g_M \qquad (2-7)$$

where $\eta = \dfrac{0.02-x}{0.02}$

and g_M : Moody correlation value

2.4. Two phase multiplier

In the present calculation we used the following expression for the frictional pressure loss.

$$P_{fric} = -\frac{1}{2}(k+\frac{fL}{D})\ X^{*}\cdot\frac{G|G|}{\bar{\rho}} \qquad (2-8)$$

$$X^{*} = 1 \qquad for\ x \leqq 0.0 \quad \text{or} \quad x \geqq 1.0$$

$$= \Phi^{2}\frac{\bar{\rho}}{\rho_{fs}} \qquad for\ 0.0 < x < 1.0$$

where X^{*} : Modified two phase multiplier
and Φ^{2} is given as follows ; (see figs. 2-3 to 2-6)

interpolation of Martinelli-Nelson's table [19]	P ≦ 100psia
double interpolation of Thom's(250psia) [19] and Martinelli-Nelson's(100psia) [18] values.	100psia < P < 250psia
interpolation of Thom's table [18]	250psia ≦ P

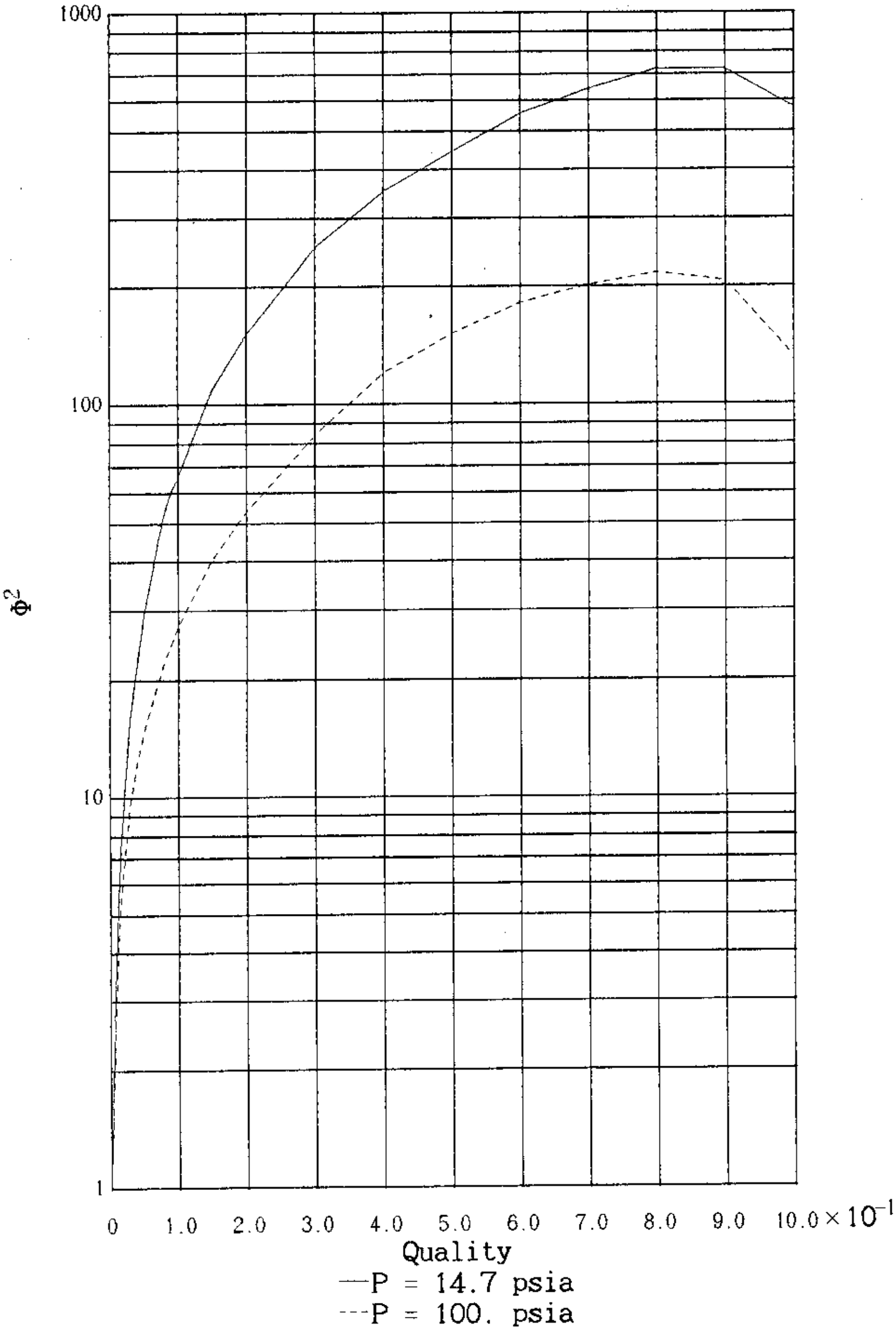

Fig. 2 - 3 Two phase multiplier : Martinelli-Nelson

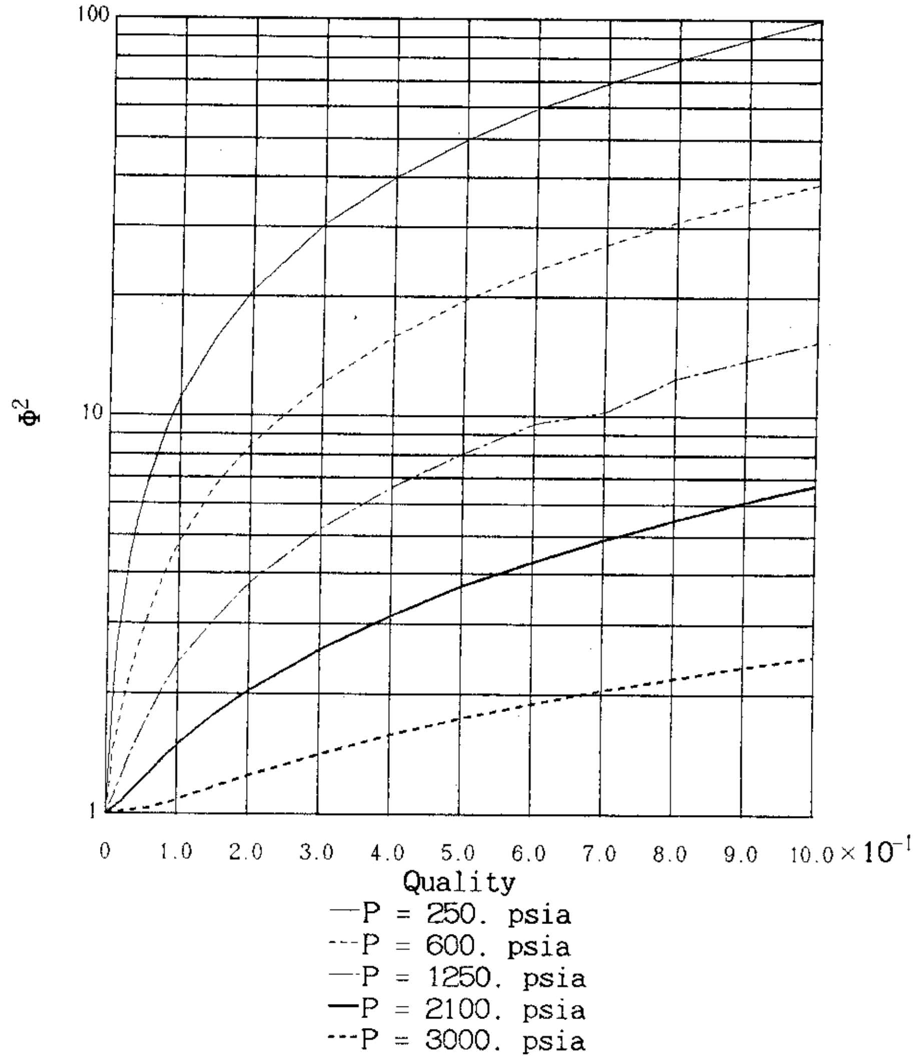

Fig. 2 - 4 Two phase multiplier : Thom

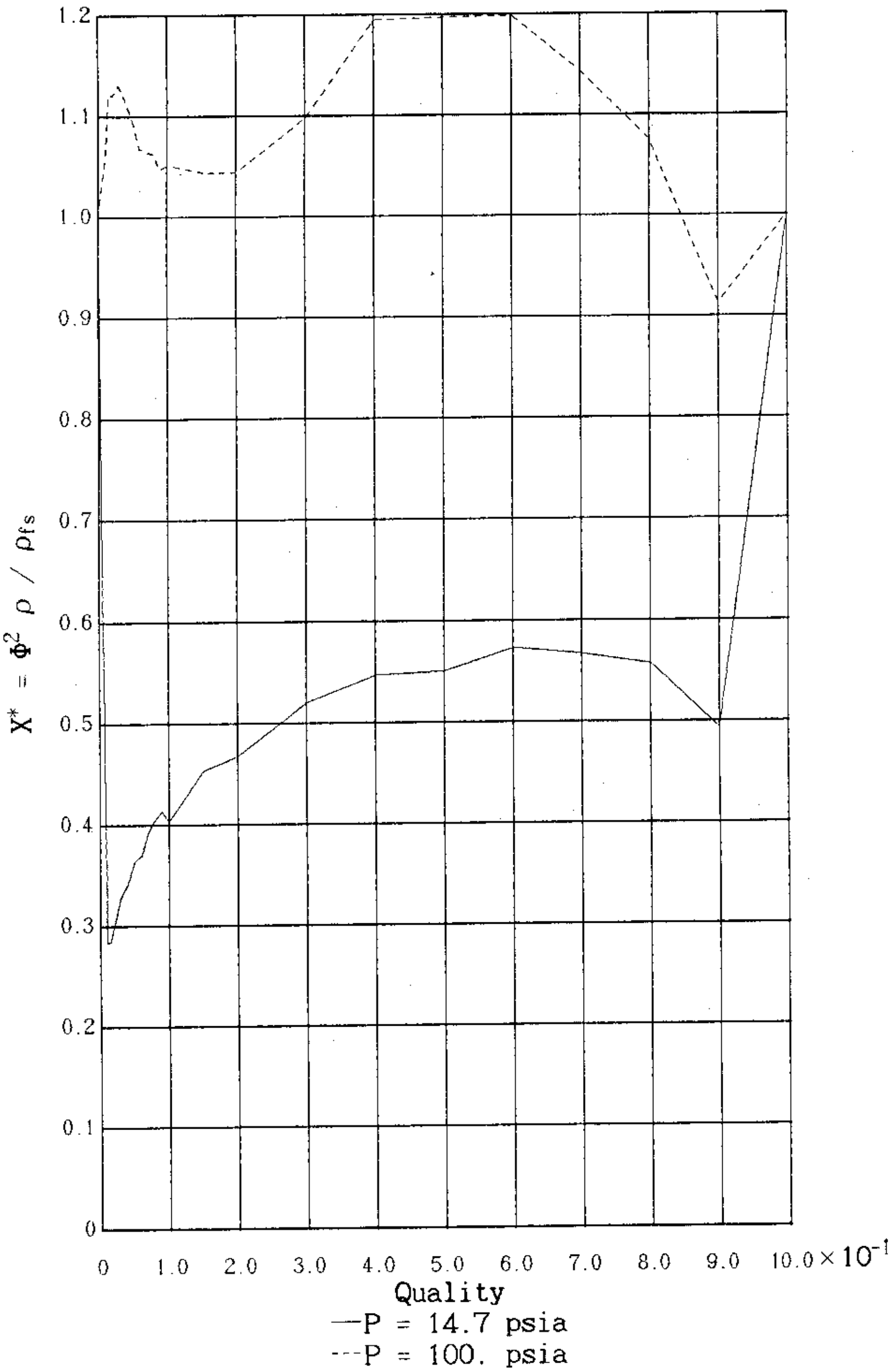

Fig. 2 - 5 Modified two phase multiplier : Martinelli-Nelson

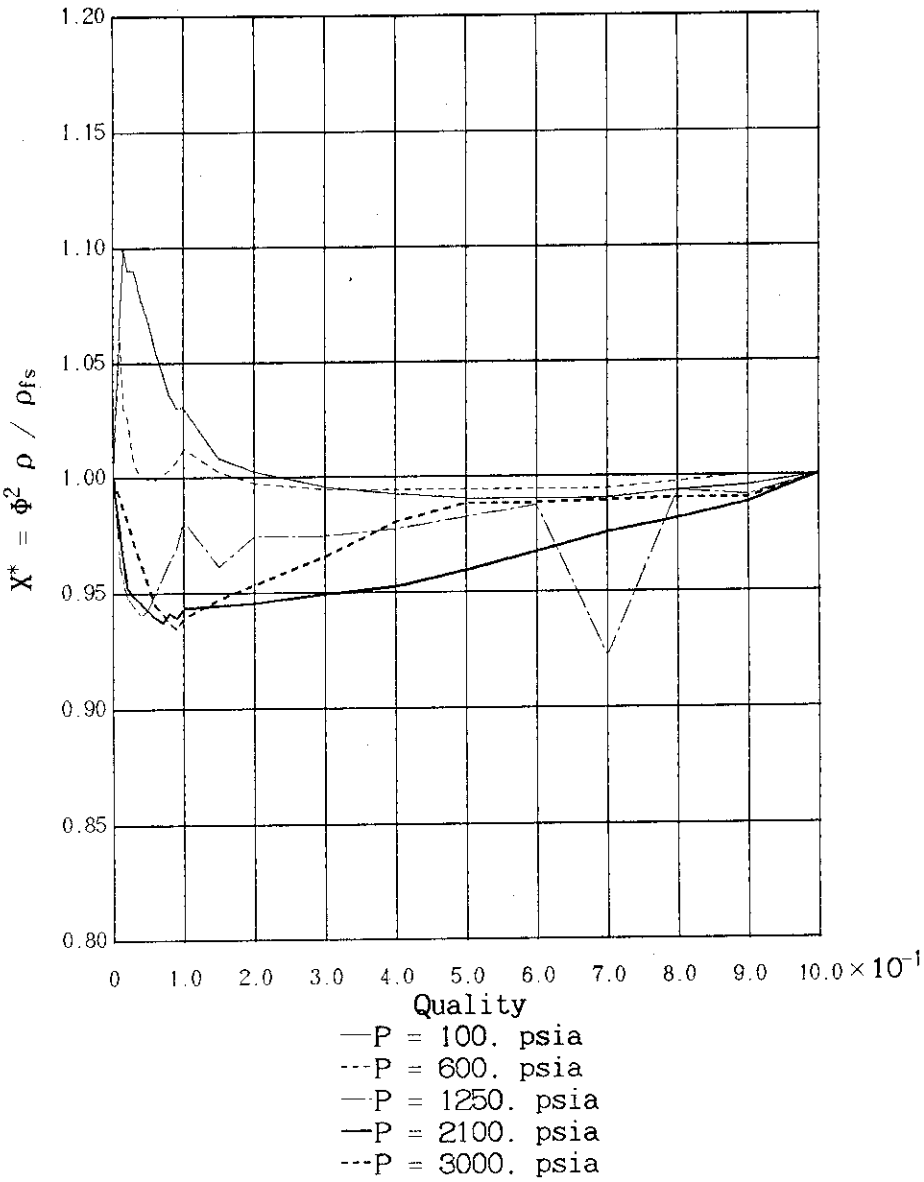

Fig. 2 - 6 Modified two phase multiplier : Thom

3. Description of input data

Most of the input data was made based on those used in THYDE-P1 Sample Calculation Runs 20 [6] and 21 [10], which were very similar to those of the RELAP4-EM/MOD5 sample problem [14].

The input data used in the present calculation are listed in App. A-1 and A-2. The first data set, App. A-1, is for the first calculation starting from the initial steady state and the other, App. A-2, is for restarting from a restarting dump point of the previous run.

In this section, we will give the main input data in use for the present calculation.

3.1. Nodalization

The nodalization scheme in the present calculation is shown in fig. 3-1.

Broken loop	Nodes	1 to 10
Intact loop	Nodes	11 to 20
Downcomer	Node	21
Lower plenum	Node	22
Average core channel	Nodes	23 to 28
Hot core channel	Nodes	29 to 34
(nodes 23,28,29,34 are non-heated parts)		
Core bypass	Node	35
Core crossflow	Node	36
Upper plenum	Nodes	37
Upper head	Nodes	38
Linkage nodes to pressurizer	Nodes	39 and 40
Linkage nodes to PIS.	Nodes	41 and 42
Linkage nodes to ACC.	Nodes	43 and 44
Pressurizer	Node	45
S.G. secondary	Nodes	46 and 47
Accumulator	Nodes	48 and 49

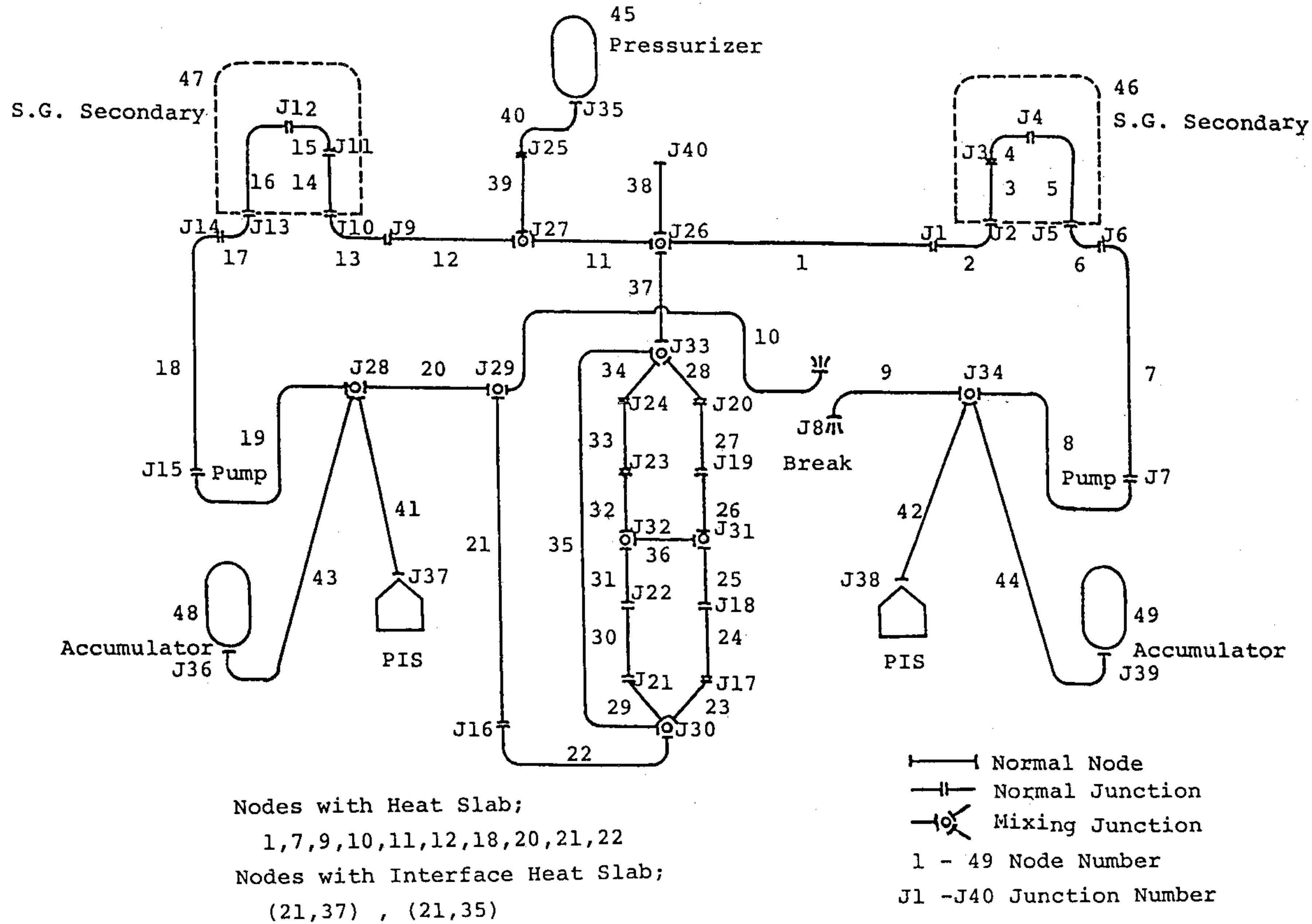

Fig. 3-1 Nodalization Scheme

Table 3-1 Node geometrical data

Node No.	Description	Flow area A (m^2)	Node length L (m)	Node volume V (m^3)
1	Broken loop hot leg	0.4266	5.240	2.235
2	SG inlet plenum	2.8953	1.665	4.821
3	SG U-tube	0.9952	5.000	4.976
4	SG U-tube	0.9952	5.460	5.434
5	SG U-tube	0.9952	10.460	10.410
6	SG outlet plenum	2.8953	1.665	4.821
7	Broken loop cold leg	0.4865	7.340	3.571
8	Pump	0.4266	5.576	2.379
9	Broken loop cold leg	0.3837	2.825	1.084
10	Broken loop cold leg	0.3837	3.130	1.201
11	Intact loop hot leg	1.2798	2.000	2.560
12	Intact loop hot leg	1.2798	3.240	4.147
13	SG inlet plenum	8.6859	1.665	14.462
14	SG U-tube	2.9856	5.000	14.928
15	SG U-tube	2.9856	5.460	16.301
16	SG U-tube	2.9856	10.460	31.229
17	SG outlet plenum	8.6859	1.665	14.462
18	Intact loop cold leg	1.4594	7.340	10.712
19	Pump	0.5750	5.576	7.137
20	Intact loop cold leg	1.2798	5.955	6.855
21	Downcomer	2.7435	7.248	19.885
22	Lower plenum	4.8578	6.075	29.511
23	non-active core in average	4.3552	0.230	1.002
24	Active core in average	4.3552	0.800	3.484
25	Active core in average	4.3552	0.800	3.484
26	Active core in average	4.3552	0.800	3.484
27	Active core in average	4.3552	0.800	3.484
28	non-active core in average	4.3552	0.230	1.002
29	non-active core in hot	0.0222	0.230	5.11×10^{-3}
30	Active core in hot	0.0222	0.800	1.78×10^{-2}
31	Active core in hot	0.0222	0.800	1.78×10^{-2}
32	Active core in hot	0.0222	0.800	1.78×10^{-2}
33	Active core in hot	0.0222	0.800	1.78×10^{-2}
34	non-active core in hot	0.0222	0.230	5.11×10^{-3}
35	Core bypass	0.2419	3.660	0.885
36	Core cross flow	9.079×10^{-4}	0.100	9.08×10^{-5}
37	Upper plenum	9.2941	4.341	40.346
38	Upper head	3.8568	3.658	14.108
39	Pressurizer surge line	0.0661	15.00	0.991
40	Pressurizer surge line	0.0661	14.30	0.945
41	Pumped injection duct	0.2192	12.00	2.630
42	Pumped injection duct	0.0731	12.00	0.877
43	Accumulator duct	0.1161	120.00	13.932
44	Accumulator duct	0.0387	120.00	4.644

Table 3-2 Loss coefficients of nodes

Node No.	K	K^{Af}	K^{Ar}	K^{Ef}	K^{Er}
1	0.023	0.043	0.084	0.0	0.0
2	0.021	3.73	1.97	0.0	0.0
3	0.011	0.033	0.048	0.0	0.0
4	0.008	0.0	0.0	0.0	0.0
5	0.017	0.0	0.0	0.033	0.048
6	0.030	0.0	0.0	3.73	1.97
7	0.029	0.042	0.077	0.0	0.0
8	4.864	0.055	0.015	0.203	0.203
9	0.028	0.0	0.0	0.0	0.0
10	0.019	0.0	0.0	0.0	0.0
11	0.024	0.043	0.083	0.0	0.0
12	0.028	0.0	0.0	0.0	0.0
13	0.013	3.73	1.97	0.0	0.0
14	0.025	0.033	0.048	0.0	0.0
15	0.021	0.0	0.0	0.0	0.0
16	0.027	0.0	0.0	0.033	0.048
17	0.029	0.0	0.0	3.73	1.97
18	0.029	0.042	0.077	0.0	0.0
19	4.867	0.055	0.015	0.203	0.203
20	0.011	0.0	0.0	0.0	0.0
21	1.032	0.0	0.0	0.0	0.0
22	1.398	0.0	0.0	0.0	0.0
23	6.416	0.74	0.74	0.0	0.0
24	6.160	0.0	0.0	0.0	0.0
25	6.072	0.0	0.0	0.0	0.0
26	6.218	0.0	0.0	0.0	0.0
27	6.044	0.0	0.0	0.0	0.0
28	6.737	0.0	0.0	0.0	0.0
29	5.295	1.284	2.482	0.0	0.0
30	5.642	0.0	0.0	0.0	0.0
31	5.570	0.0	0.0	0.0	0.0
32	5.574	0.0	0.0	0.0	0.0
33	4.661	0.0	0.0	0.0	0.0
34	6.194	0.76	0.34	0.0	0.0
35	47.856	0.77	0.83	0.87	0.78
36	6.919	0.0	0.0	0.0	0.0
37	0.021	0.0	0.0	0.0	0.0
38	5.0	1.491×10^4	1.491×10^4	0.0	0.0
39	5.0	0.41	0.87	0.0	0.0
40	5.0	0.0	0.0	0.0	0.0
41	10.0	0.0	0.0	0.0	0.0
42	10.0	0.0	0.0	0.0	0.0
43	10.0	0.109	0.049	0.0	0.0
44	10.0	0.109	0.049	0.0	0.0

3.2. Initial thermal-hydraulic state

The geometrical data and loss coefficient for each node are listed in Tables 3-1 and 3-2 respectively. And the initial mass flux and enthalpy at node 1 were set as ;

$G = 9.0 \times 10^3$ (kg/m$^2 \cdot$ sec)

$h = 360$ (Kcal/kg)

to be used for the initial distributions of the flow rate and the specific enthalpy in the network.

3.3. Break data

The double-ended guillotine break was assumed to occur at junction 8 at 0.01 second after the calculation started.

3.4. Steam Generator data

U-tube pitch	3.0×10^{-2}	m
Number of U-tubes of one unit	3265	
Initial secondary system pressure	62	atm
Initial specific enthalpy of feed water	222	kcal/kg
Initial mass flow rate of feed water	474	kg/sec
Initial subcooled water level	4.0	m
Initial void fraction of saturated region	0.95	

Table 3 - 3 Initial heat flux

Node No.	Heat flux (kcal/m^2 sec)
14	65.65
15	49.24
16	41.03

The feed water was assumed to be cut off at 0.4 sec after LOCA initiation.

3.5. Pump data

Pump data were made based on those used in the RELAP4/MOD5 sample calculation. They are as follows :

Rated speed	1185 (rpm)
Rated flow	5.583 (m^3 / sec)
Rated torque	43250 (J / rad)
Rated head	9.754 (m)
Rated density	747.6 (Kg / m^3)

The data of the single-phase head and torque homologous curves are shown in figs. 3-2 and 3-3, respectively. And the head difference homologous curves are shown in fig.3-4 , which are taken from the RELAP4/MOD5 built-in data of Westing-House pump. The head and torque multipliers as functions of void fraction are shown in fig.3-5.

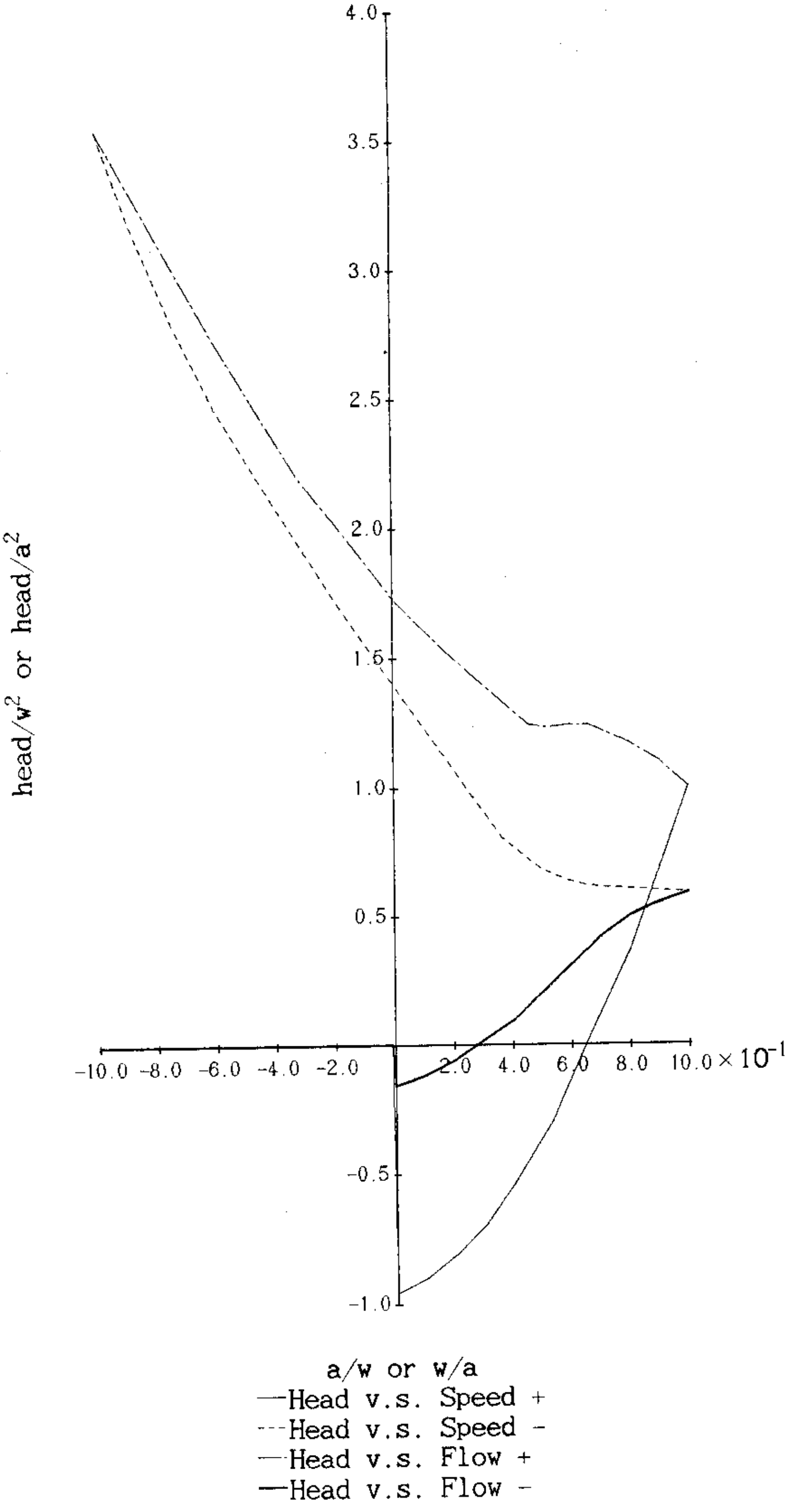

Fig.3-2 Single-phase homologous head curve

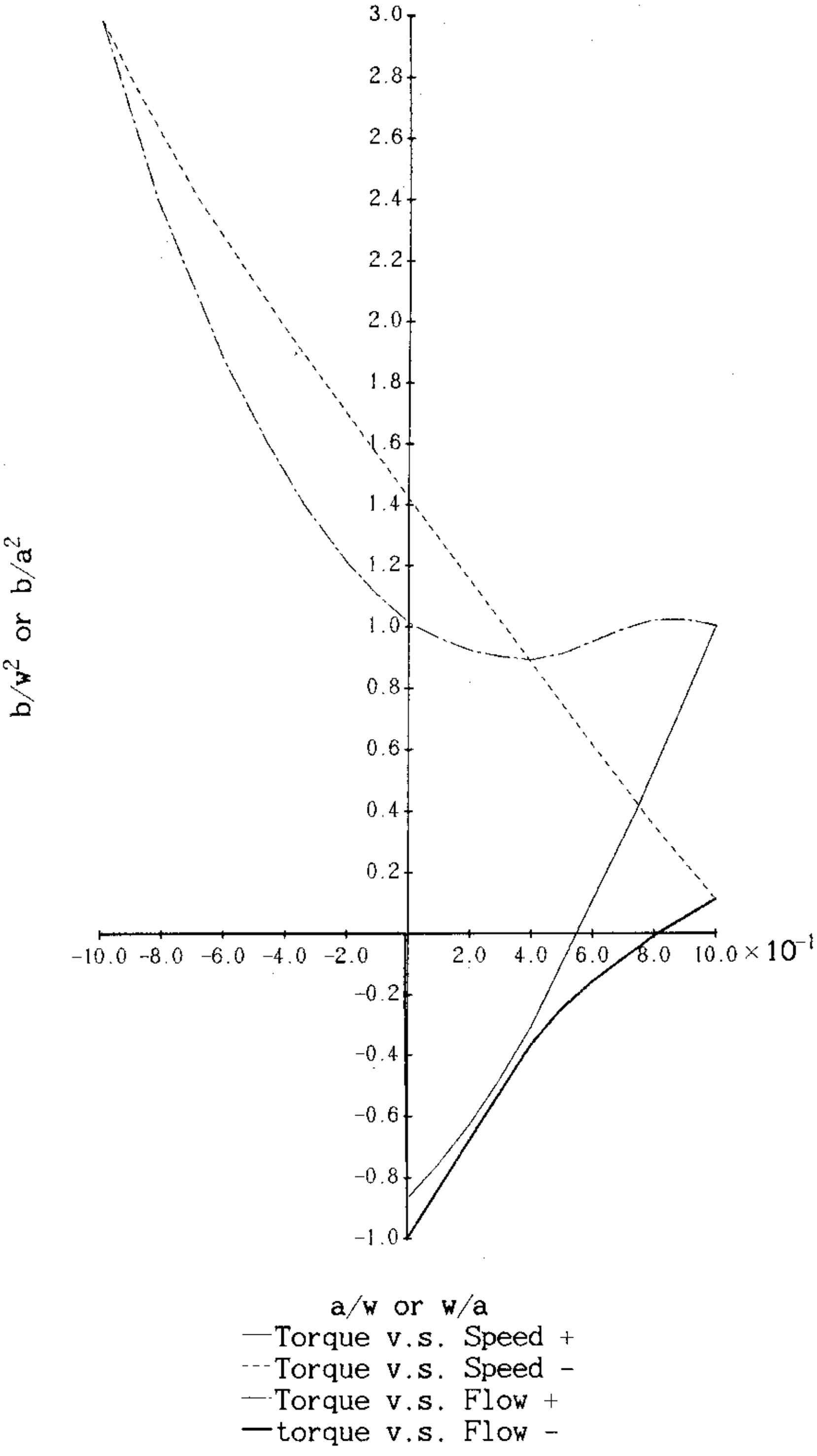

Fig.3-3 Single-phase homologous torque curve

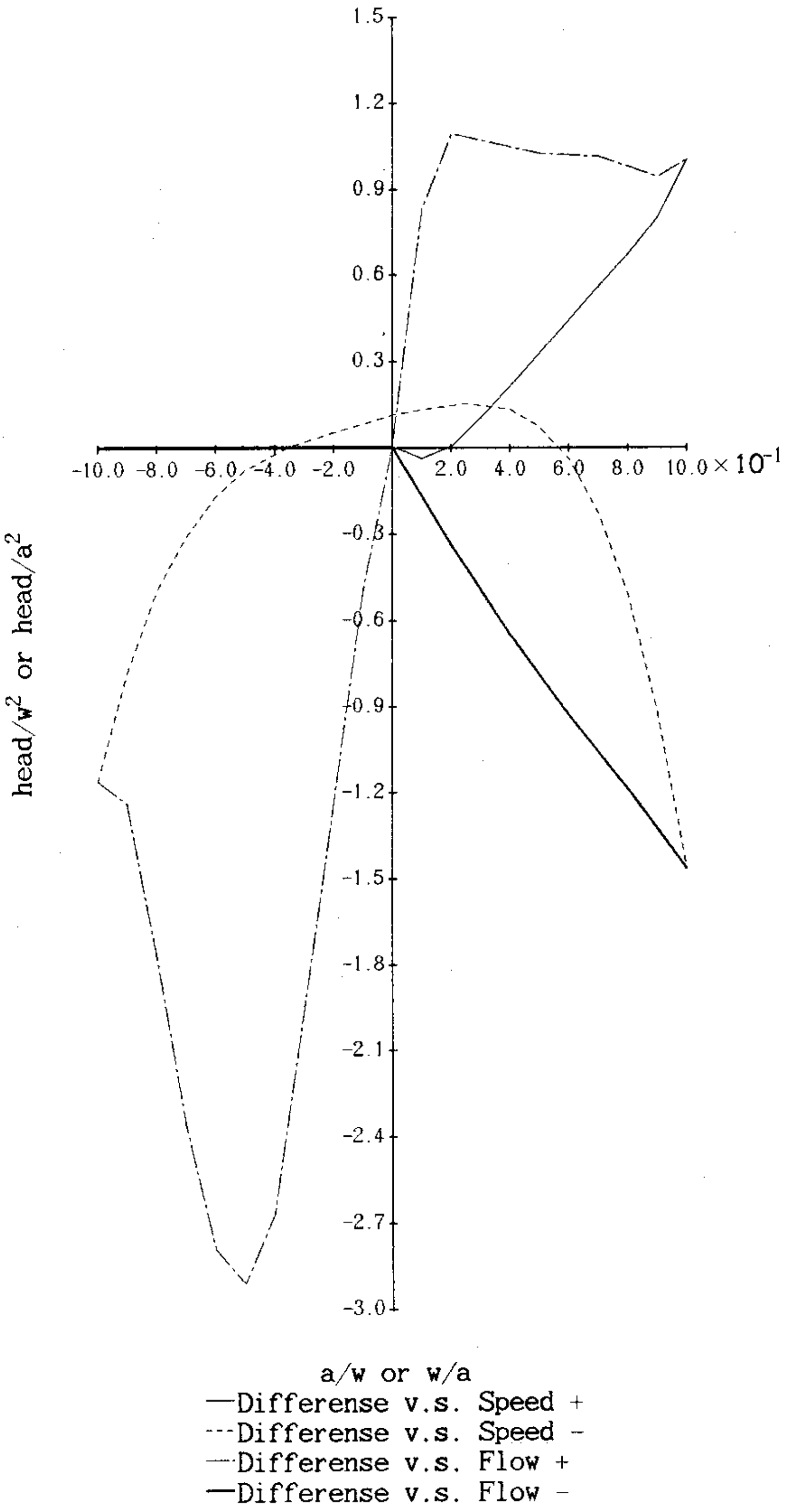

Fig.3-4 Head differense homologous curve

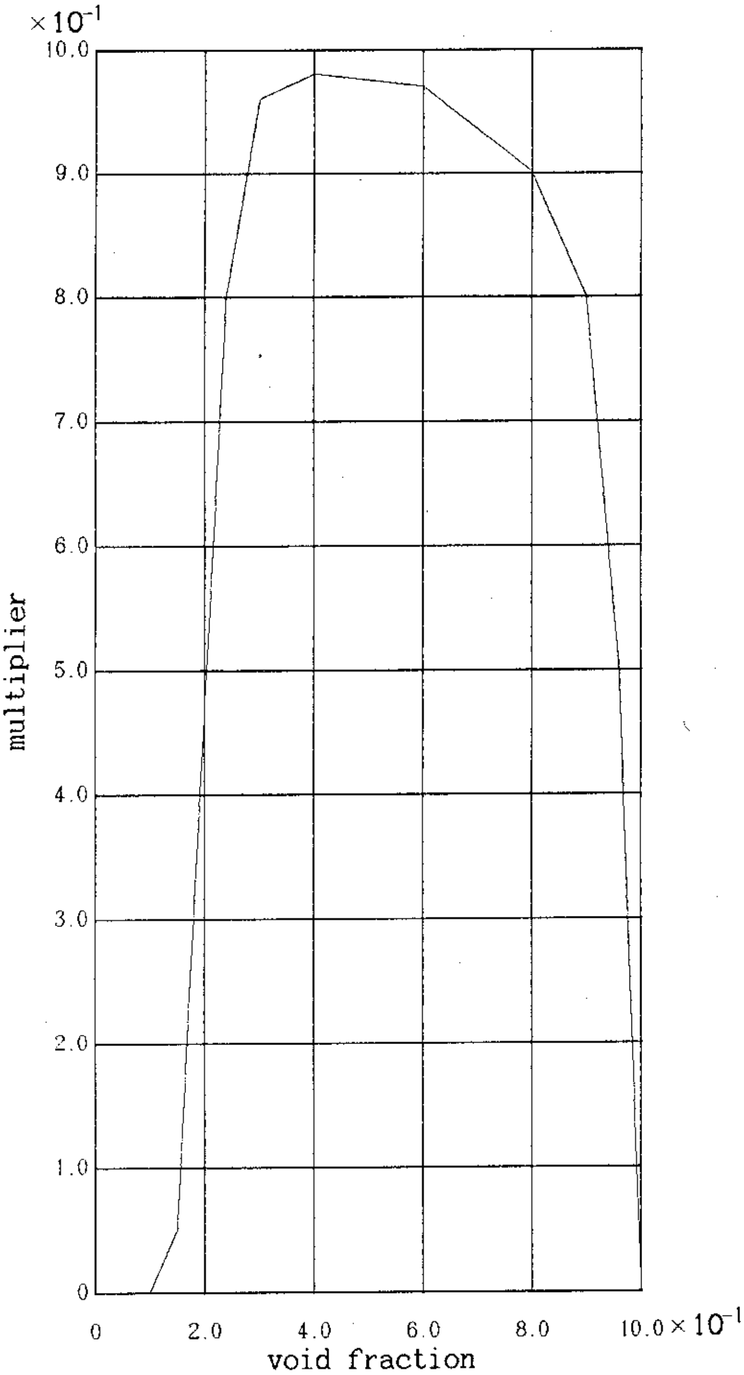

Fig.3-5 Head multiplier curve

3.6. Core data

The core was divided radially into two regions , i.e. an average channel and a hot one. The radial peaking factor of the hot one was assumed as 1.30.

Table 3 - 4 initial heat flux and number of fuel rods

	average channel region		hot channel region	
	node no.	heat flux (kcal/m.sec)	node no.	heat flux (kcal/m.sec)
initial heat flux	23 24 25 26 27 28	non-heated 156.0 234.0 234.0 156.0 non-heated	29 30 31 32 33 34	non-heated 203.0 304.0 304.0 203.0 non-heated
number of rods	39170		200	

Reactor thermal power	3479	MWt
Fuel length	3.66	m
Plenum gas volume	1.235×10^{-5}	m^3
Clad outer diameter	1.0732×10^{-2}	m
Clad thickness	6.187×10^{-4}	m
Pellet diameter	9.3146×10^{-3}	m
Fuel rod pitch	1.42×10^{-2}	m

where the last four values are those at a full power operating condition.

3.7. Pressurizer data

The initial condition for pressurizer were :

Cross sectional area	3.58	m^2
Height	15.56	m
Stand pipe length	0.1	m
Initial subcooled water level	9.0	m
Initial void fraction of saturated region	0.99	

3.8. ECCS data

Accumulator data

Initial water volume	23.2 m^3
Initial nitrogen volume	10.0 m^3
Specific enthalpy of water	
for cold leg injection	51.7 kcal/kg
for L.P. injection	h_{fs}
Initial pressure	44 atm

Pumped injection data

Specific enthalpy of water	
for cold leg injection	37.8 kcal/kg
for L.P. injection	h_{fs}
Mass flow rate	220 kg/sec for one loop

3.9. Heat slab data

As the heat slab models were newly adopted into the THYDE-P1, there was no data of them in the previous Sample Calculation Runs. So heat slab data were made based on those of the RELAP4-EM/MOD5 sample problem [14)]

Table 3 - 5 Geometry and number of heat slabs

inner node	outer node	No. of slabs	shape	No. of region	length of slabs	inner radius (width)*	outer radius (thickness)*
-	21	1	Rect.	1	4.573	(8.019)	(0.03556)
21	-	1	Cyl.	2	7.303	2.197	0.2199
22	-	1	Cyl.	2	2.871	2.195	0.1405
11	-	3	Cyl.	2	2.00	0.3682	0.06351
12	-	3	Cyl.	2	3.182	0.3682	0.06351
1	-	1	Cyl.	2	5.182	0.3682	0.06351
18	-	3	Cyl.	2	7.315	0.3938	0.06732
7	-	1	Cyl.	2	7.315	0.3938	0.06732
20	-	3	Cyl.	2	6.400	0.3493	0.06031
9	-	1	Cyl.	2	3.200	0.3493	0.06031
10	-	1	Cyl.	2	3.200	0.3493	0.06031
37	21	1	Cyl.	1	3.174	1.8797	0.05715
35	21	1	Cyl.	1	4.267	1.8797	0.05715

(   ) * is for rectangular shape.

3.10. Container pressure

No particular model for the container was provided except the temporal behavior of the container pressure which was a function of time , i.e. ;

Time (sec)	0.0	7.5	15.0	30.0	1000.0
Pressure (atm)	1.0	2.7	4.0	4.0	4.0

3.11. Time constants of relaxation model for density change [6)]

Time constants τ_d were set as follows ;

Table 3 - 6 Time constants for relaxation model

Time (sec)	τ_D	Nodes and/or (junctions)
0.0 - 13.8		none
13.8 - 18.7	0.08	10 20
18.7 - 33.1	0.08 1.0	10 20 9
33.1 - 45.8	1.0 10.0	9 10 19 20 43 44 (29) 21
45.8 - END	1.0 10.0	9 10 19 20 21 23-34 43 44 (29) 22

3.12. Maximum time step used in the present calculation

The maximum time step width allowed in the present calculation was given by input as follows ;

$$\Delta t_{max} = 0.001 \text{ sec.} \quad \text{for} \quad t < 0.3 \text{ sec.}$$
$$= 0.008 \text{ sec.} \quad \text{for} \quad 0.3 < t < 60.0 \text{ sec.}$$
$$= 0.016 \text{ sec.} \quad \text{for} \quad 60.0 < t < 90.0 \text{ sec.}$$
$$= 0.032 \text{ sec.} \quad \text{for} \quad 90.0 < t$$

4. Calculated results and discussions.

In a postulated LOCA, it has been conventional to divide the whole process into the three phases, i.e. blowdown, refill and reflood phases. As for the end of blowdown, it is usually defined as the time when the system pressure has decreased almost to that of the containment. And for the end of refill, it is defined as the time when the lower plenum is filled with water, which is called BOCREC. In the present calculation they are 29.5 sec. and 46.1 sec., respectively.

Therefore we call the period before 29.5 sec. as BLOWDOWN PHASE, the period between 29.5 sec. and 46.1 sec. as REFILL PHASE and the rest as REFLOOD PHASE for convenience. The chronology of events is summarized in Table 4-1, compared with the results of WREM code. [19),20),21)] The detailed discussions about the events will be made in the following subsections.

Note that the expression like "at T sec." represents "at T sec after the initiation of LOCA" in this section.

4.1. Blowdown phase

In this subsection, the detailed discussion about the blowdown phase will be presented.

4.1.1. Pressure transient

The calculated pressure transient from 0 to 48 sec. are shown in figs. 4-1 to 4-6. They show the pressures at the core center, the break points, the upper plenum, the pressurizer, the S.G. primary and secondary in the broken loop, and those of S.G. in the intact loop, respectively.

The system pressure decreased very quickly form 1.63×10^7 Pa. (initial pressure) to 1.31×10^7 Pa. in 0.18 sec. just after the initiation of LOCA. And after that, the choking at the break points

Table 4 － 1 Chronology of events

Time (sec) THYDE-P	Time (sec) WREM	Events
0.01	0.01	Break took place and pumps were tripped off, and core scrammed.
0.18	---	Voiding started at center of hot channel.
0.20	---	Voiding started at center of average channel.
0.28	---	Voiding started at upper head.
0.4	---	S.G. feed waters were tripped off.
1.5	1.3	Voiding started at lower plenum.
1.9	---	Voiding started at down comer.
5.2	1.1	ACC injection to broken loop started.
14.5	13.2	ACC injection to intact loop started.
22.5	8.4	Pressurizer emptied.
25.01	25.01	Pumped injections tripped on.
29.5	23.5	End of blow down
34.1	25.02	ECC water started to penetrate downcomer. (EOBP)
37.7	27.0	ECC water filled up cold leg.
38.9	---	ECC water reached downcomer. (L.P. injection started)
46.1	41.5	Reflooding started. (BOCREC)
70.5	40.4	Acc injection ended.
72.	---	Bottom of core node in average channel quenched.
86.	---	Bottom of core node in hot channel quenched.
96.0	---	Burst occured in hot channel.
192.	---	Burst occured in average channel.
294.	---	Lower half of average channel quenched.
333.	---	Lower half of hot channel quenched.

and voiding at the core made the gradient rather slow. At 4.3 sec. the break flow of the core side became a two-phase flow and that made the gradient less steep.

At 29.5 sec., the system pressure is almost equal to that of the containment (about 4×10^5 Pa.), and it is the end of blowdown.

The pressures at the break points, the upper plenum and the S.G. primary showed a very similar behavior except that that of the pump-side break point showed a rather faster transient for about 4 seconds. And that of the pressurizer showed very gradual transient because of the choking at the surge line ; i.e. it decreased slowly with an almost constant gradient until 22.5 sec., when the water level in the pressurizer reached the minimum level, and then it decreased quickly because of steam releasing. Compared with the results of the RELAP4/EM-BLOWDOWN calculation, it can be said that the THYDE-P evaluated the pressure transient milder. Such a tendency is more marked at the pressurizer.

The pressure at the pressurizer caught up with that of the system at 12 sec. in RELAP4/EM, and at 46 sec. in THYDE-P1-EM. Such a difference of the system pressure transients is caused by that of the break flow, which will be discussed in the next subsection, and the difference of pressure transient at the pressurizer is caused by the difference of the critical flow at the pressurizer surge line, which will be shown in the other subsection, 4.1.5.

4.1.2. Break flow

The break flow rates and their qualities are shown in figs. 4-7 to 4-10. **Note** that as the negative flow means discharging at the core side of the break, so does the positive flow at the pump side.

At the core side of the break, the discharge flow decreased swiftly until 4.3 sec., because it was a single phase flow. And after that, the two-phase critical flow made the gradient slow. The quality began increasing after 5 sec. because of decompression boiling, and was suddenly stopped at 17.5 sec. by the ACC water whose injection had begun at 14.5 sec. ACC water also made the flow rate high. PIS water injection, which was started at 25.01 sec., made it subcooled at 28 sec.

At the pump side of the break, a similar behavior was observed, but no subcooled critical flow could be seen and the transient was about 4 or 5 seconds faster. That is, the decompression was so rapid that vioding at the pump side break began at a very early stage, at 0.5 sec., and the quality increased up to 9 sec. when it started to decrease due to ACC water whose injection had begun at 5.2 sec. A slight increase of flow rate could also be seen at about 10 sec. but PIS water whose injection started at 25.01 sec made it subcooled after 28 sec.

When these results are compared with those of the RELAP4/EM calculation, it can be said that the flow rate at the core side of the break point are calculated to be considerably small by THYDE-P1-EM from 3 sec. to 10 sec. As the quality of the break flow in this period was between 0.0 to 0.1, it can be said that these difference are caused by the smoothing method between the subcooled and saturated regimes, and by the value of the discharge coefficients (C_D). They are 0.91 for Zaloudek and 0.6 for Moody in THYDE-P1-EM, while both are 1.0 in RELAP4/EM. These values used in the present calculation were chosen by the experience of the BE calculation of many experiments, which would represent the discharge flow realistically.

4.1.3. Core flow

As shown in figs. 4-11 and 4-12, the core flow at the hot channel and at the average channel showed quite similar behavior. That is ; at first, just after the rupture, a reverse flow occurred at the bottom of the core and continued up to 2 sec. After that, forward flow took place and persisted up to 8 sec. caused by the voiding at the L.P. and the downcomer which began at 1.5 sec. and 1.9 sec. respectively. At the top of the core, a reverse flow occurred at 1 sec and continued until 2 sec. This time lag of one second can be explained by the voiding at the core center which started at a very early stage. After 2 sec. the behavior was quite similar to that of the core bottom.

The differential pressure across the core, which denotes the core flow and water accumulation in the core, is shown in fig. 4-13.

In the RELAP4/EM calculation, a reverse flow took place at 5 sec. and the flow rate was larger. As this flow was supplied from the upper head and the pressurizer, it came from the difference of the pressurizer surge flow and the difference of noding at the upper plenum and the hot-leg linkage junction.

4.1.4. Intact loop flow

The pump outlet flow and its quality are shown in figs. 4-14 and 4-15 respectively.

Up to 5 sec., the flow decreased slowly, for it is a single-phase flow. At 5 sec. the voiding began and the two-phase flow made it decrease rapidly.

As shown in fig. 4-16, the hot leg inlet flow decreased and then became a reverse flow at 6 sec. This is caused by both the decompression in the core and the injection from the pressurizer, but the latter contributed mainly.

The cold leg outlet flow is shown in fig. 4-17 and it showed a similar behavior to that of the pump outlet flow. The main difference between them are caused by the ECC injection. That is ; ACC injection started at 14 sec. which stopped voiding at the cold leg and the quality was suddenly reduced from 0.9 to 0.2, and the PIS injection, which began at 25.01 sec. made it subcooled at 29 sec., and increased the mass flow rate. The mass flow rate was larger by 1700 kg/sec at the cold leg than that of the pump outlet flow. This difference was equal to the mass flow rate of the ACC injection.

Comparing them with the results of the RELAP4/EM calculation, we can see that the pump outlet flow and the cold leg outlet flow matched well. But after 17 sec. the cold leg outlet flow was about 1.6 times as large as that of the THYDE-P1-EM. It is because the ECC behavior differs. And in RELAP4/EM, the hot leg inlet flow became a reverse flow at 5 sec., which is mainly caused by the difference of the pressurizer surge flow and the difference of the noding scheme at the upper plenum.

The pressurizer surge flow and the water level in the pressurizer are shown in figs. 4-18 and 4-19, respectively.

4.1.5. Broken loop flow

The pump outlet flow and its quality are shown in figs. 4-20 and 4-21, respectively. They show almost the same behavior as those of the pump side break flow in the early phase of blowdown, except that after 10 sec. the break flow was larger by 500 kg/sec and the quality decreased gradually because of the ACC injection. The hot leg inlet flow is shown in fig 4-22. It was a forward flow at any time and the flow rate was twice as large as that of the RELAP4/EM calculation. As seen in the noding scheme, this flow was supplied from the intact loop hot leg or from the core. After 10 sec. when the flow was a reverse flow in the core, it was supplied from the intact loop hot leg. The division rate between the two sources differs very much between THYDE-P1-EM and RELAP4/EM. The difference mainly comes from the difference of the noding scheme. That is, in THYDE-P1-EM, water entered a small volume mixing junction, mixing junction number 26, and divided into two passes without any gravitational effect. While in RELAP4/EM water entered a large volume node, the upper plenum, and divided into two directions. The gravitational effect was taken into account in the downward flow, which causes the core reverse flow. So the most part of flow went toward the core in the RELAP4/EM calculation but the considerable part went toward the broken loop hot leg in the THYDE-P1-EM calculation.

4.1.6. ECC behavior

The ECC behavior is shown in figs. 4-23 and 4-24. ACC injection started when the pressure of the linkage junction decreased under 44 atm. It was at 5.3 sec. at the broken loop, and at 14.5 sec. at the intact loop. PISs started at 25.01 sec. at both loops by trip conditions. ACC water stopped voiding at the cold leg and increased the flow rate, and PIS water made the coolant subcooled in both broken and intact loops.

Comparing them with the results of the RELAP4/EM calculation, we observe that ACC injection is delayed in THYDE-P1-EM. That is because the decompression was estimated milder in THYDE-P1-EM. And in RELAP4/EM, the ACC injection mass flow rates were about 1.6 times as large as those in the THYDE-P1-EM, i.e. 2700 kg/sec for intact loop and 800 kg/sec for broken loop in RELAP4/EM, while 1700 kg/sec for intact loop and 500 kg/sec for broken loop in THYDE-P.

Though it may seem that ECCs stopped at 34.1 sec. in the THYDE-P1-EM calculation, it was only for convenience's sake and the ACC injection really stopped at 70.5 sec. ACC discharge continued and the water mass in the ACCs were kept being reduced continually as shown in figs. 4-25 and 4-26. (see subsection 2.1.)

4.1.7. Downcomer and Lower Plenum

The mass flow rates and their qualities at the downcomer and the L.P. are shown in figs. 4-27 to 4-30. The results of THYDE-P1-EM and RELAP4/EM are quite similar to each other. A reverse flow occurred just after the rupture and became a forward flow caused by voiding which started at 3 sec. in the L.P. and at 4 sec. in the downcomer, and again returned to a reverse flow at 6.5 sec in both nodes. After that, the quality rose rapidly because of the high enthalpy reverse flow from the core. At 17 sec. the reverse flow rate decreased and hence the quality dropped a little, but soon recovered and it kept being superheated up to 34.1 sec.

As shown in fig. 4-28, no forward flow could be seen between 4 to 6 sec in the RELAP4/EM calculation. That is partly because the break flow was too large to allow a reverse flow to occur at the downcomer or L.P.

4.1.8. Temperature and HTC at core

The temperature at the center of the fuel, the temperature and the HTC at the cladding surface, and the quality of the coolant are shown in figs. 4-31 to 4-38.

It can be seen that the temperature at the center of the fuel suddenly fell just after the rupture due to the scram, and kept almost constant value after 10 sec.

The cladding surface temperature rose quickly for 3 seconds just after the rupture, because the decrease of the flow rate and the flashing at the core made the cooling condition worse. But after 3 sec. it stopped rising until 8 sec. for the sake of the low quality forward flow caused by the voiding at the L.P. and the downcomer. After that, a reverse flow took place and it made the coolant superheated. The HTC showed the minimum value at 10 sec., and the cladding surface temperature showed the maximum value at 11 or 12 sec. The peak temperature was 948 K in the average channel, and 1,041 K in the hot channel.

After 12 sec. the increase of reverse flow rate, and the drop of the coolant quality caused by the pressurizer surge flow improved heat transfer until 24 sec., but again the surface temperature tended to increase because of the small HTC of superheated steam forced convection.

In the RELAP4/EM-HOT CHANNEL calculation, the peak cladding surface temperature is higher by 100 K than that of the present calculation, and the time is earlier by 4 or 5 seconds. That is because the RELAP4/EM calculation evaluates the larger discharge flow . It made the system decompression rapid and the coolant in the core becomes superheated much earlier. And the cladding surface temperature rose to the peak on a stretch because no forward flow caused by voiding at the downcomer and the L.P. was calculated at 4 or 5 sec.

After 8 sec., the temperature dropped swiftly. This is because of the large amount of the reverse flow at the core, which changes the heat transfer mode from superheated steam forced convection to film boiling.

4.1.9. Comparison to the RELAP4/EM calculation

Comparing the present results with those of the RELAP4/EM calculation, it can be said that the overall behavior is very alike. But as for the time , it is somehow late in THYDE-P1-EM. It is mainly because the injection flows are small in THYDE-P1-EM compared with RELAP4/EM. That is, to say about ACC injection, the average flow rate to the intact loop was 1700 Kg/sec in THYDE-P1-EM, while it was 2700 Kg/sec in RELAP4/EM. Similarly it was 500 Kg/sec and 800 Kg/sec in the broken loop respectively. As for the pressurizer surge flow at 1.0 sec., it was about 1300Kg/sec in THYDE-P1-EM but 2500 Kg/sec in RELAP4/EM. These differences, which may be due to the difference in C_d , cause the delay of the pressurizer empty time or ACC injection stop time.

The difference in the period from the end-of-blowdown to EOBP comes mainly from the difference in the noding. That is, in the THYDE-P1-EM calculation the cold leg outlet flow enters junction 29, which is a mixing junction and has small volume without height. While in the RELAP4/EM calculation it enters the large node, upper half of the downcomer, the height of which is about 3 meters with a considerable gravitational force. Ignoring this gravitational force in THYDE-P1-EM, EOBP could not be observed even at 50 sec. or later. In order to minimize this difference, THYDE-P1-EM was modified to consider ρgh (h = 0.699 m = diameter of the cold leg) term at the downcomer top mixing junction, but the effect seemed to be small yet. The same thing can be said about the upper plenum. As the reverse flow rate differed so much between the THYDE-P1-EM and RELAP4/EM calculation, we should have considered a gravitational term at the upper plenum junction in the present calculation.

4.2. Refill phase

The refill phase starts at 29.5 sec. and ends at 46.1 sec. As for the refill phase, there is little to be discussed. That is mainly because many unrealistic assumptions were adopted in this phase in order to execute an equivalent calculation and to make up an equivalent initial reflood conditions to those of the WREM/J2 code. As these methods were presented in the subsection 2.2., they are strictly based on those used in the RELAP4/EM and RELAP-FLOOD calculations. They were adopted to simulate the following models which had been used in the WREM/J2 code. Those are :

1. The total ECC mass injected is subtracted from the cold-leg, the downcomer and/or the lower-plenum, just after EOBP.
2. ECC injection point is changed from the cold-leg to the lower-plenum in starting RELAP-FLOOD calculation.
3. BOCREC time used in the RELAP-FLOOD calculation is not the one calculated by RELAP4/EM, but is evaluated by a manual calculation as below:

$$T_{BOCREC} = T_{EOBP} + \Delta T_{fill} + \Delta T_{fall}$$

T_{EOBP} : EOBP-time calculated in RELAP4/EM

ΔT_{fill} : time needed to fill the cold-leg and L.P.

ΔT_{fall} : time needed to free-fall the downcomer

Consequently T_{BOCREC} differs from that computed in the RELAP4/EM-BLOWDOWN calculation..

4.2.1. Fuel temperature and HTC

The temperatures at the fuel center and at the cladding surface are shown in figs. 4-31 to 4-34. As seen in them, they increased linearly in this phase because an adiabatic calculation had been executed. And the gradients of them are quite similar to those of the RELAP4/EM-HOT CHANNEL calculation.

HTCs were set as zero in the refill phase, which can be seen in figs. 4-35 and 4-36. The qualities at the core dropped to 1.0 because an adiabatic condition gave no heat to the coolant in the core nodes, which are shown in fig. 4-37 and 4-38.

4.2.2. Other variables

As seen in fig. 4-23 and 4-24, ECC injections to the cold-leg were stopped at 34.1 sec. But ACC ejections were kept hypothetically, and water mass left in ACC were reduced gradually as shown in figs. 4-25 and 4-26. That was evaluated by equation (2-9).

Hypothetical ECC injection to the lower-plenum started at 38.9 sec. and the BOCREC was at 46.1 sec. The cold-leg heating (see subsection 2.1.5.) started at 34.1 sec. and ended at 40.3 sec. (node 9), 41.2 sec. (node 10) and 41.6 sec. (node 20).

The effect of this heating can be seen in fig. 4-9 and 4-10. It disturbed the flow a little. That is, the pump outlet flow in the intact loop became a reverse flow and its quality dropped because the flashing in the adjacent node, node number 20, rout water toward the pump node. But the disturbance diminished soon and the RELAP-FLOOD initial condition was satisfied at the time of BOCREC.

4.3. Reflood phase

The reflood phase begins at 46.1 sec. As it was noted in the subsection 2.2., we gave priority to the check of the FLECHT HTC correlation and of the history of the fuel and cladding surface temperature. So the results of flow calculation considerably differs from those of the RELAP4-FLOOD calculation. It is because a perfect phase separation is assumed at downcomer and core, and FLECHT CARRY OVER RATE FRACTION (CRF) was also used in the RELAP-FLOOD calculation. But they were not used at all in the present calculation because THYDE-P1-EM solves physical equation strictly even in the reflood phase calculation. Consequently the discussion and comparison will be made mainly about the thermal calculation results. And as the version SV03L02 of the THYDE-P does not have a hottest-pin calculation model, it is impossible to compare the results with those of the TOODEE2 calculation.

4.3.1. Temperature, HTC and Metal-Water reaction

The fuel center temperature, the cladding surface temperature, the HTC at the cladding outer surface and at the inner surface (gap conductance), the M-W reaction heat generation rate, and the thickness of the cladding oxide layer are shown in figs. 4-39 to 4-64. They show the transients from 45.8 sec. to 400 sec. Each variable is shown for the four types of rods. They are the non-burst rod in the average channel, the non-burst rod in the hot channel, the burst rod in the average channel and the burst rod in the hot channel. The burst occurred at 96 sec. in the hot channel, and at 192 sec. in the average channel. The burst nodes were node 32 and node 26, respectively, which were the same as the peak power nodes at the steady state.

The fuel center temperature of both channels showed similar behavior with a constant difference about 100 K. Maximum temperature was 1,283 K at 243 sec. in the hot channel, and 1,160 K at 196 sec. in the average channel. As for the burst rods, the fuel temperature of the burst nodes rose after the burst, and the maximum temperature was 1,456 K at 243 sec in the hot channel, and 1,225 K at 243 sec in the average channel. It is because the gap conductance of the burst nodes suddenly dropped to 1/50 by the steam as shown in fig 4-53 and 4-54. Its effect can be seen in the cladding surface temperature of the burst rods. As shown in figs. 4-45 and 4-46, the cladding surface temperature suddenly fell down just after the burst. It is because a small gap conductance made the amount of heat supply very small.

The cladding surface temperature of the non-burst rods are shown in figs. 4-43 and 4-44. The average channel temperature is shown in fig. 4-43 along with the results of the RELAP-FLOOD calculation. Though they cannot be compared directly because of the difference of noding, it can be said that they agree well. The difference of noding is that the slabs 1 to 3 of the RELAP-FLOOD calculation are equivalent to nodes 24 and 25 of the THYDE-P1-EM calculation.

The HTCs at the cladding surface are shown in figs. 4-47 to 4-50. HTC behaviors agreed with those of the RELAP-FLOOD calculation beyond our expectation, in spite of the fact that the flow calculation models, the method to identify the quenching node and the HTC formula for quenching node differs from those used in the RELAP-FLOOD calculation. The main differences of the results are summarized as follows :

1. Quenching proceeds a little too fast in the present calculation.
2. At the beginning and the ending of quench, HTC jumped up in the present calculation.
3. Sometimes HTC of the quenching node decreased in the present calculation

These differences are due to the absence of the phase separation model at the core and the L.P., and to the unusage of the FLECHT CRF in the THYDE-P1-EM calculation.

Metal-Water reaction began when the cladding temperature rose to 900 K, and became more active accompanied with the temperature rise. So the thickness of oxide showed the maximum value at the core center, node 26 and node 32, and it was 0.007 mm in the average channel, 0.018 mm in the hot channel for the non-burst rods. As for the burst rods, temperature drop due to the gap conductance decrease made it thinner at the outer surface of cladding. It was 0.006 mm in the average channel and 0.017 mm in the hot channel. But oxidization began even at the inner surface and it grew to 0.0015 mm in the average channel, 0.012 mm in the hot channel, the maximum total oxide thickness was about 0.03 mm for a burst rod in the hot channel. It is only 5% of whole cladding thickness and is safe enough.

But there is a result calculated by TOODEE-2, which estimated the maximum oxide thickness as 0.012 mm, that is only 2% of cladding, in a severer condition that the peak cladding temperature rose as high as 1300 K. So it may be said that M-W reaction is considerably large in the THYDE-P1-EM calculation as compared with the WREM/J2 calculation.

4.3.2. Other variables

Figs. 4-65 to 4-72 show the mass flow rate at the core, their quality, the differential pressure across the core, across the downcomer and between them. As seen in figs. 4-67 and 4-68, quality did not become negative even in those nodes which had already been quenched. And the differential pressure between the core top and bottom is only 5×10^3 Pa. When it is converted to water head, it is less than one meter. As for the downcomer it is twice as large as that of the core, but when it is converted, it is less than 2 meters. All these are caused by the lack of phase separation model at the core and the downcomer. Consequently we cannot make a comparison about the flow calculation between THYDE-P1-EM and WREM/J2 in the reflood phase. If we wish to do so, we should implement the phase separation model and FLECHT CRF in the THYDE-P1-EM code.

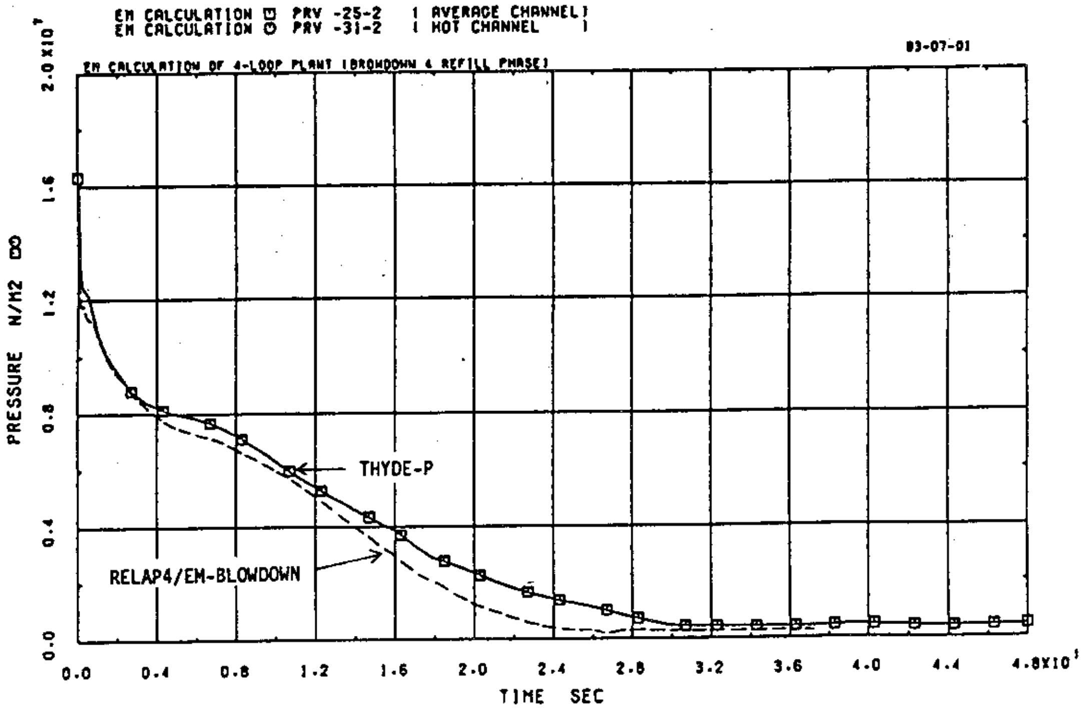

Fig. 4-1 Core pressure

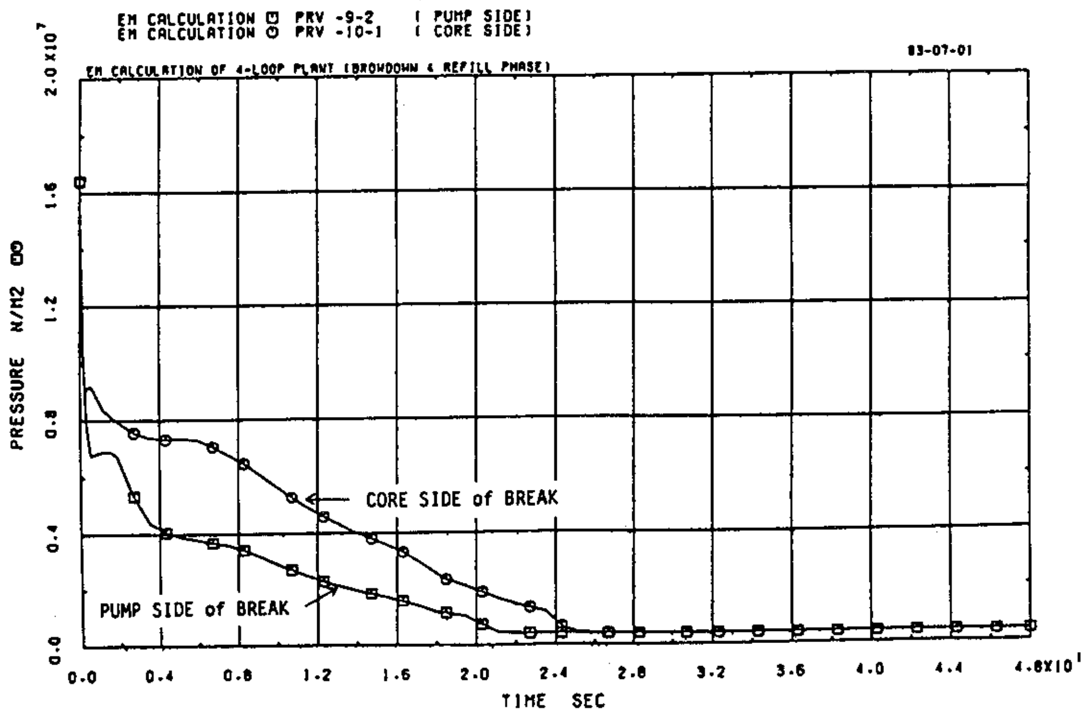

Fig. 4-2 Break point pressure

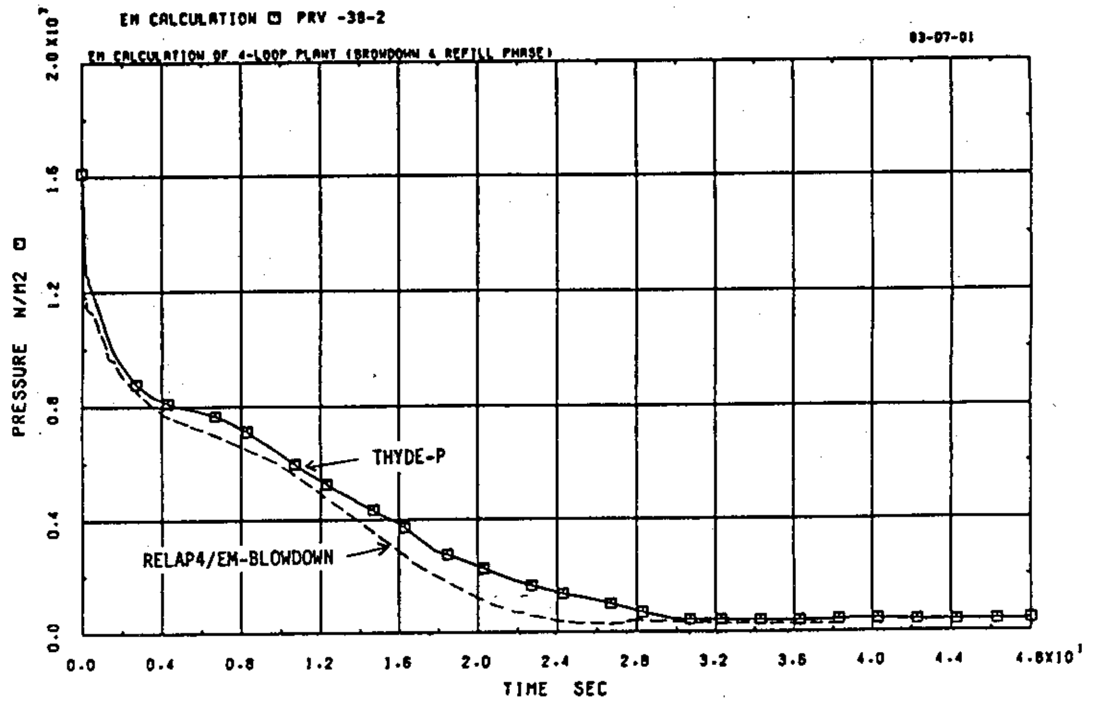

Fig. 4-3 Pressure at upper plenum

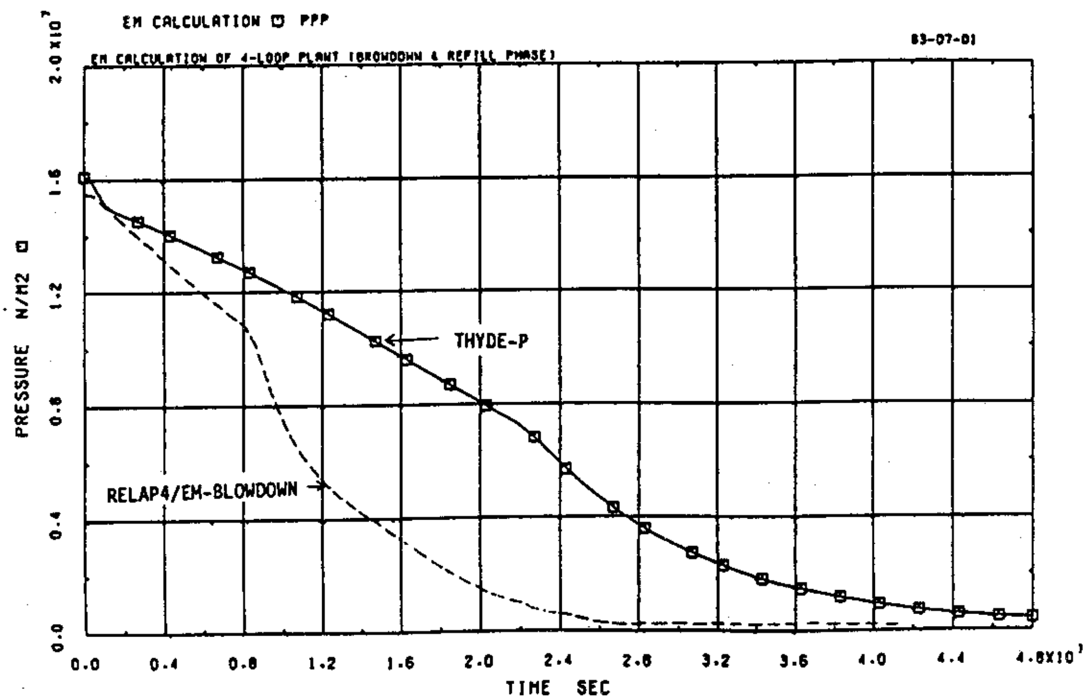

Fig. 4-4 Pressure at pressurizer

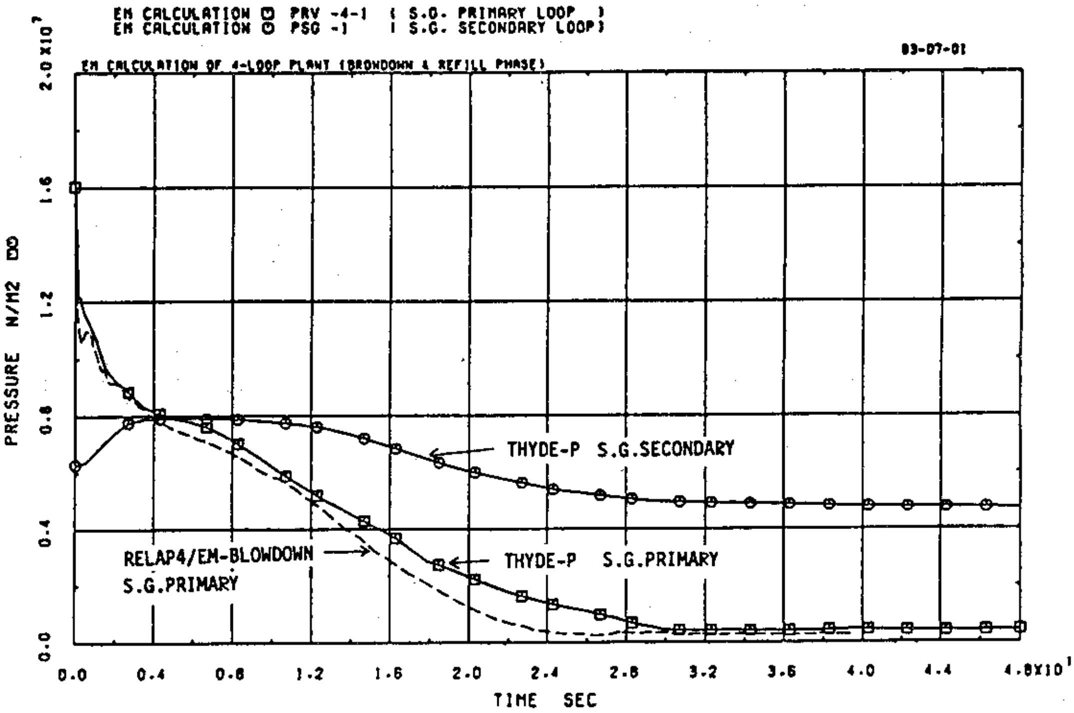

Fig. 4-5 Pressure at S.G. primary and secondary (broken loop)

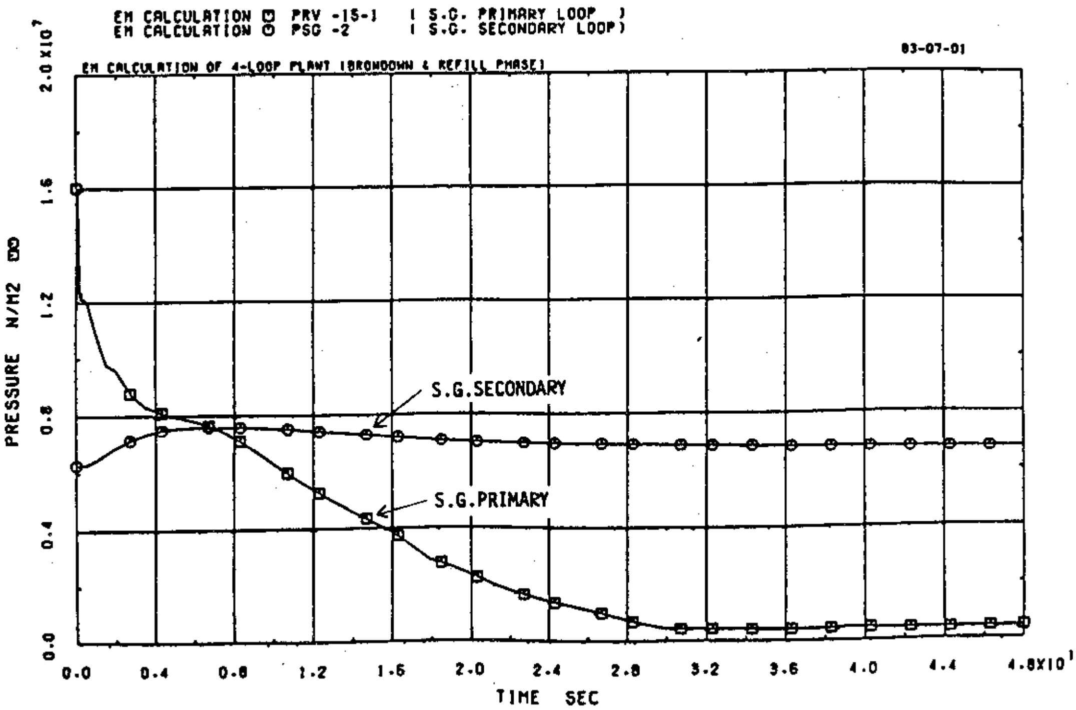

Fig. 4-6 Pressuer at S.G. primary and secondary (intact loop)

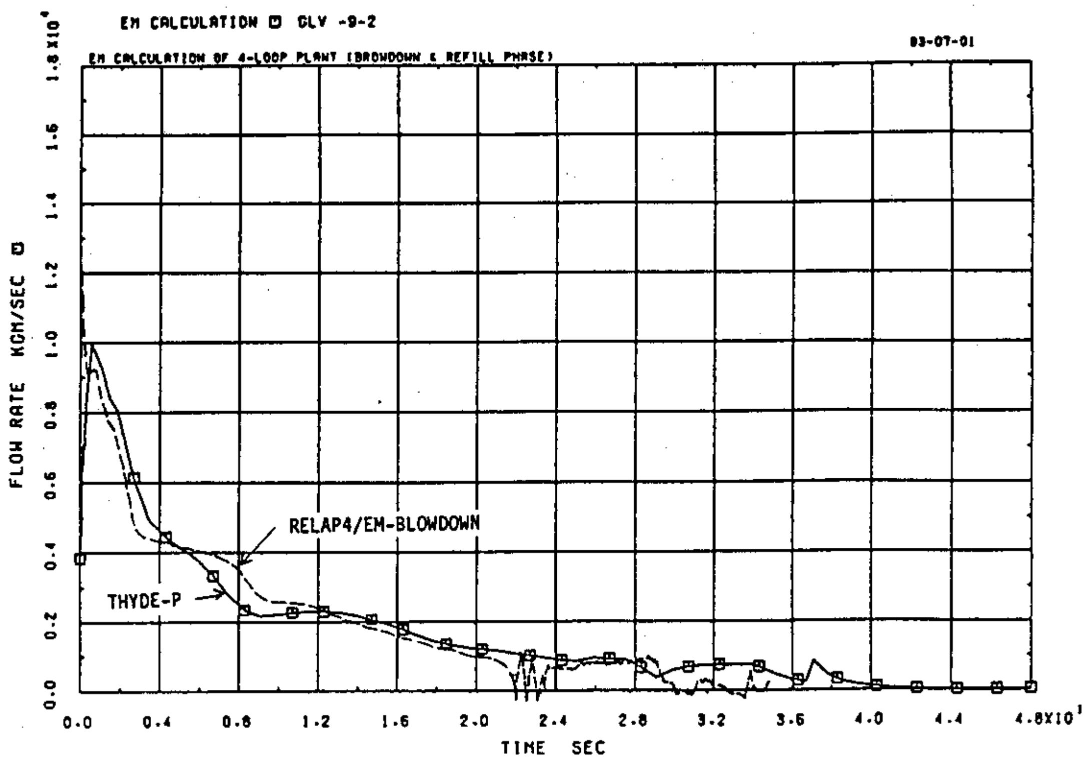

Fig. 4-7 Break flow at pump side

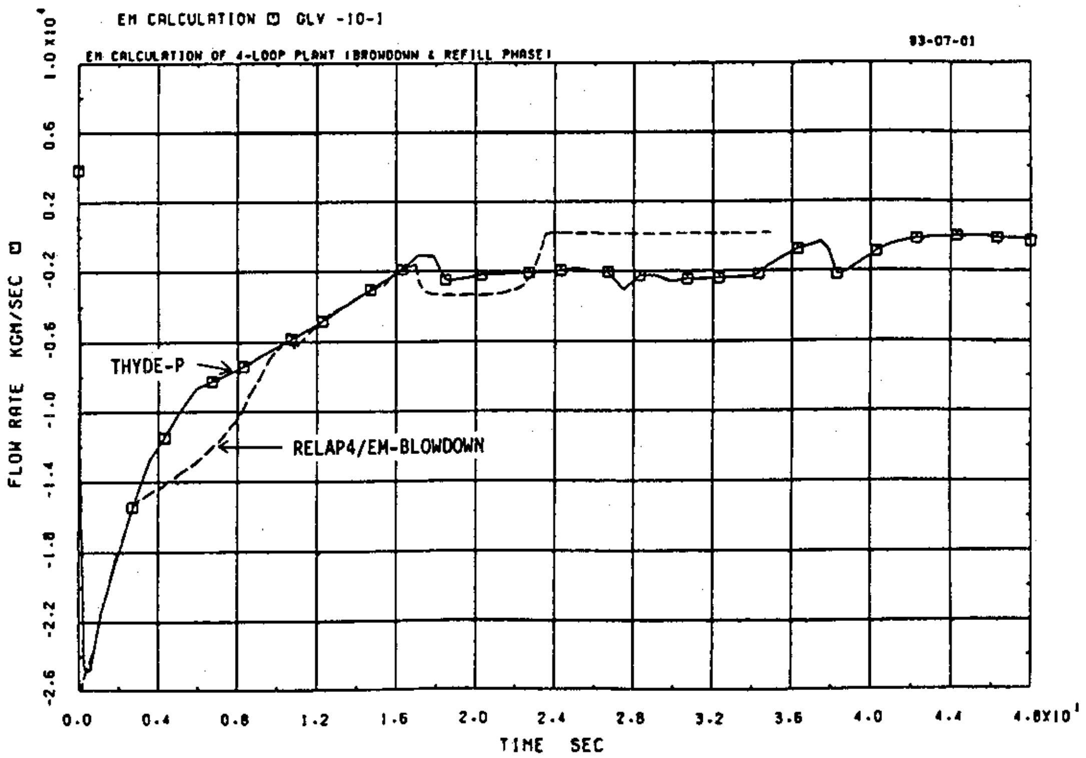

Fig. 4-8 Break flow at core side

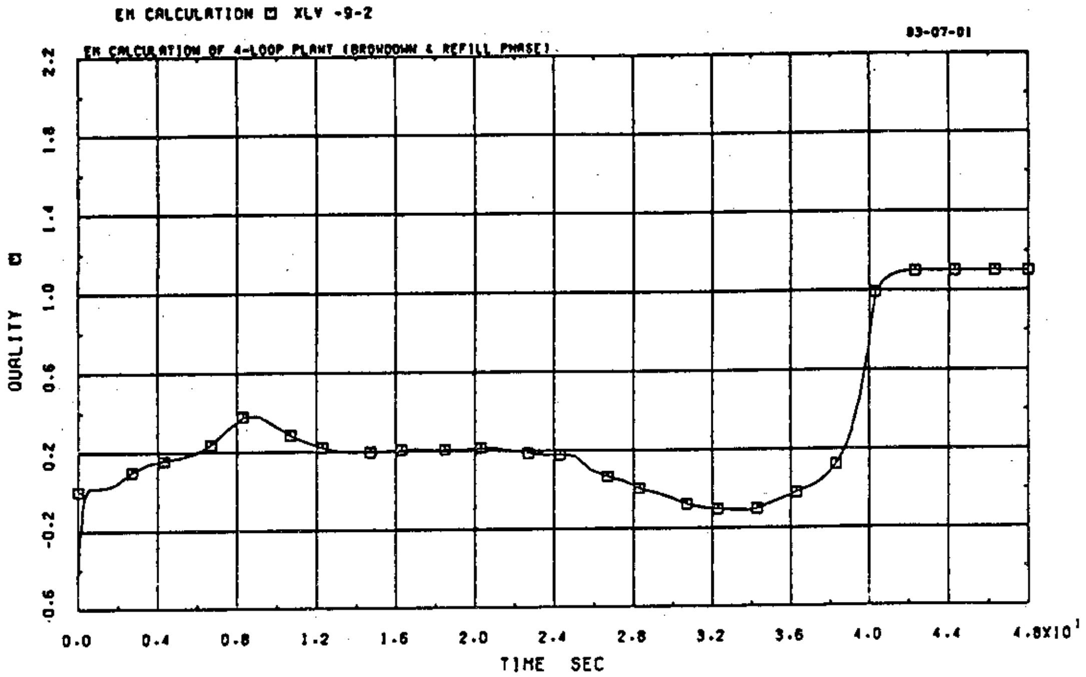

Fig. 4-9 Quality at pump side of break

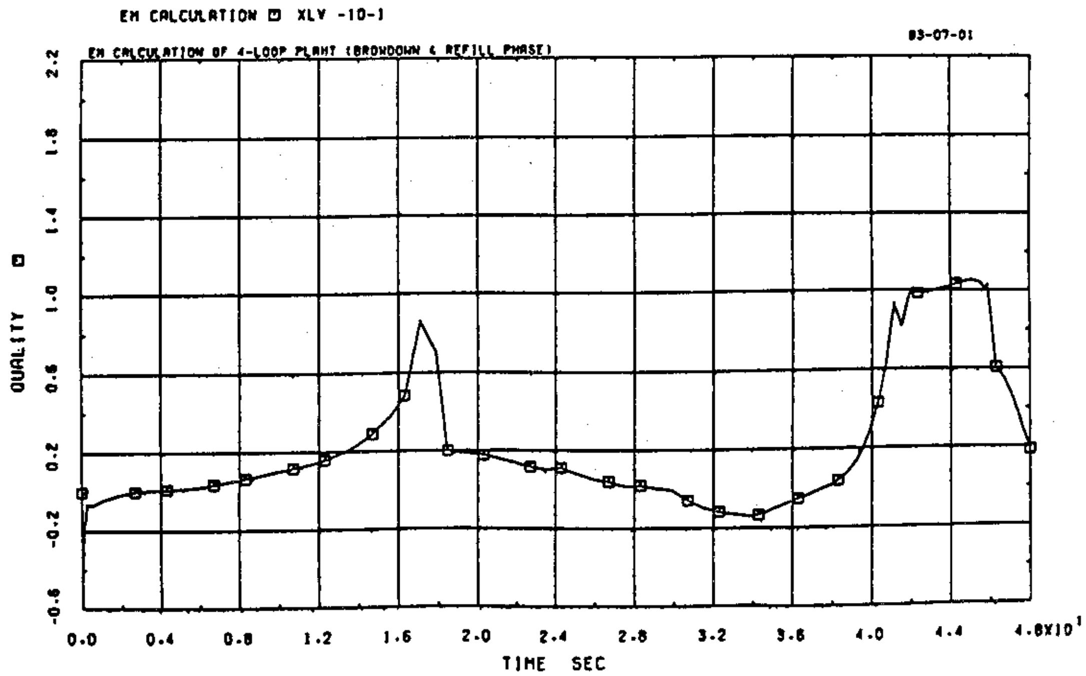

Fig. 4-10 Quality at core side of break

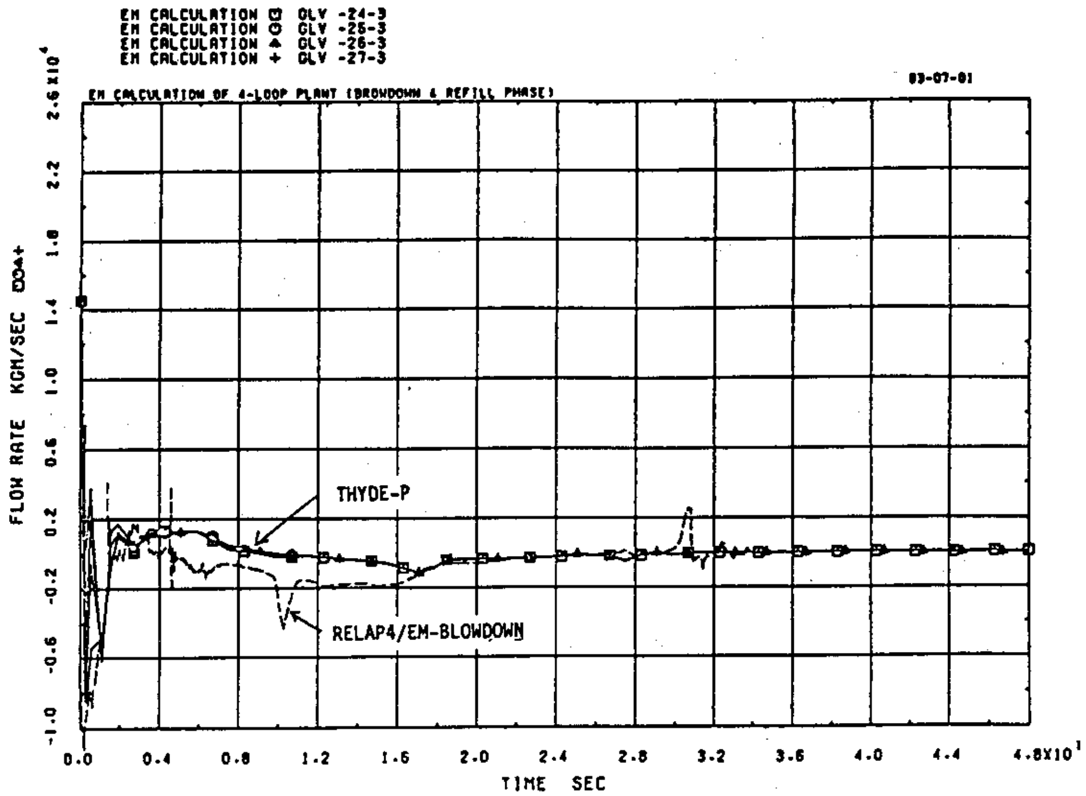

Fig. 4-11 Mass flow rate in core (average channel)

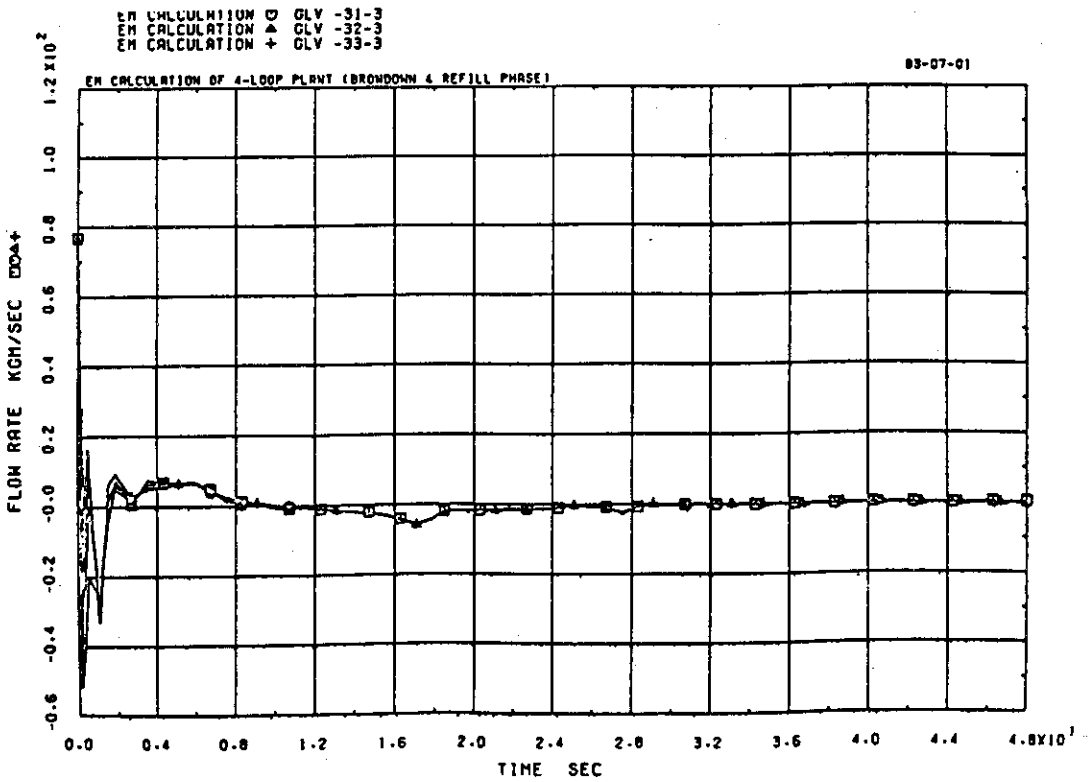

Fig. 4-12 Mass flow rate in core (hot channel)

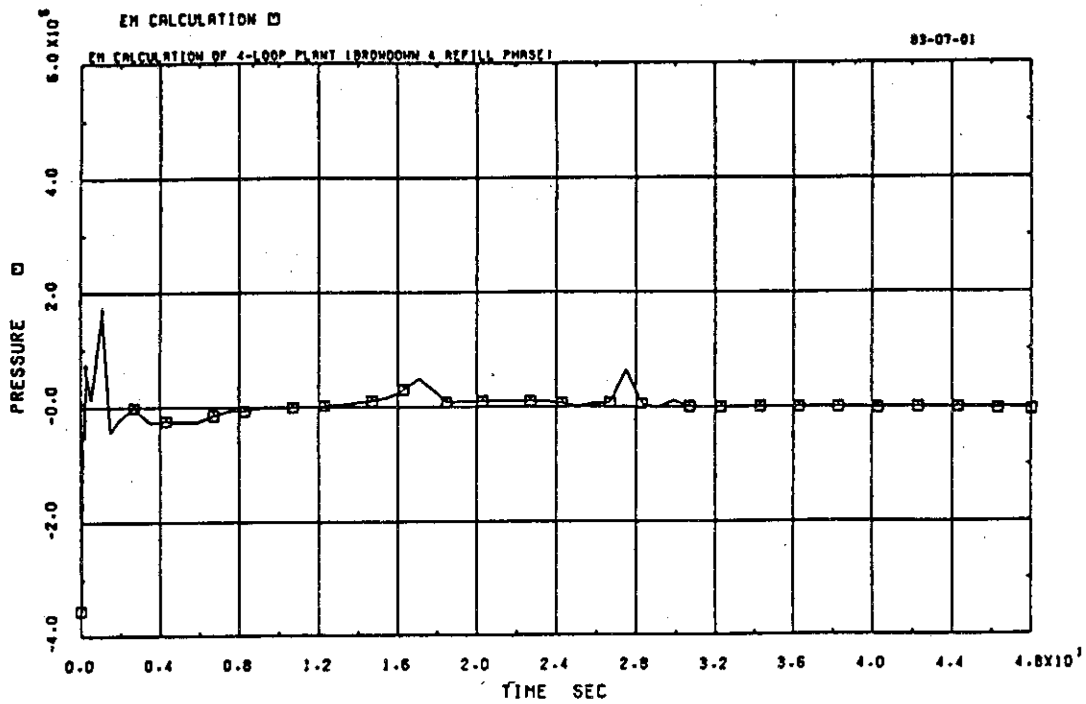

Fig. 4-13 Differential pressure across core

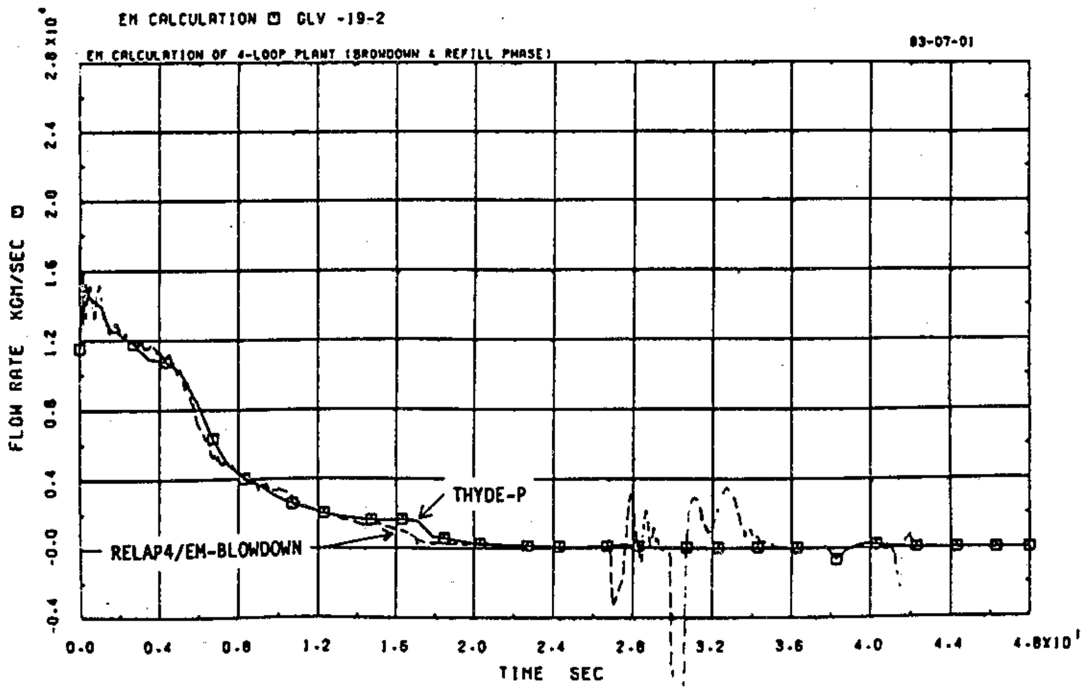

Fig. 4-14 Pump outlet mass flow rate (intact loop)

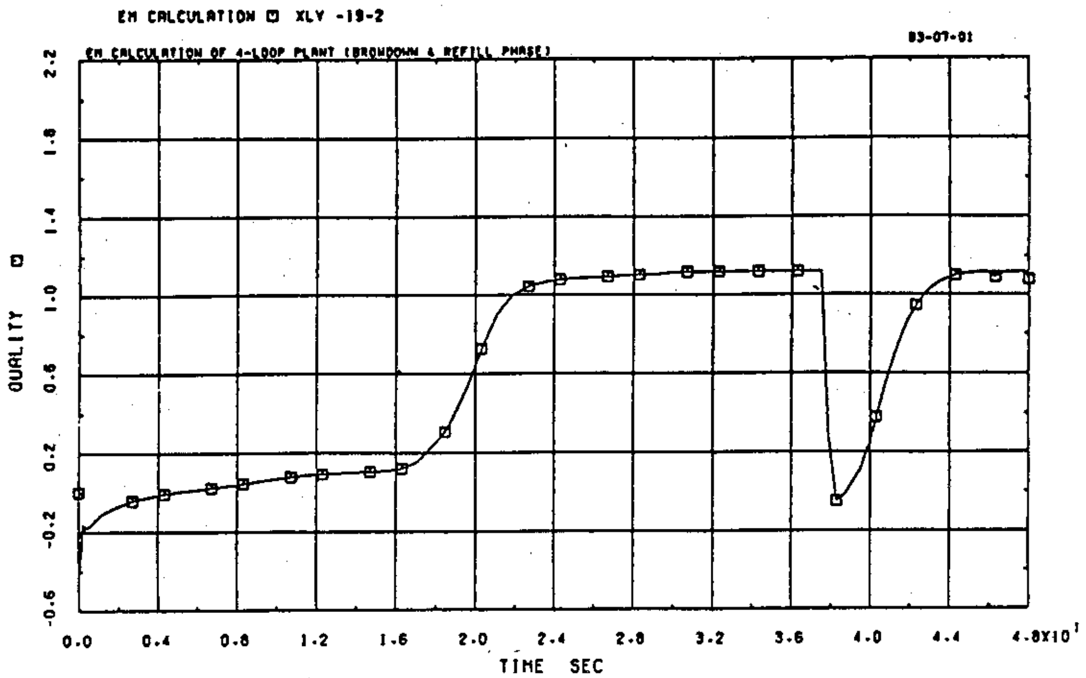

Fig. 4-15 Pump outlet quality (intact loop)

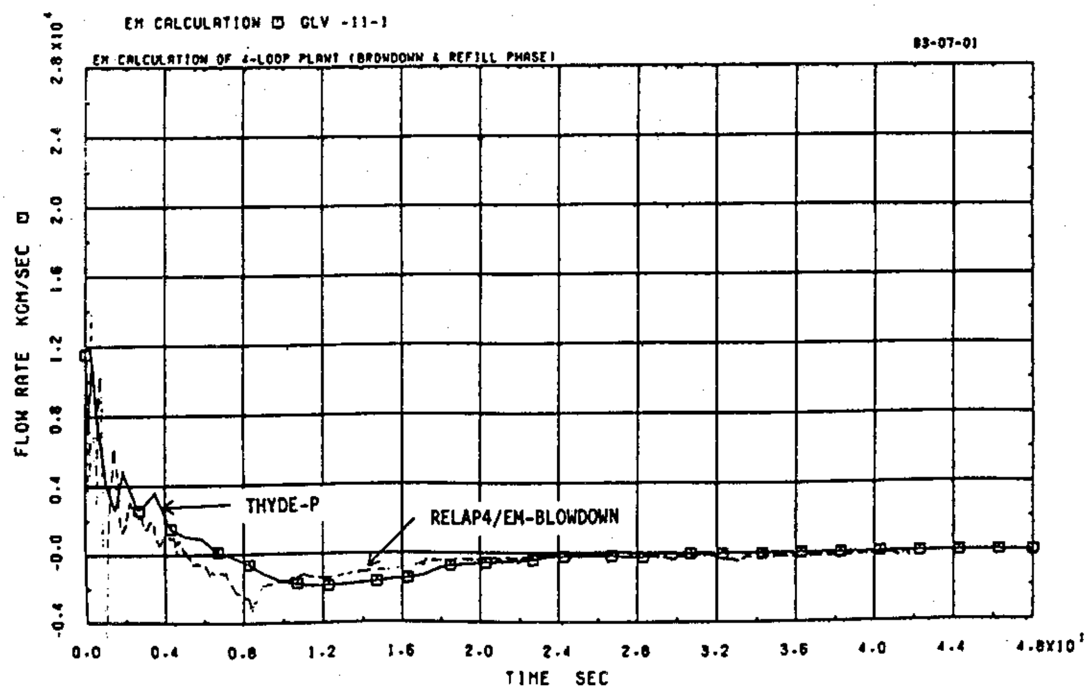

Fig. 4-16 Hot leg inlet mass flow rate (intact loop)

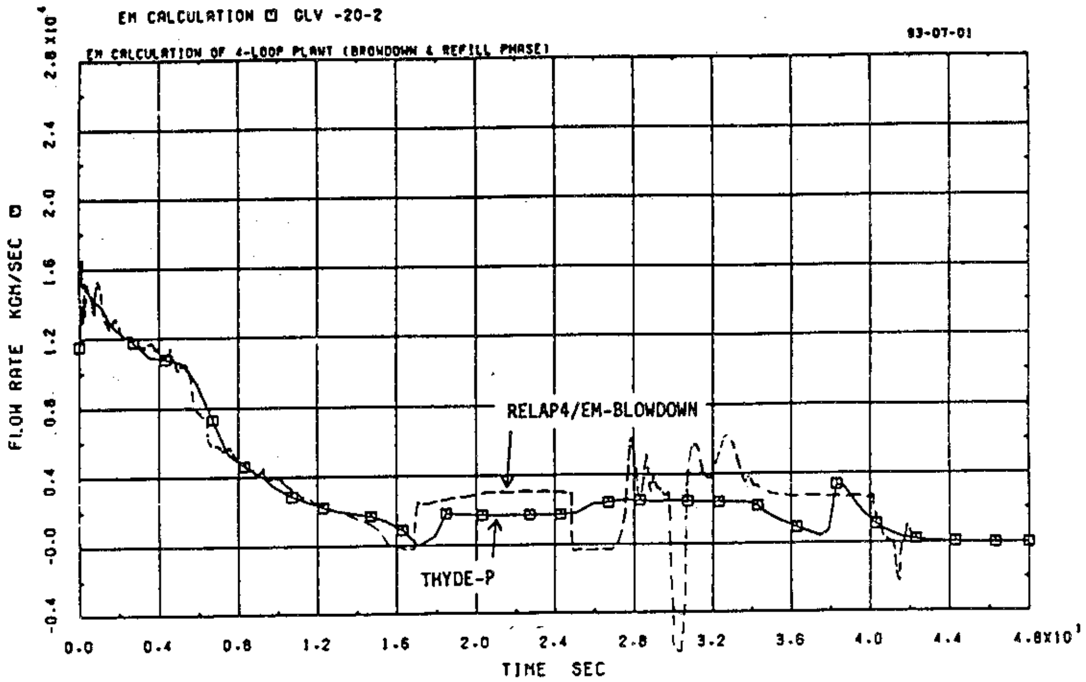

Fig. 4-17 Cold leg outlet mass flow rate (intact loop)

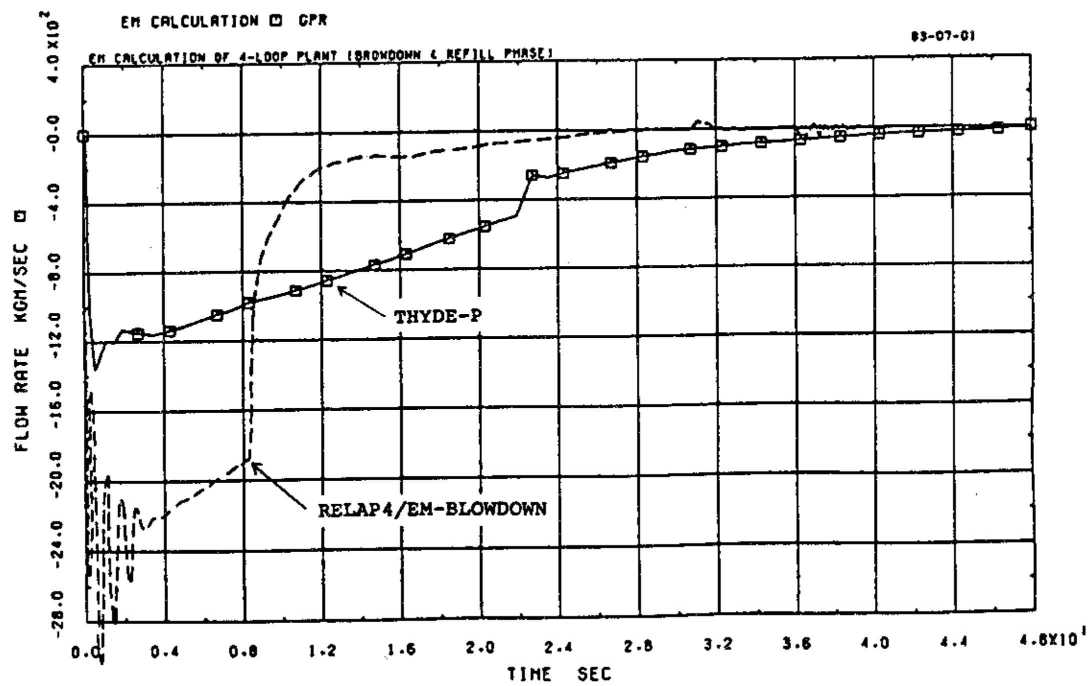

Fig. 4-18 Pressurizer surge line mass flow rate

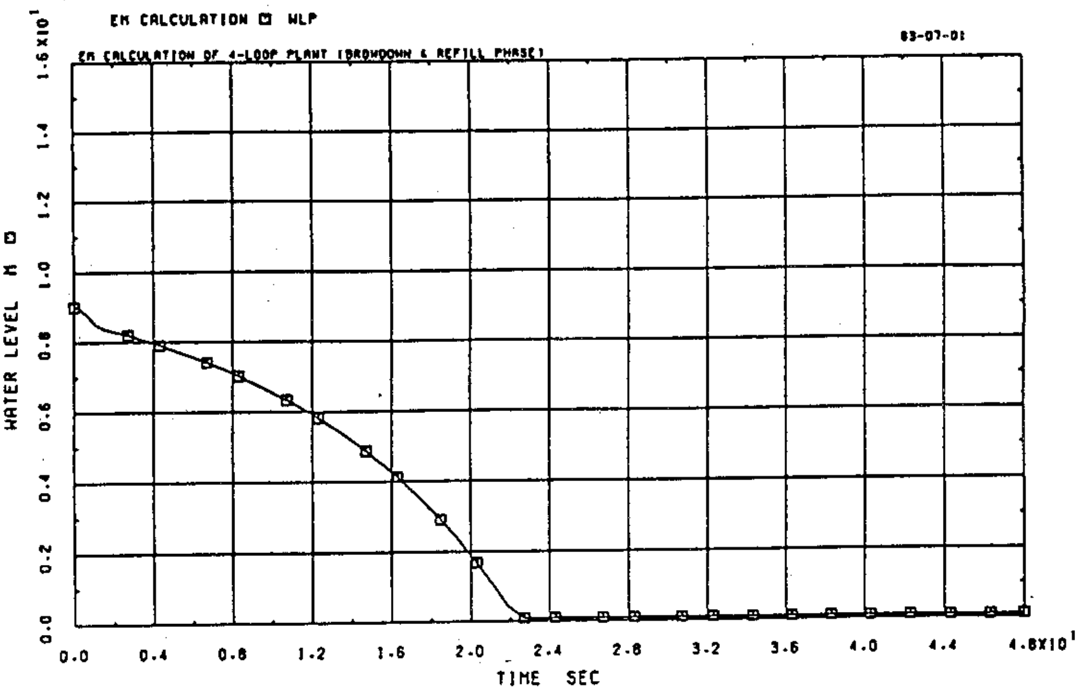

Fig. 4-19 Water level in pressurizer

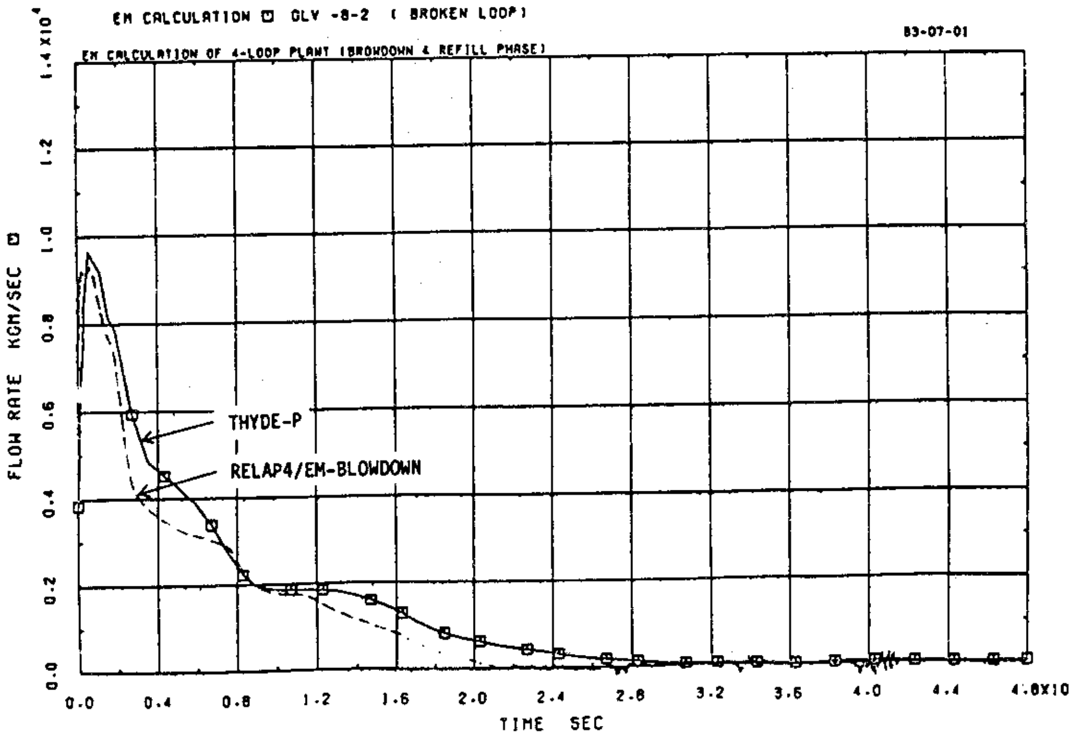

Fig. 4-20 Pump outlet mass flow rate (broken loop)

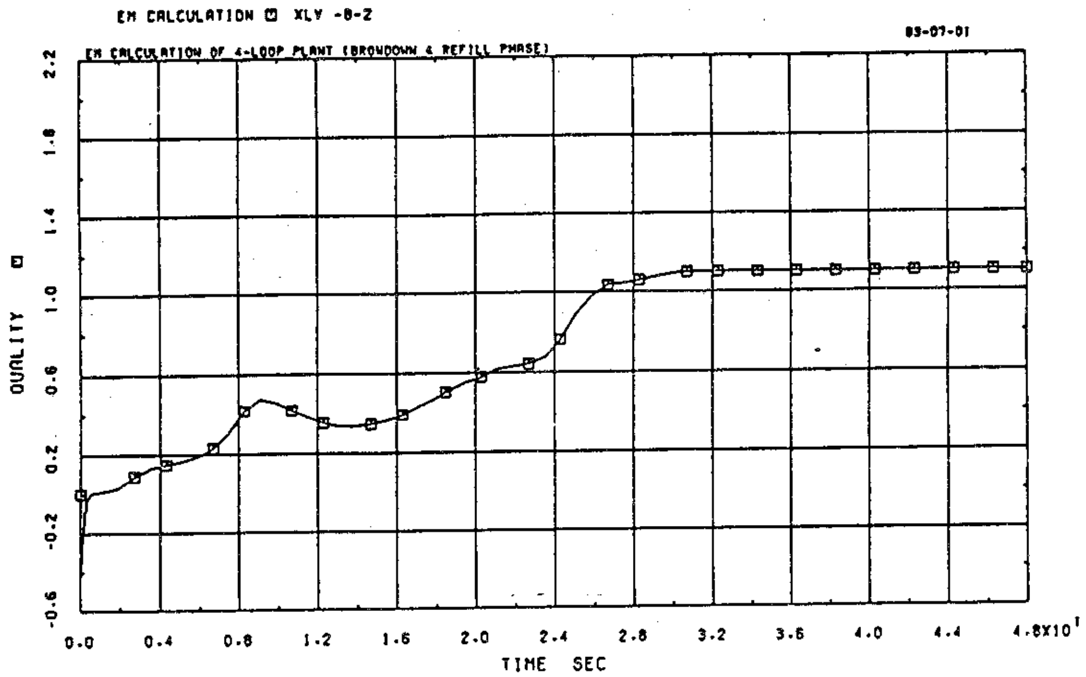

Fig. 4-21 Pump outlet quality (broken loop)

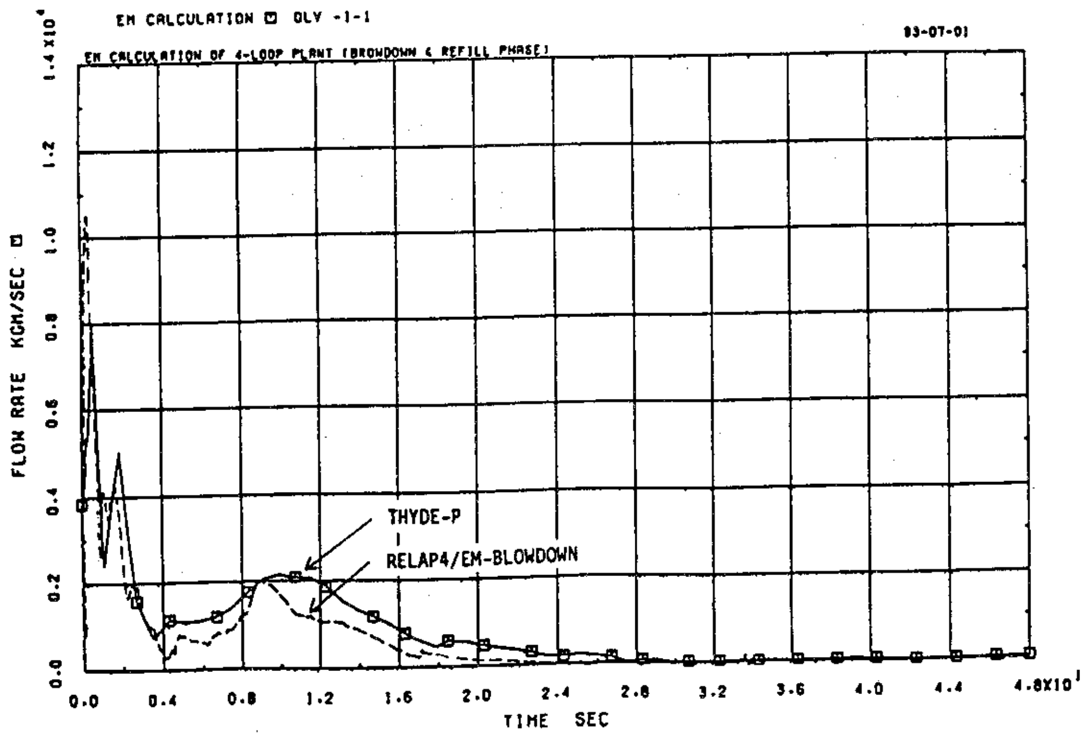

Fig. 4-22 Hot leg inlet mass flow rate (broken loop)

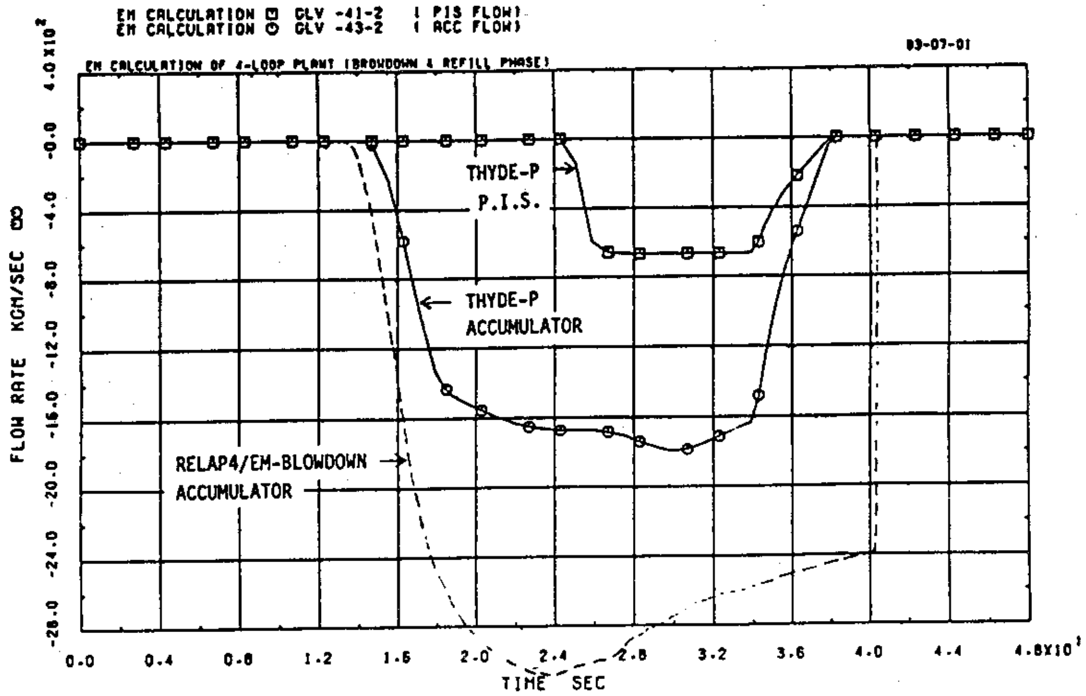

Fig. 4-23 ECC injection mass flow rate (intact loop)

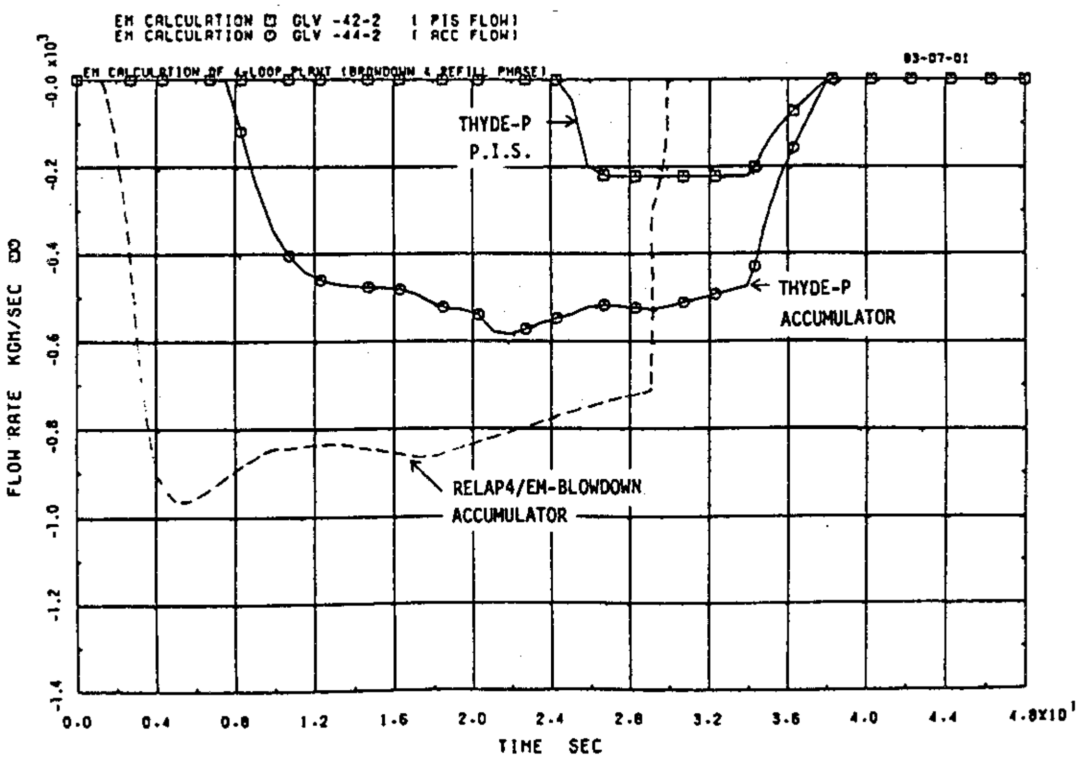

Fig. 4-24 ECC injection mass flow rate (broken loop)

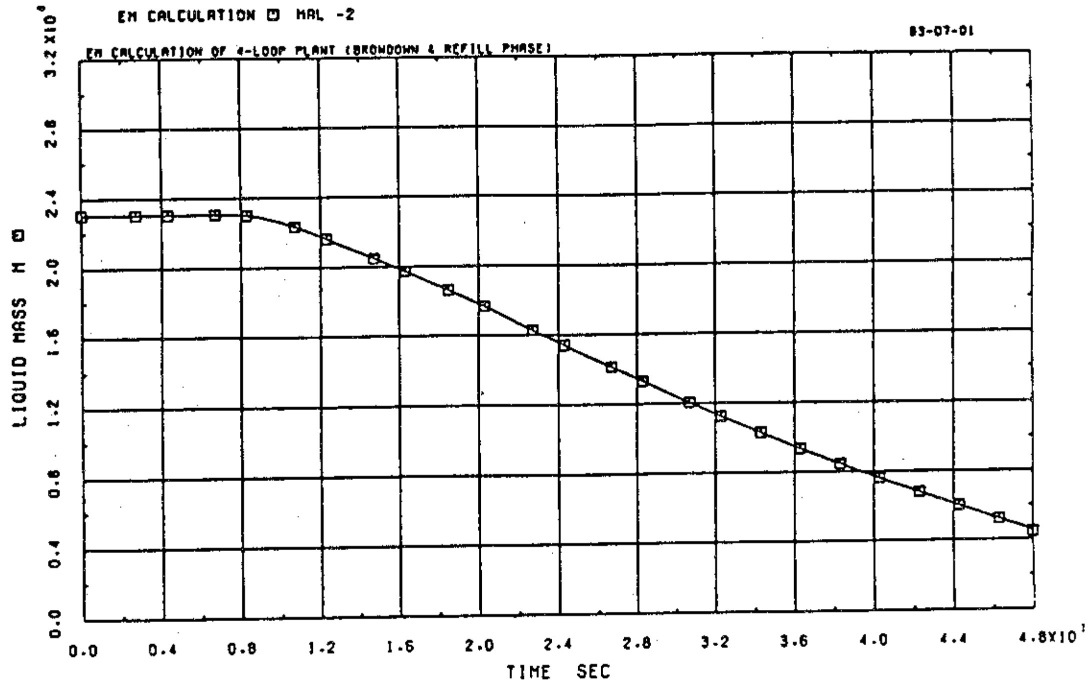

Fig. 4-25 Water mass left in ACC (intact loop)

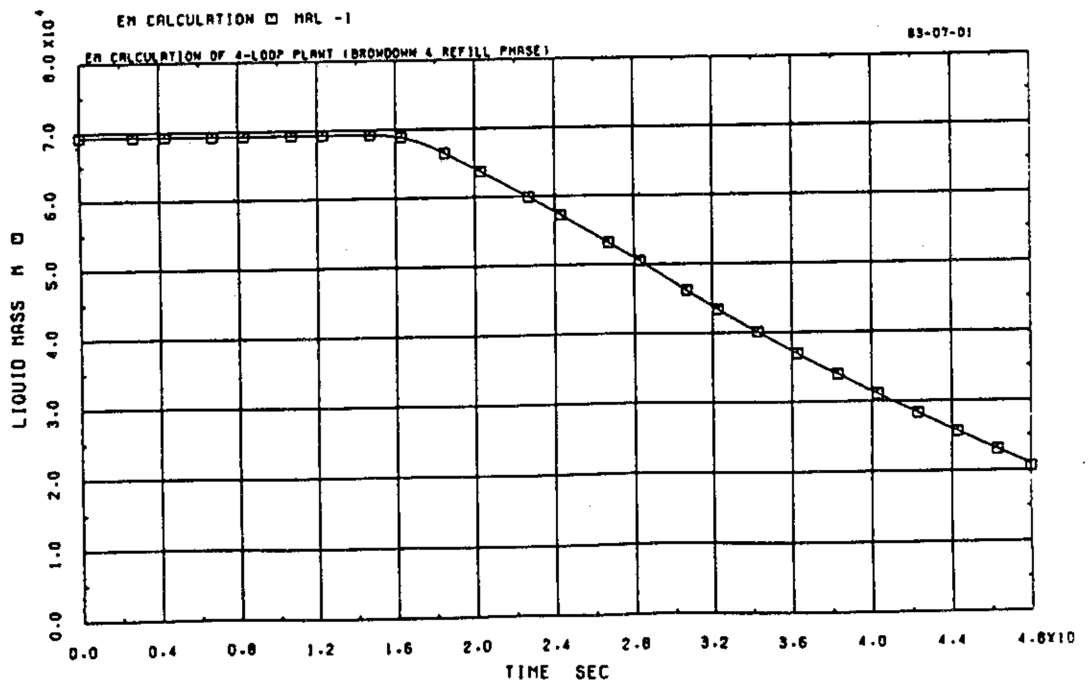

Fig. 4-26 Water mass left in ACC (broken loop)

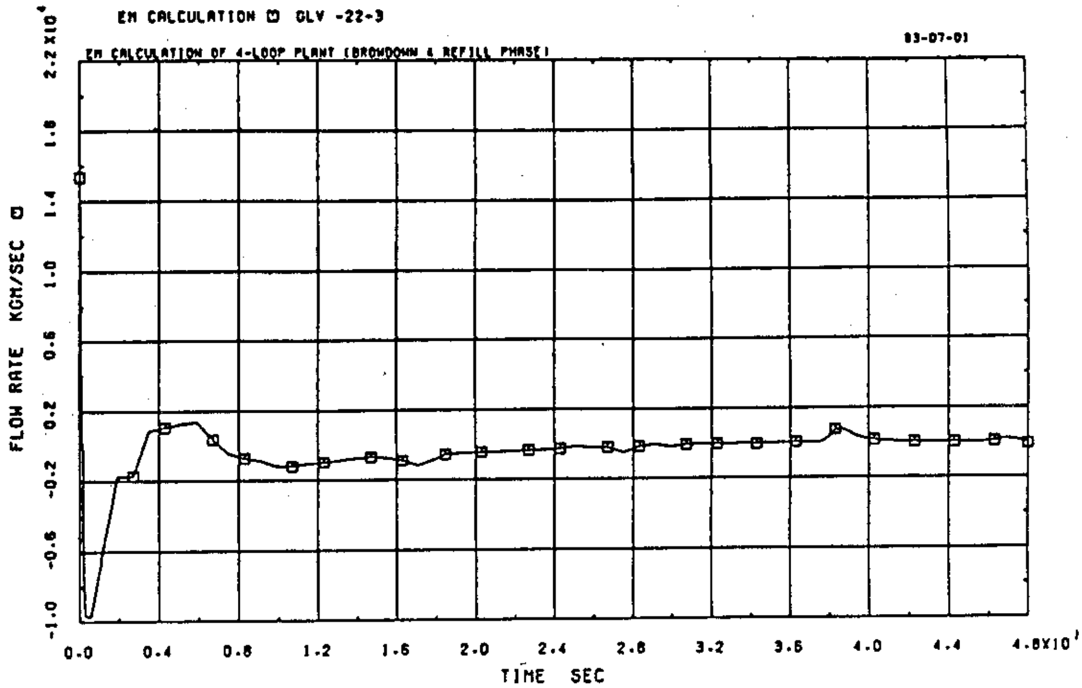

Fig. 4-27 Mass flow rate at lower plenum

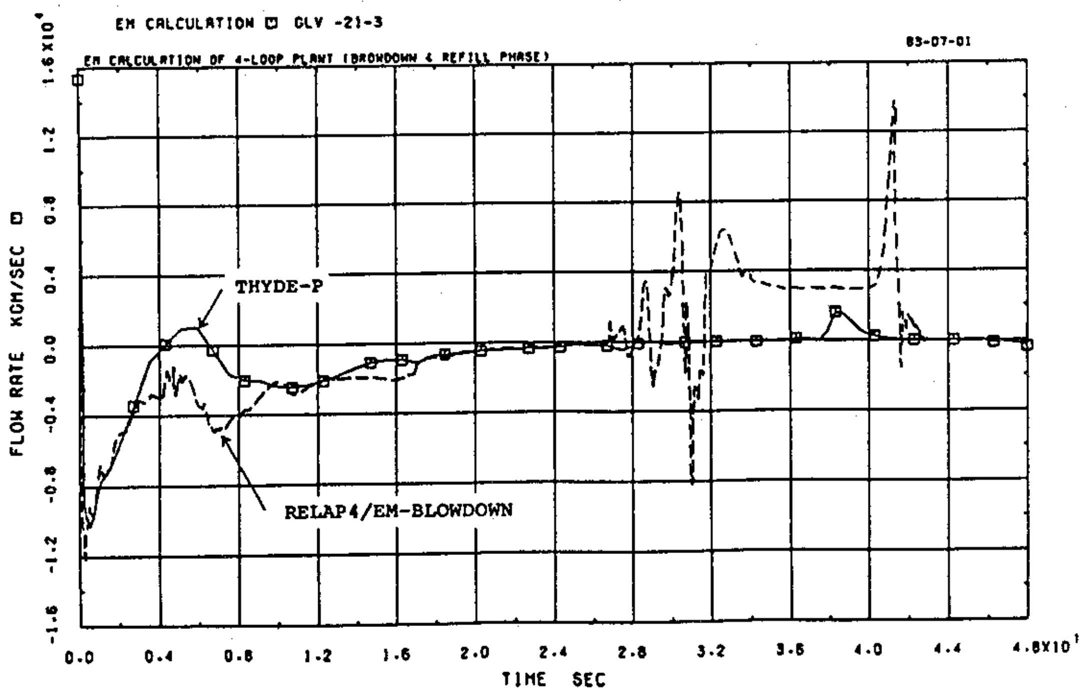

Fig. 4-28 Mass flow rate at downcomer

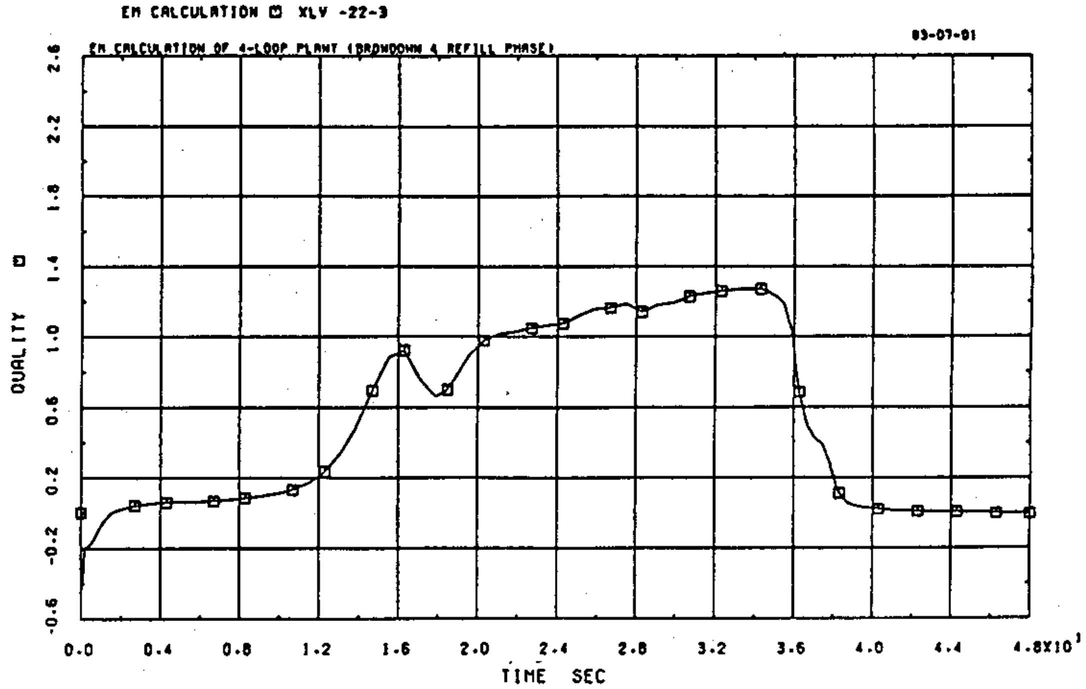

Fig. 4-29 Quality at lower plenum

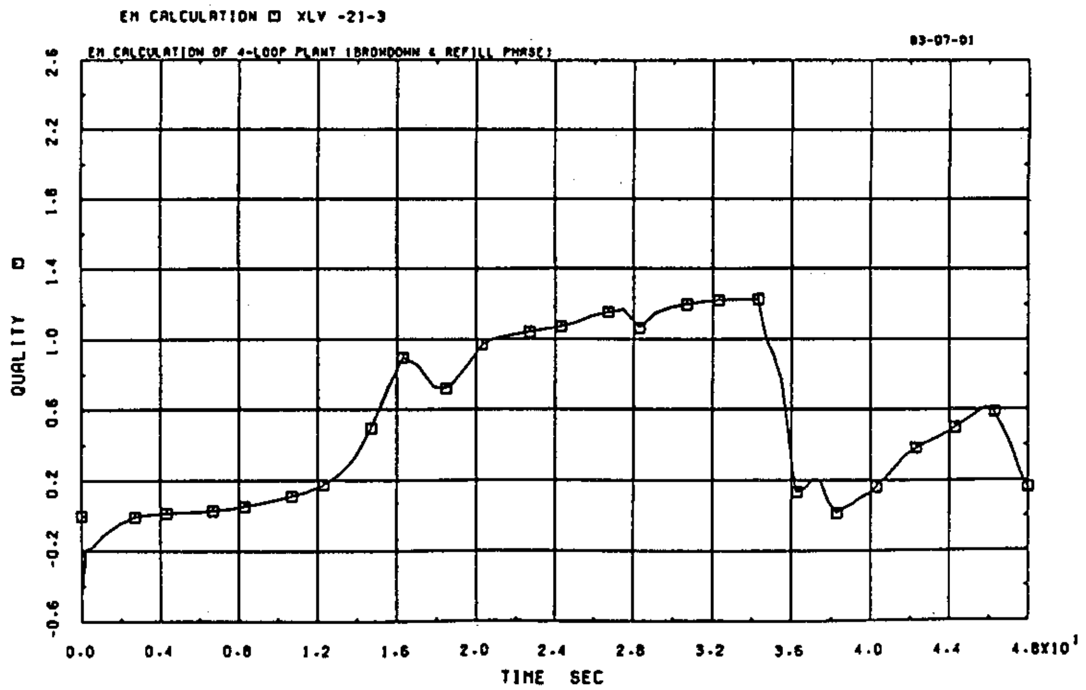

Fig. 4-30 Quality at downcomer

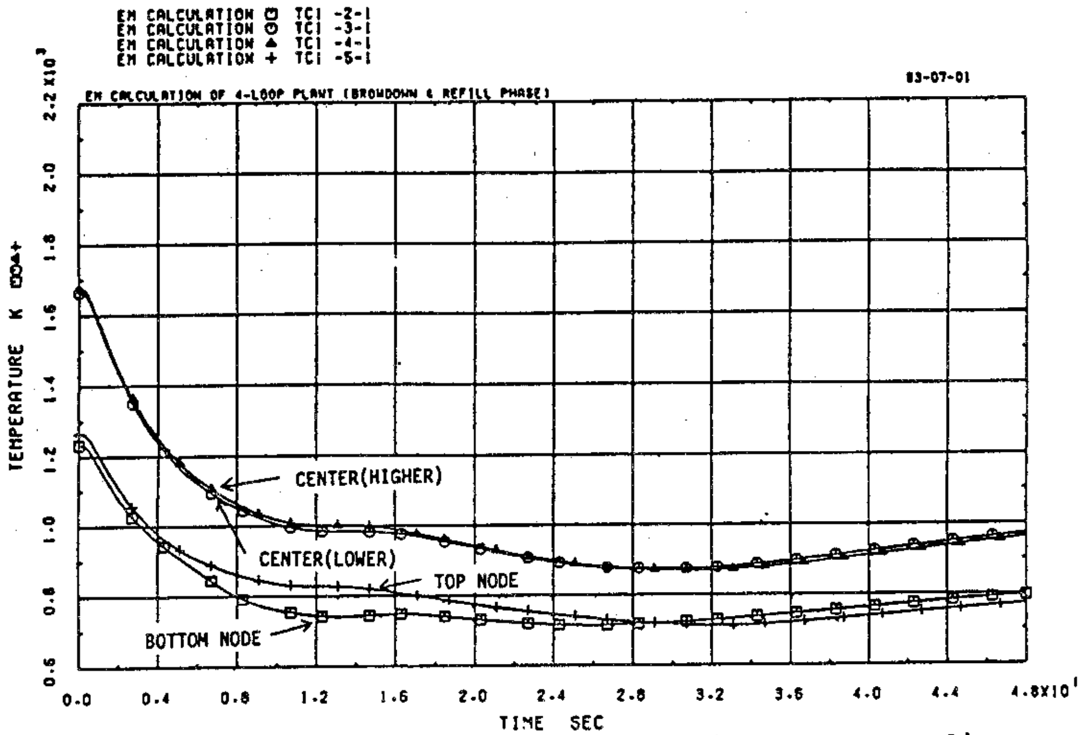

Fig. 4-31 Fuel center temperature (average channel)

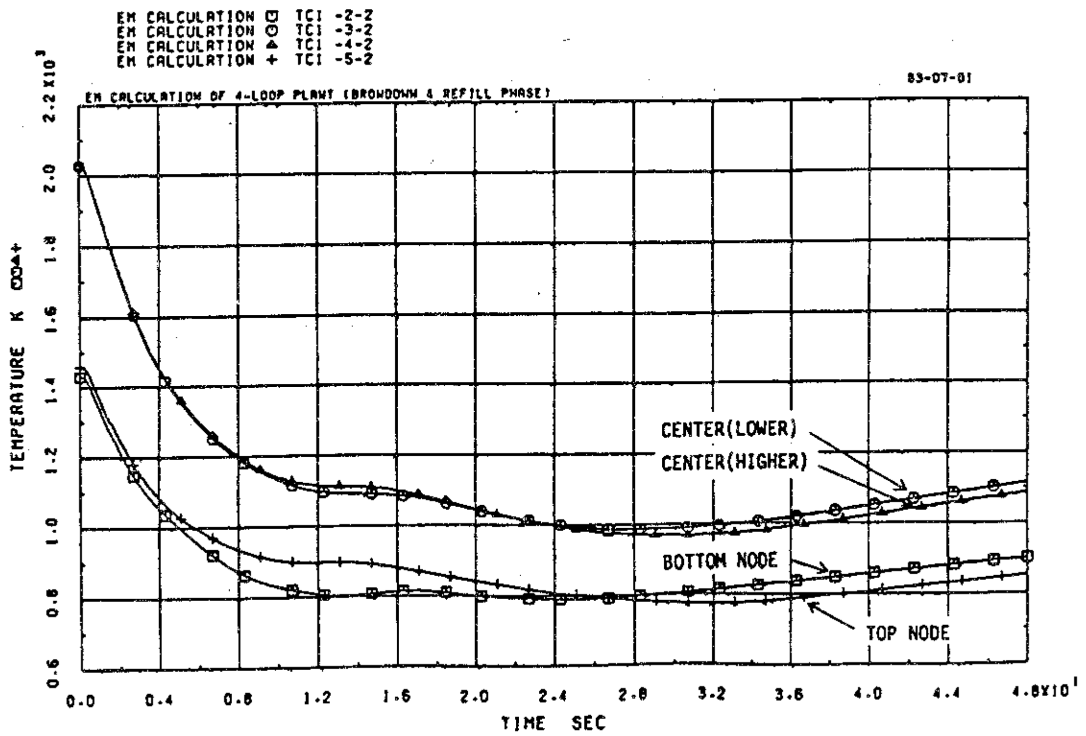

Fig. 4-32 Fuel center temperature (hot channel)

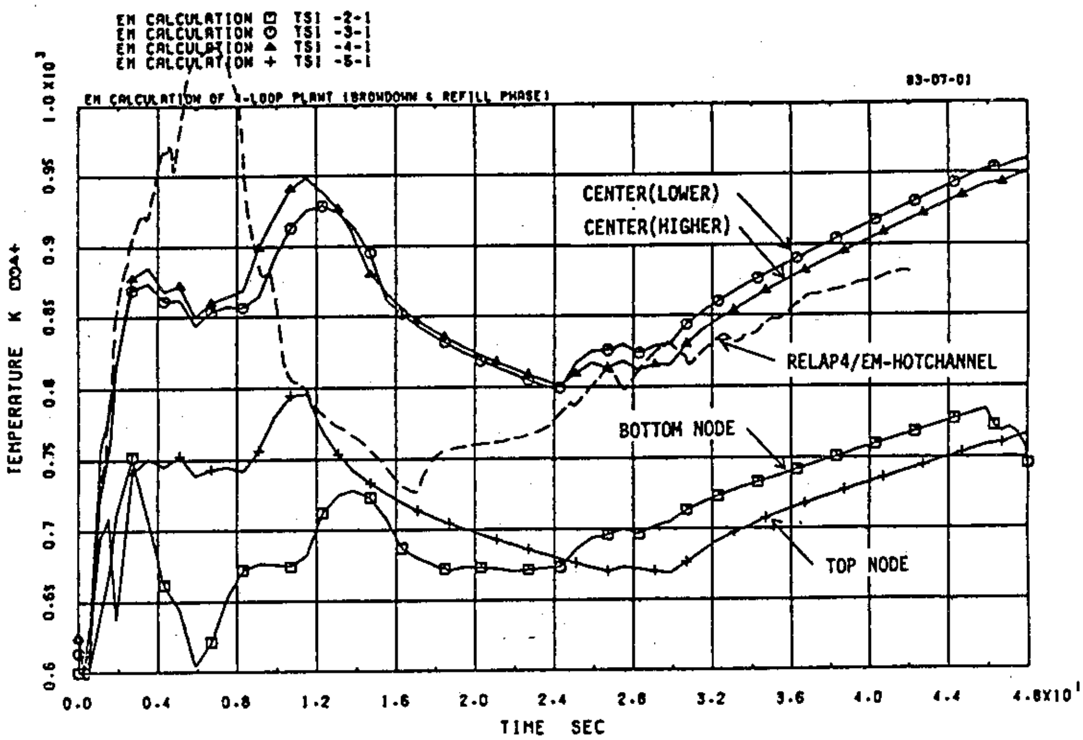

Fig. 4-33 Cladding surface temperature (average channel)

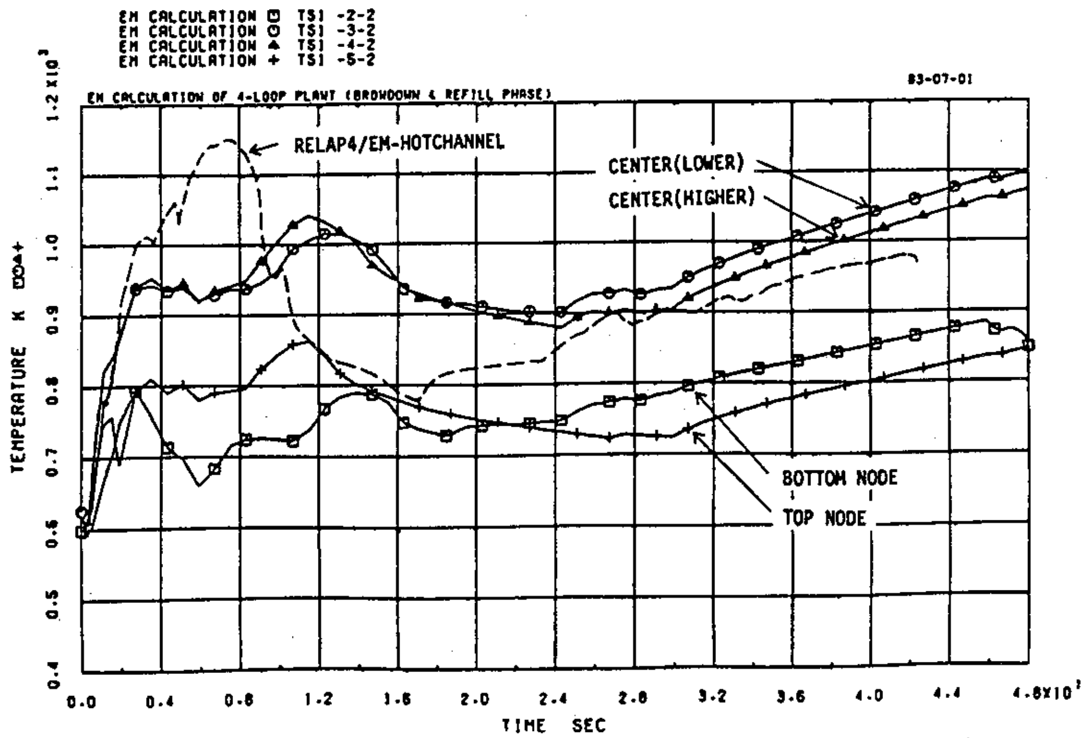

Fig. 4-34 Cladding surface temperature (hot channel)

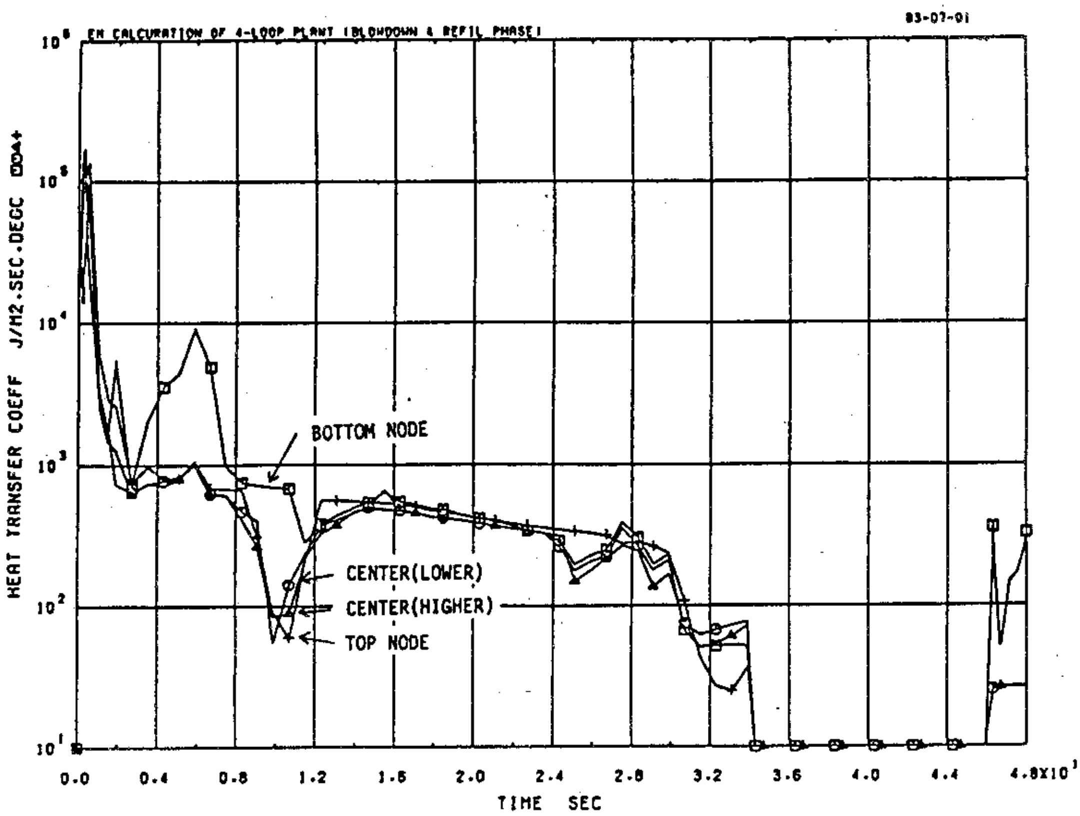

Fig. 4-35 HTC at cladding surface (average channel)

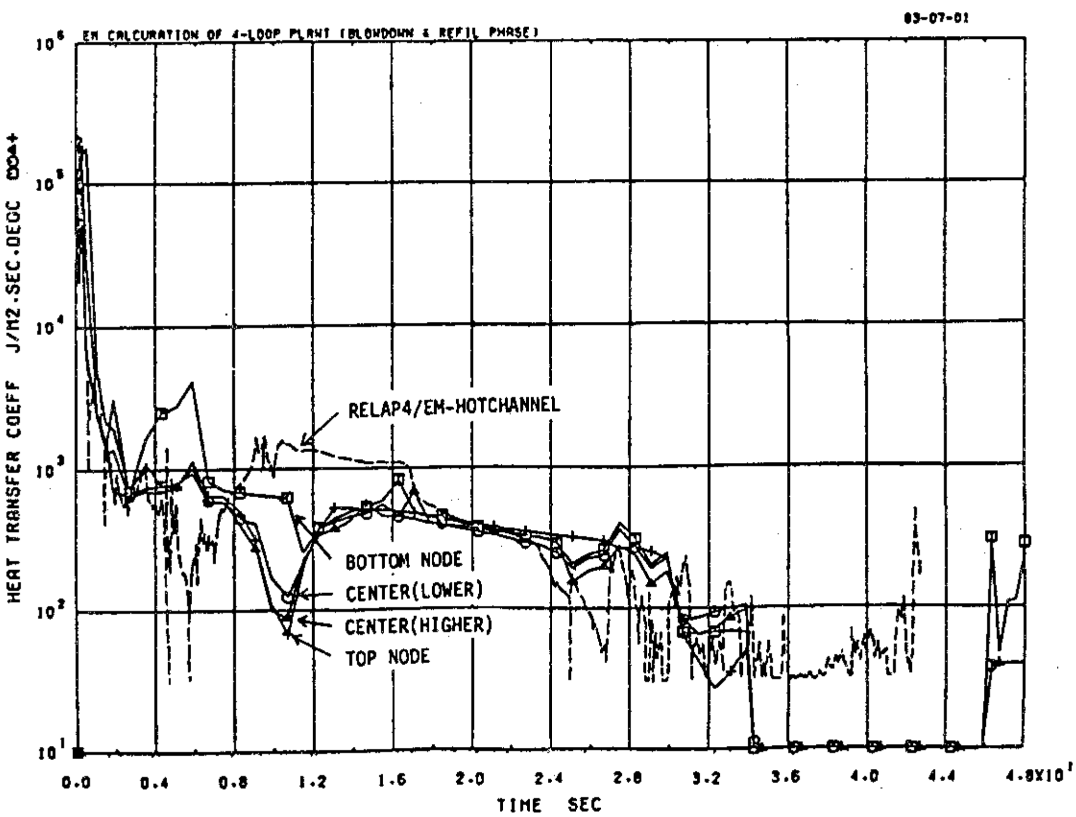

Fig. 4-36 HTC at cladding surface (hot channel)

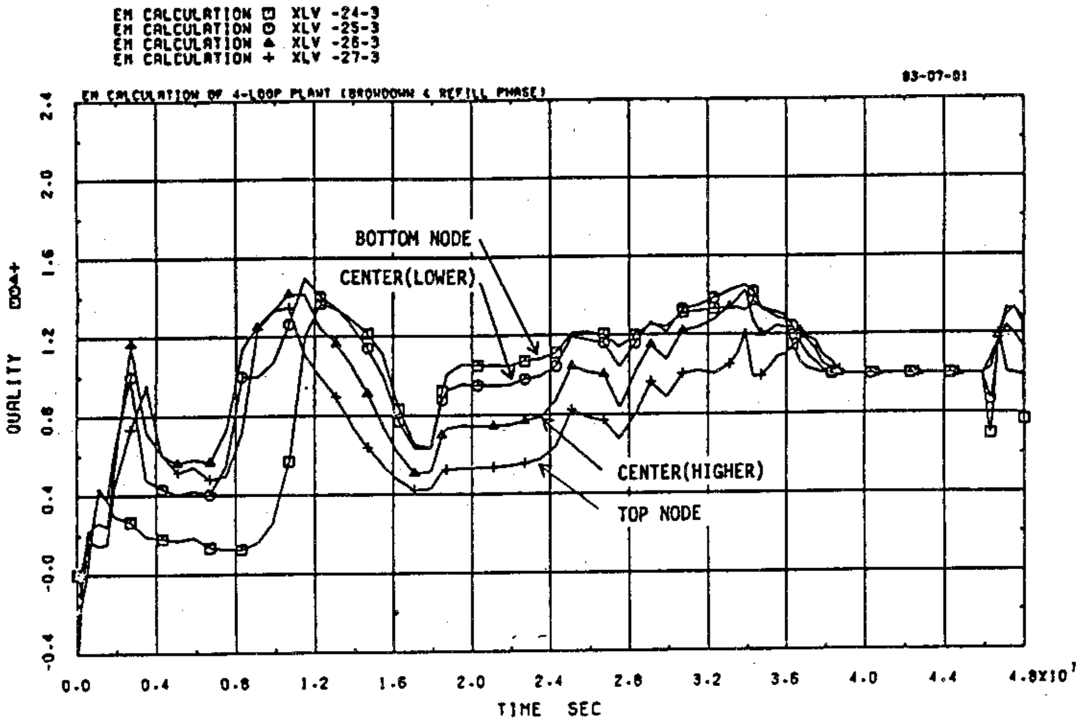

Fig. 4-37 Coolant quality in core (average channel)

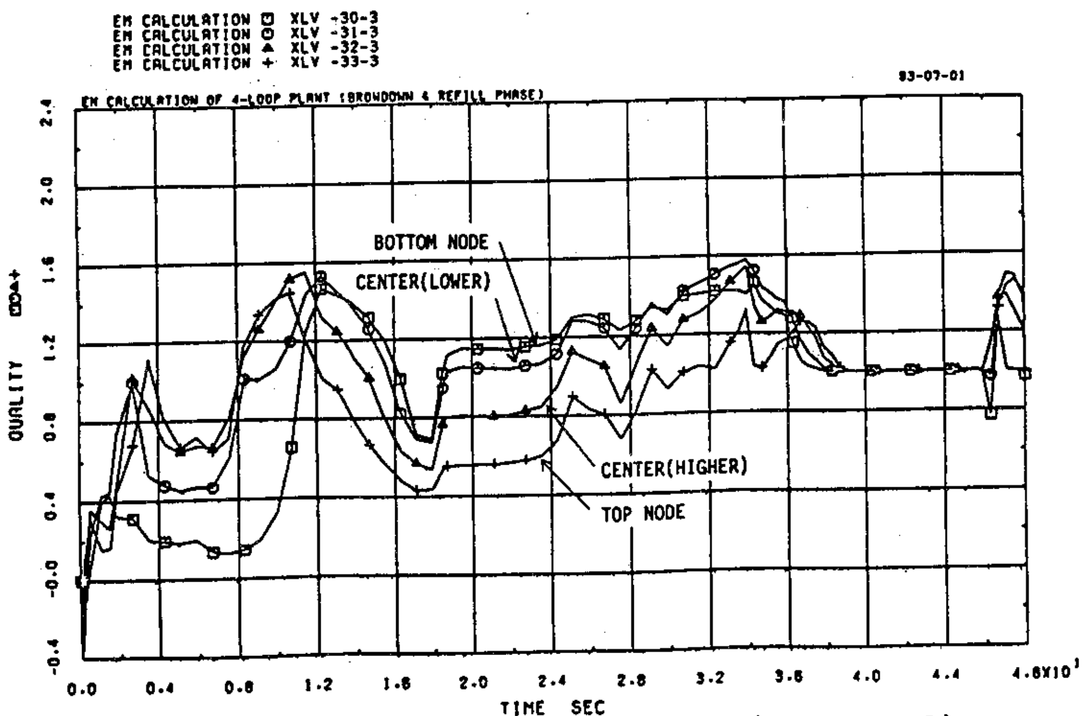

Fig. 4-38 Coolant quality in core (hot channel)

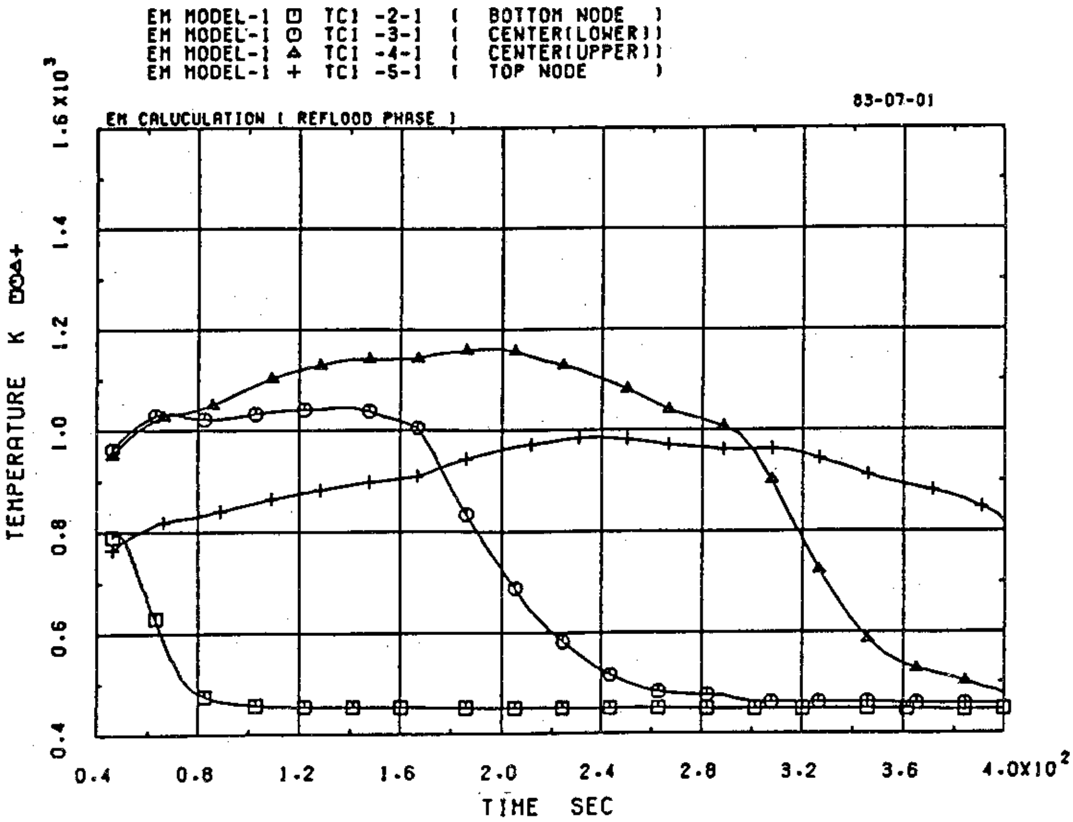

Fig. 4-39 Fuel center temperature (ave,non-burst)

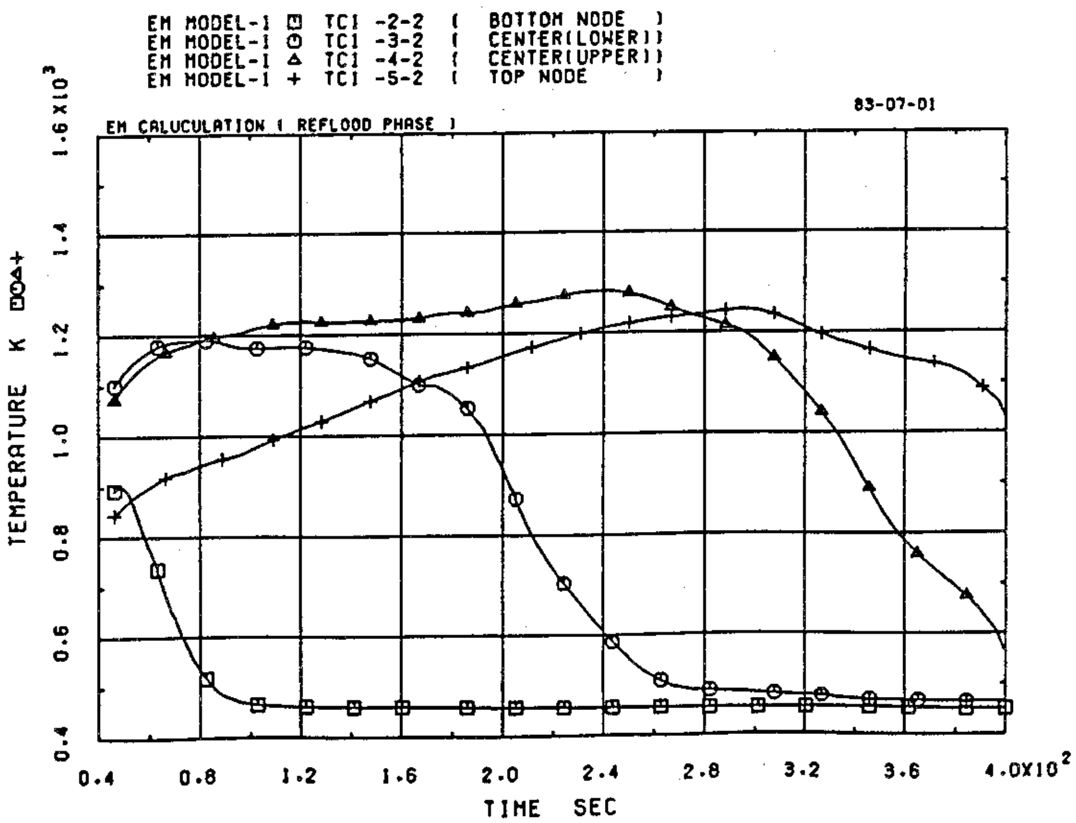

Fig. 4-40 Fuel center temperature (hot,non-burst)

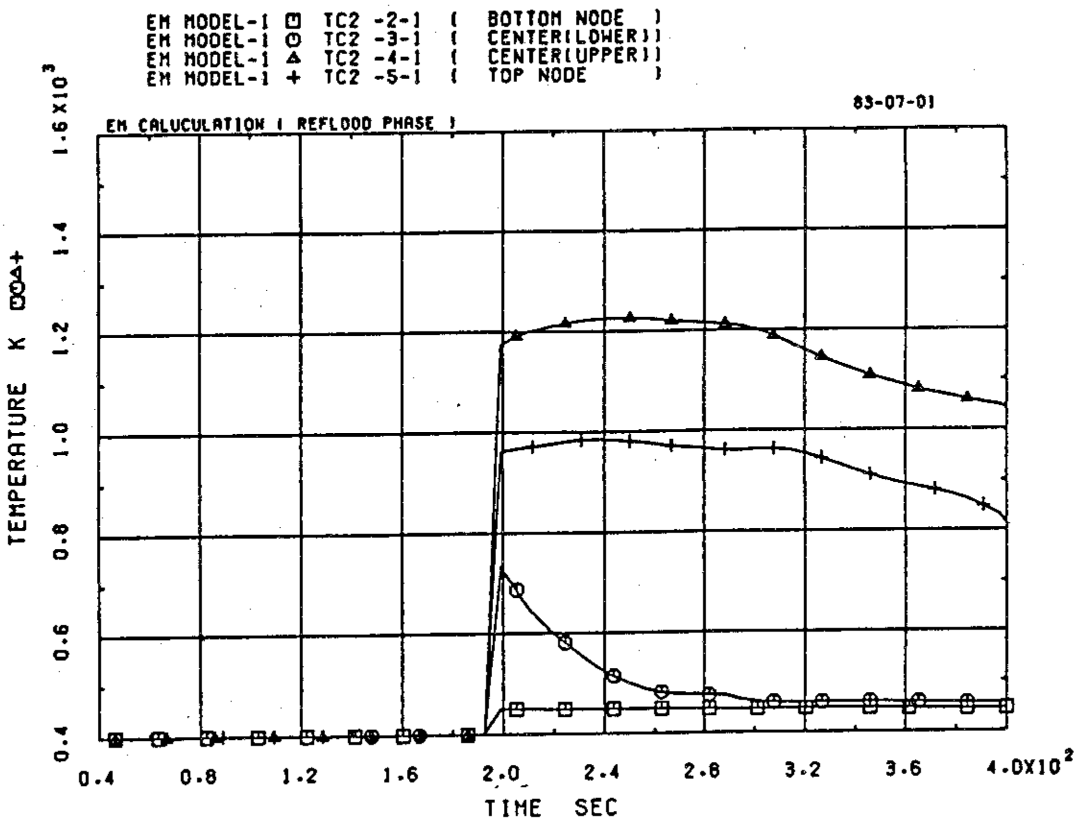

Fig. 4-41 Fuel center temperature (ave,burst)

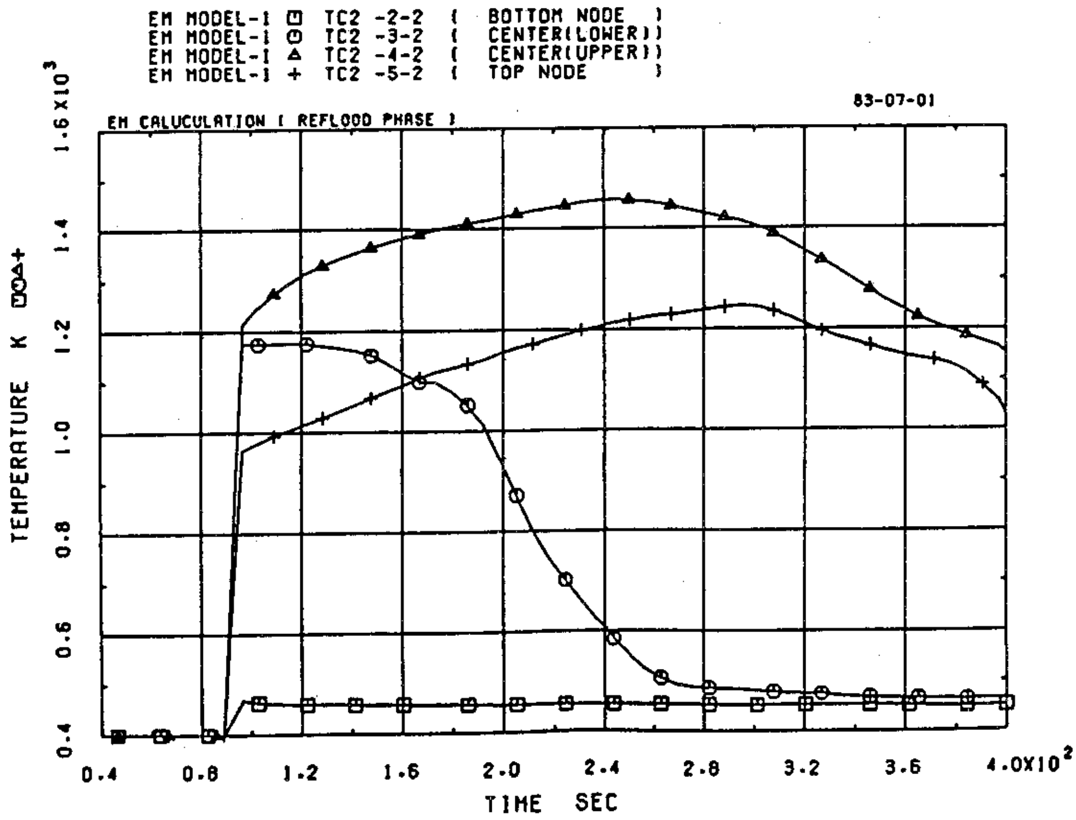

Fig. 4-42 Fuel center temperature (hot,burst)

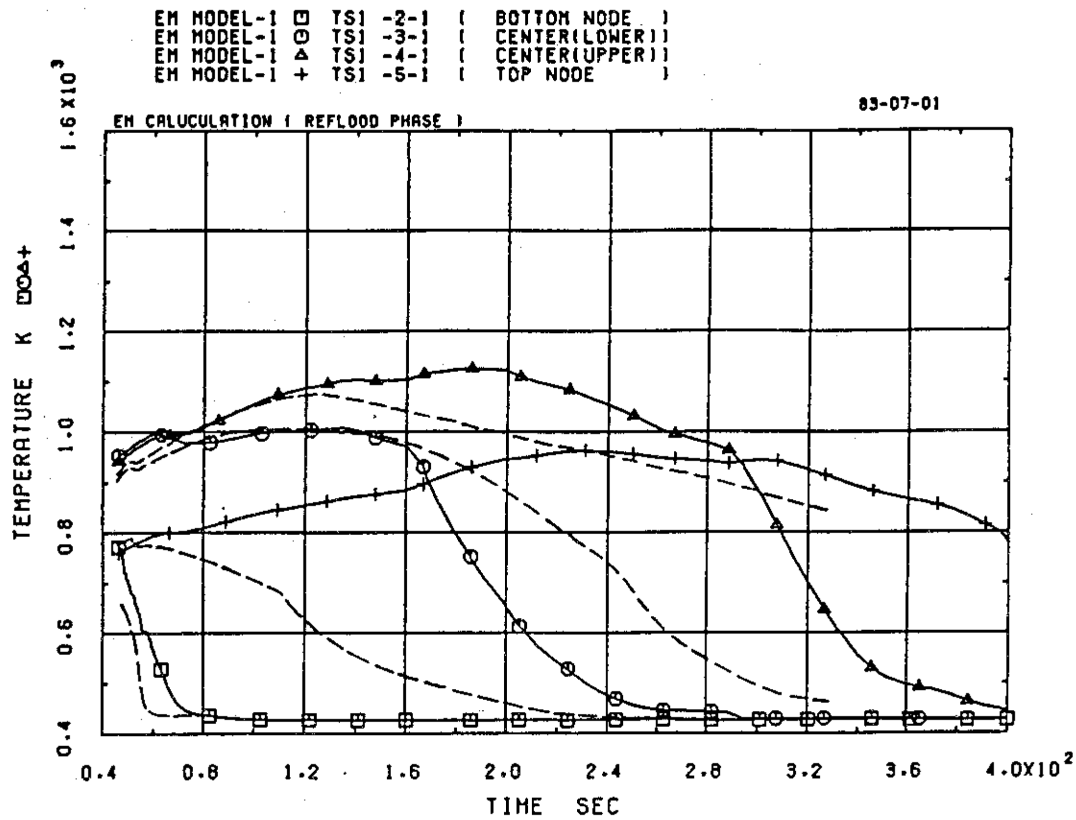

Fig. 4-43 Cladding surface temperature (ave,non-burst)

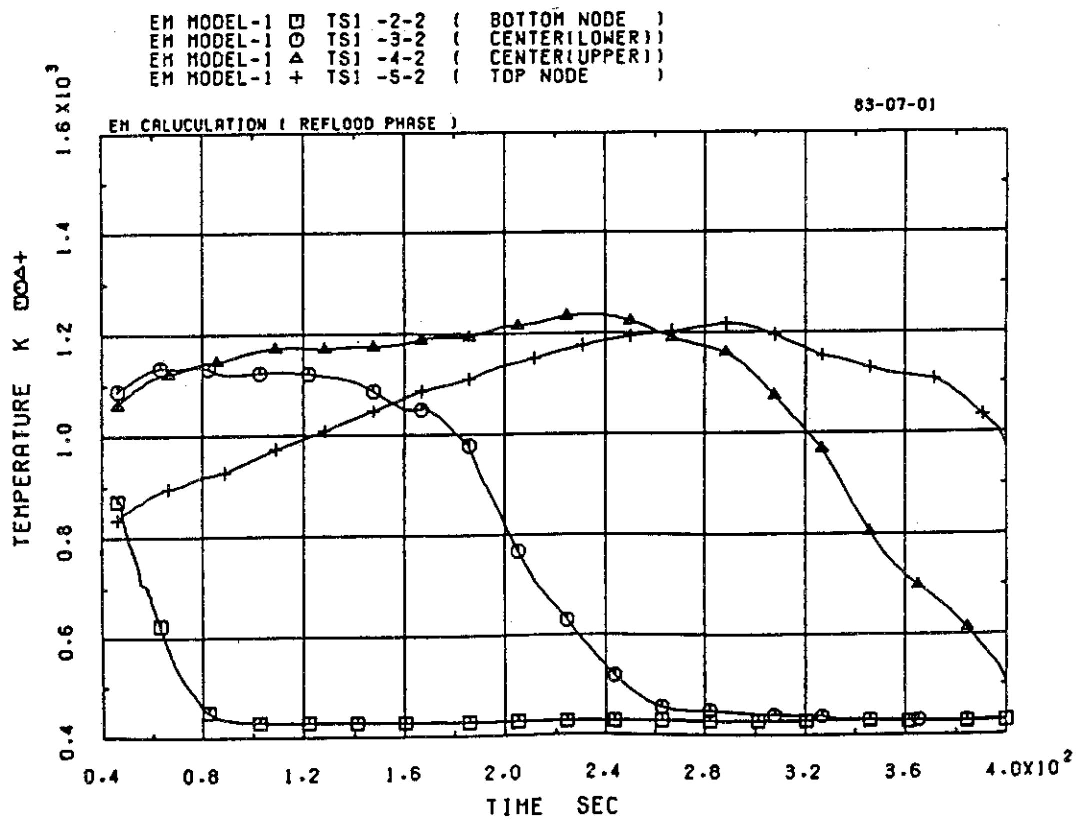

Fig. 4-44 Cladding surface temperature (hot,non-burst)

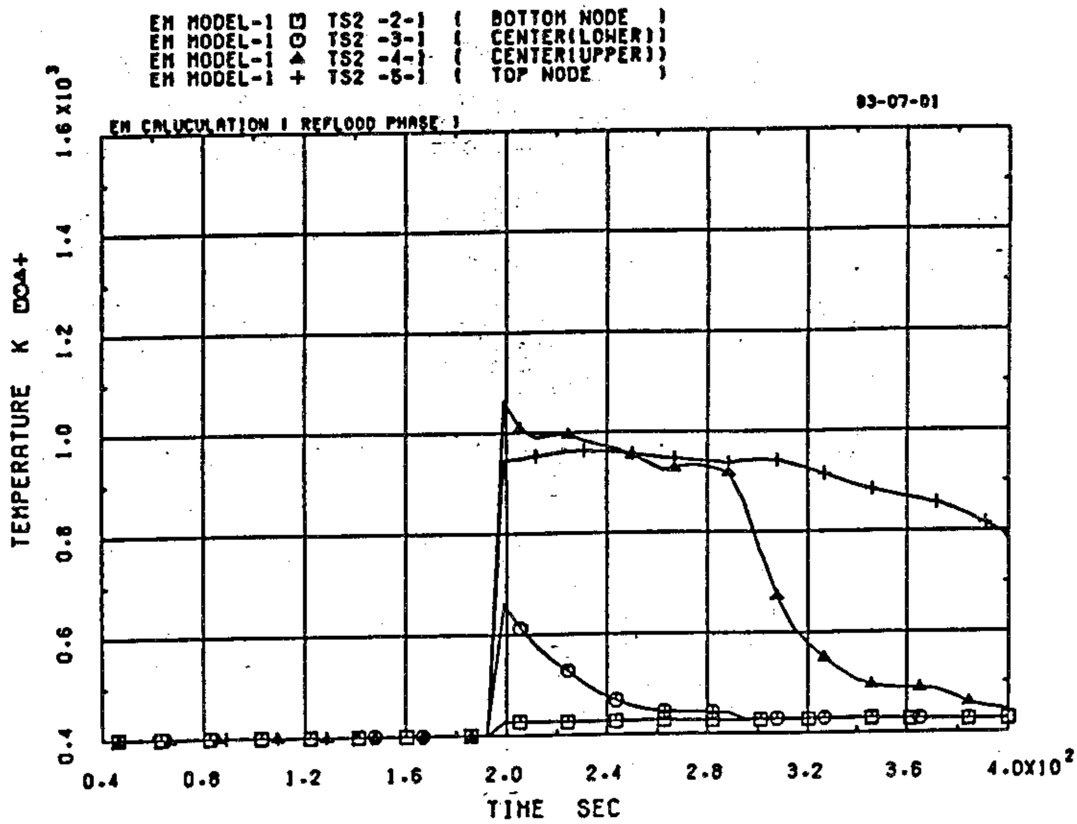

Fig. 4-45 Cladding surface temperature (ave,burst)

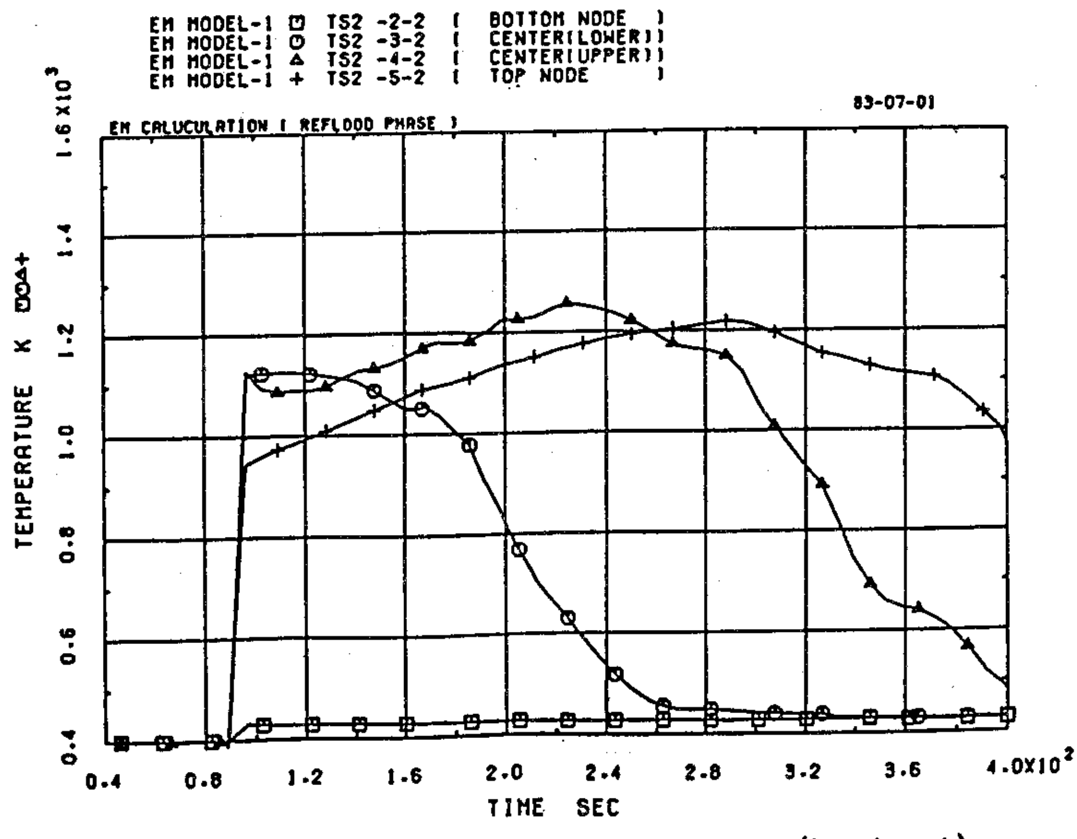

Fig. 4-46 Cladding surface temperature (hot,burst)

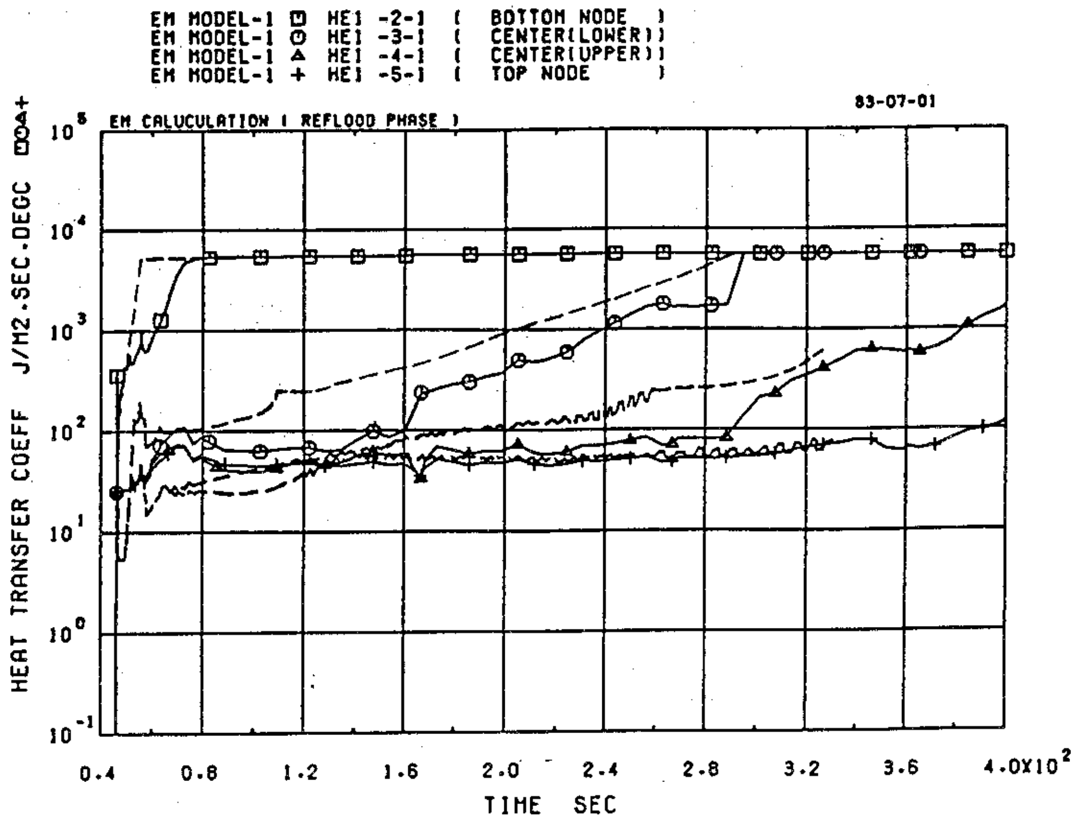

Fig. 4-47 HTC at cladding surface (ave,non-burst)

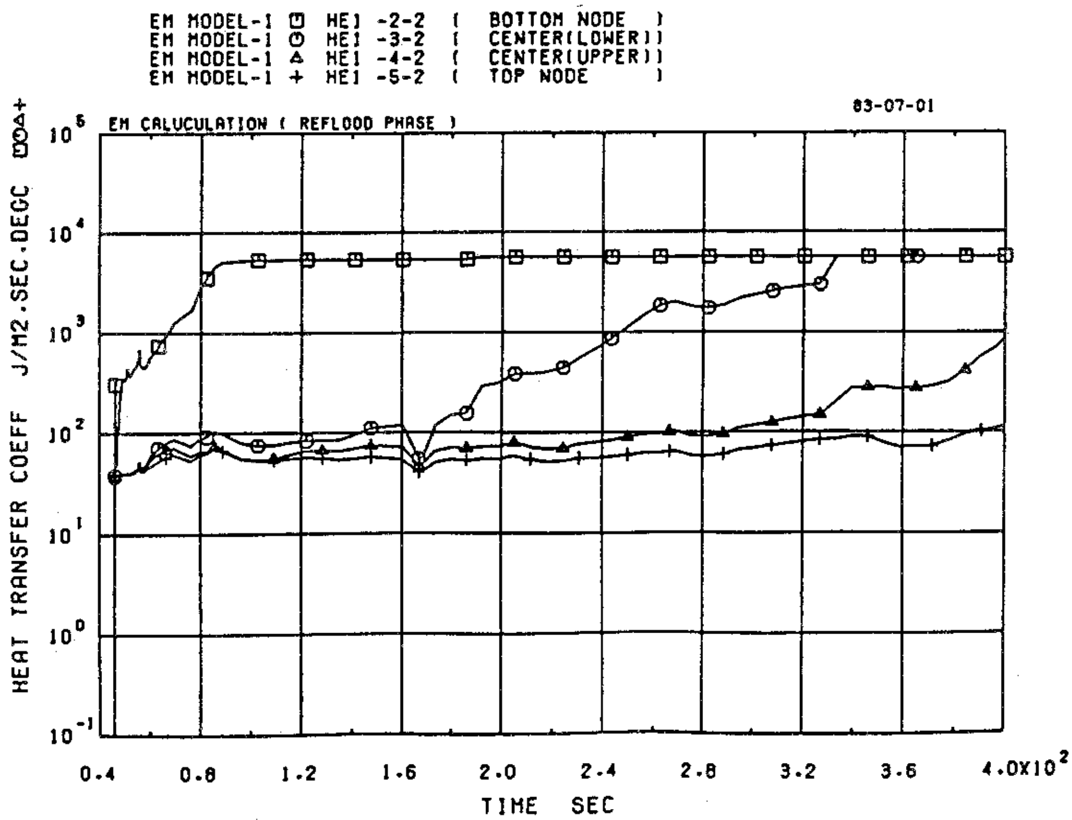

Fig. 4-48 HTC at cladding surface (hot,non-burst)

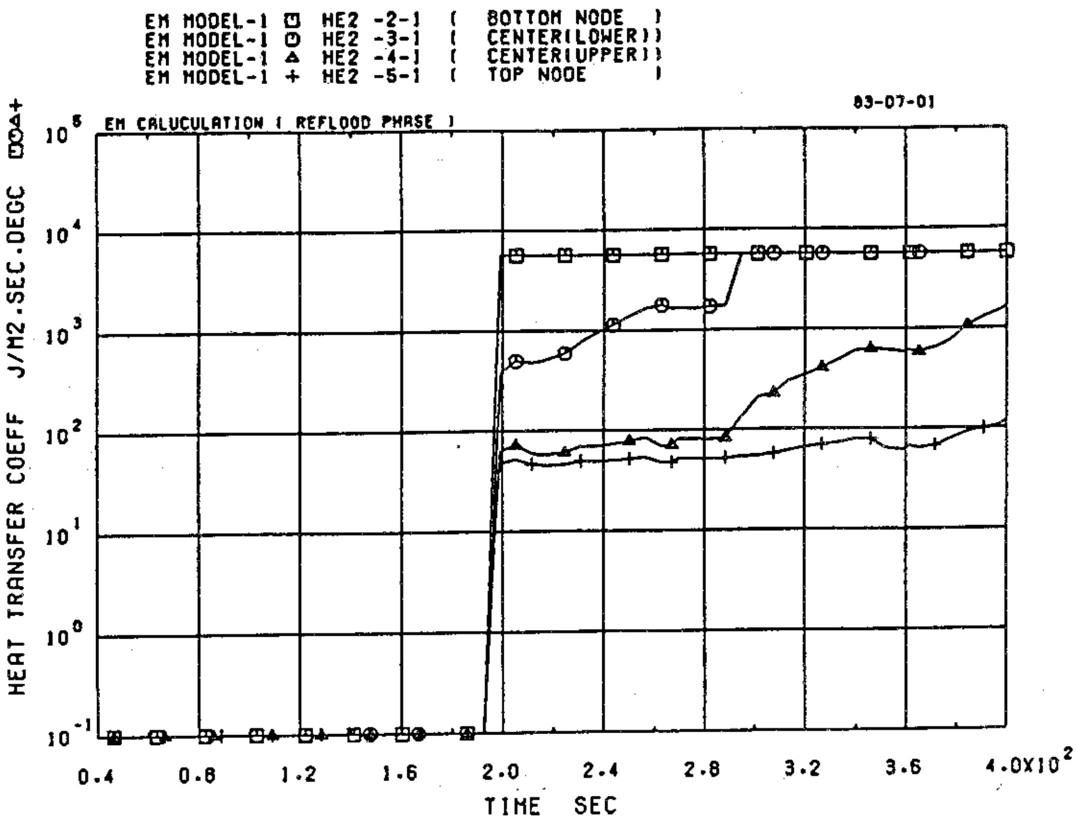

Fig. 4-49 HTC at cladding surface (ave,burst)

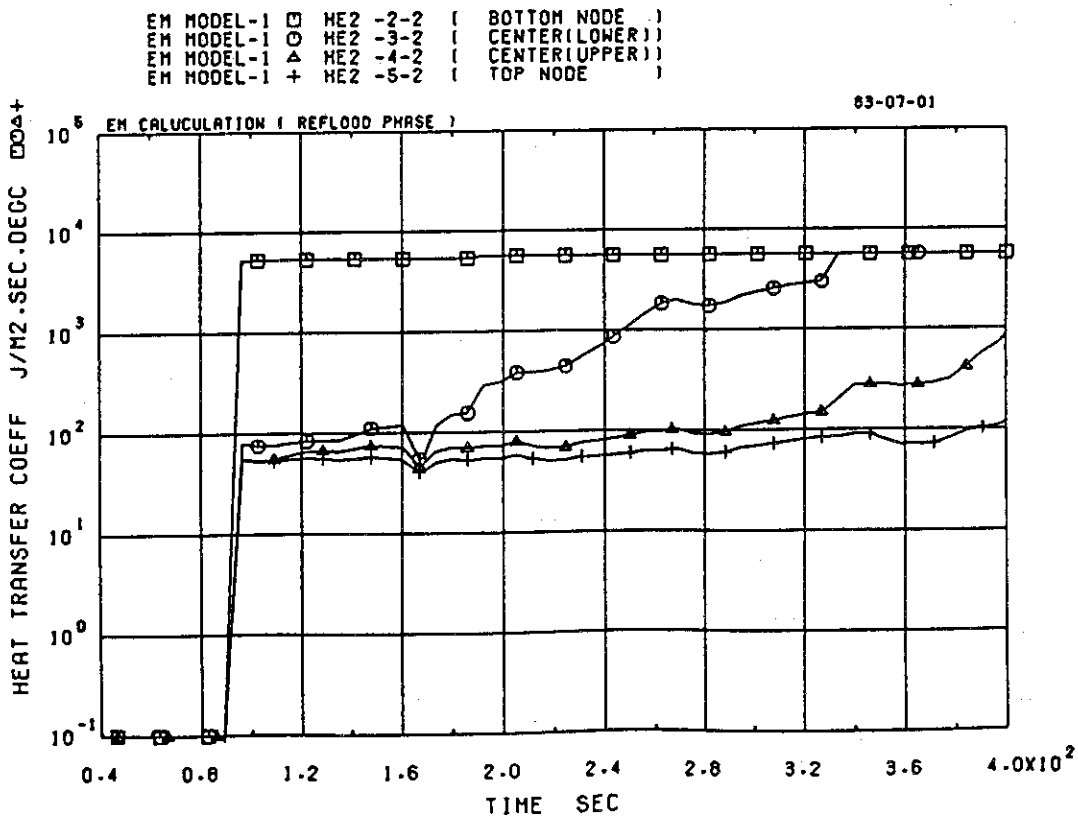

Fig. 4-50 HTC at cladding surface (hot,burst)

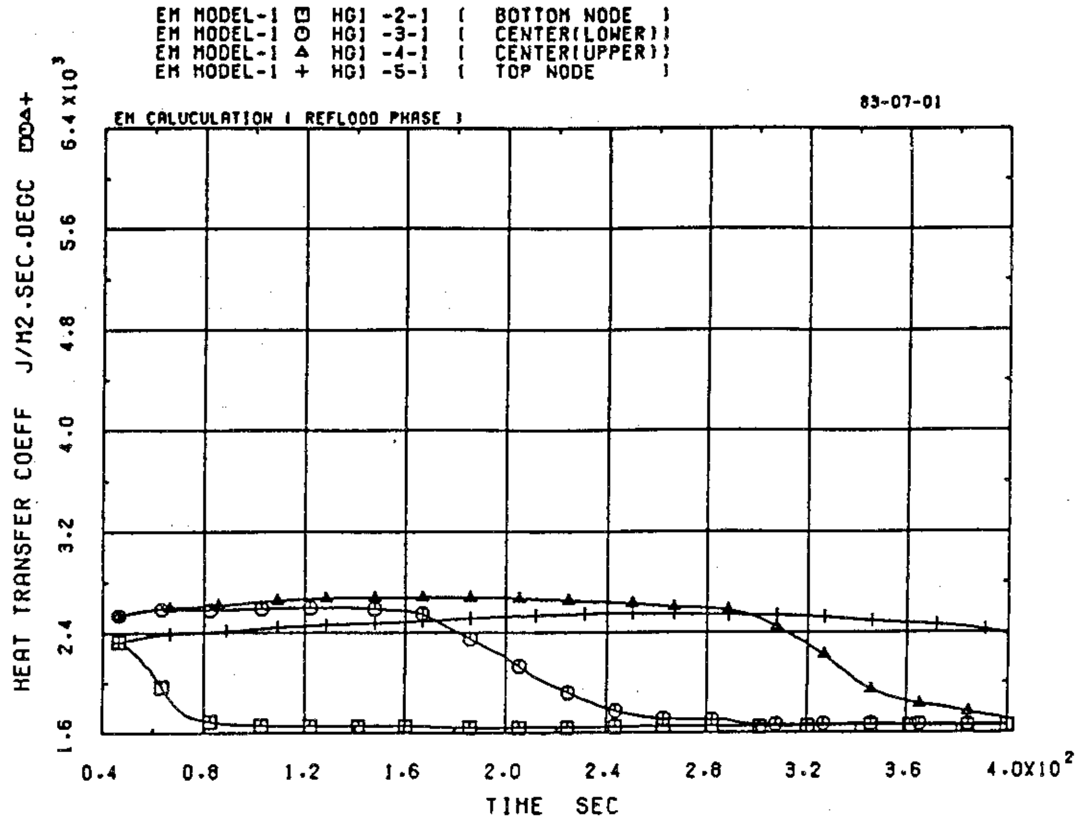

Fig. 4-51 Gap conductance (ave,non-burst)

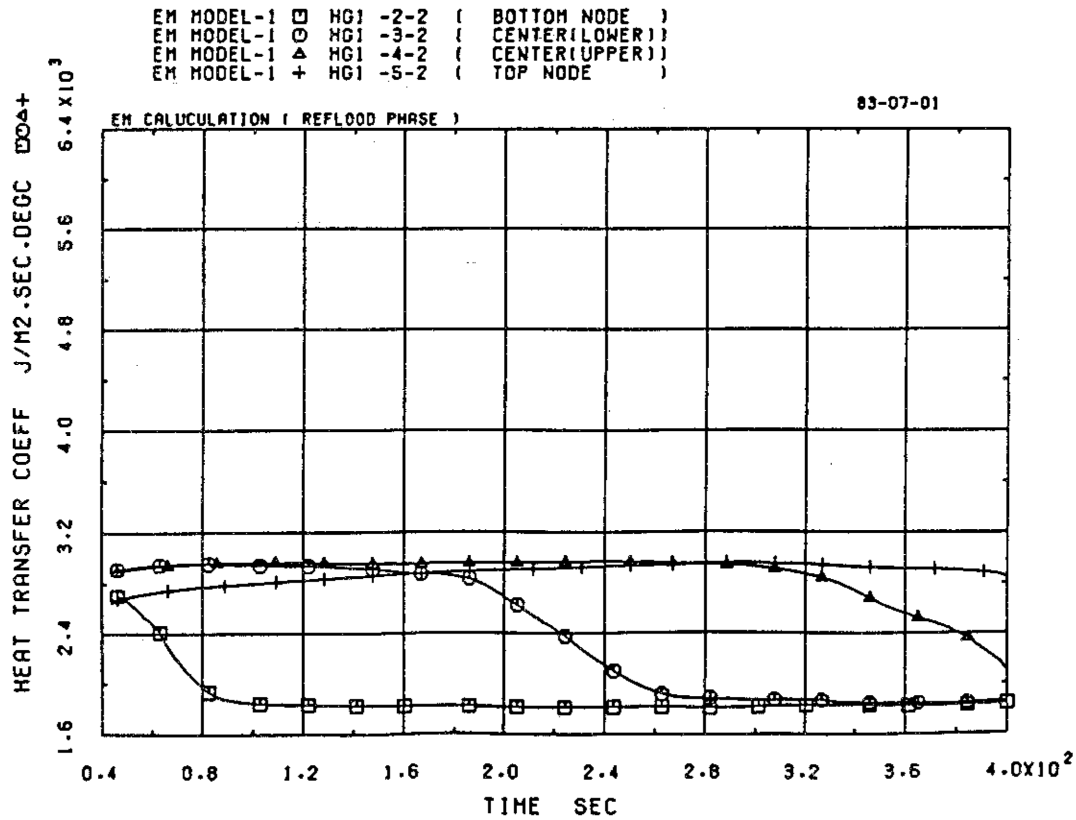

Fig. 4-52 Gap conductance (hot,non-burst)

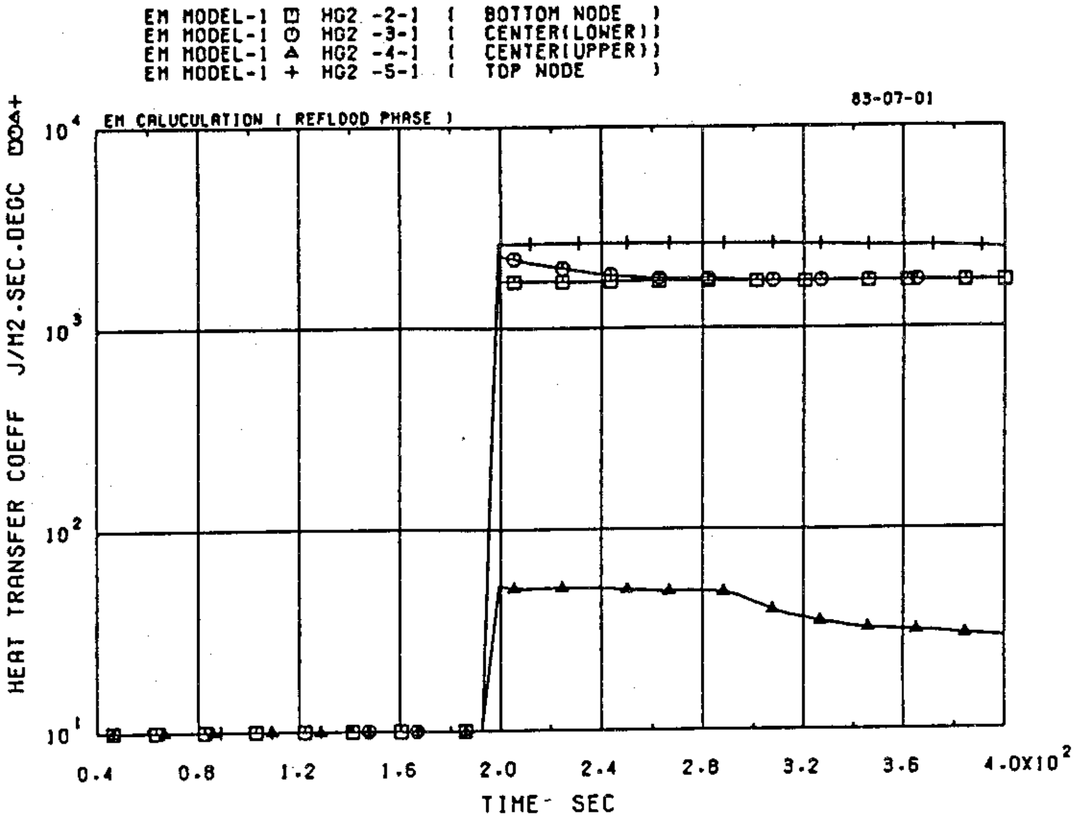

Fig. 4-53 Gap conductance (ave,burst)

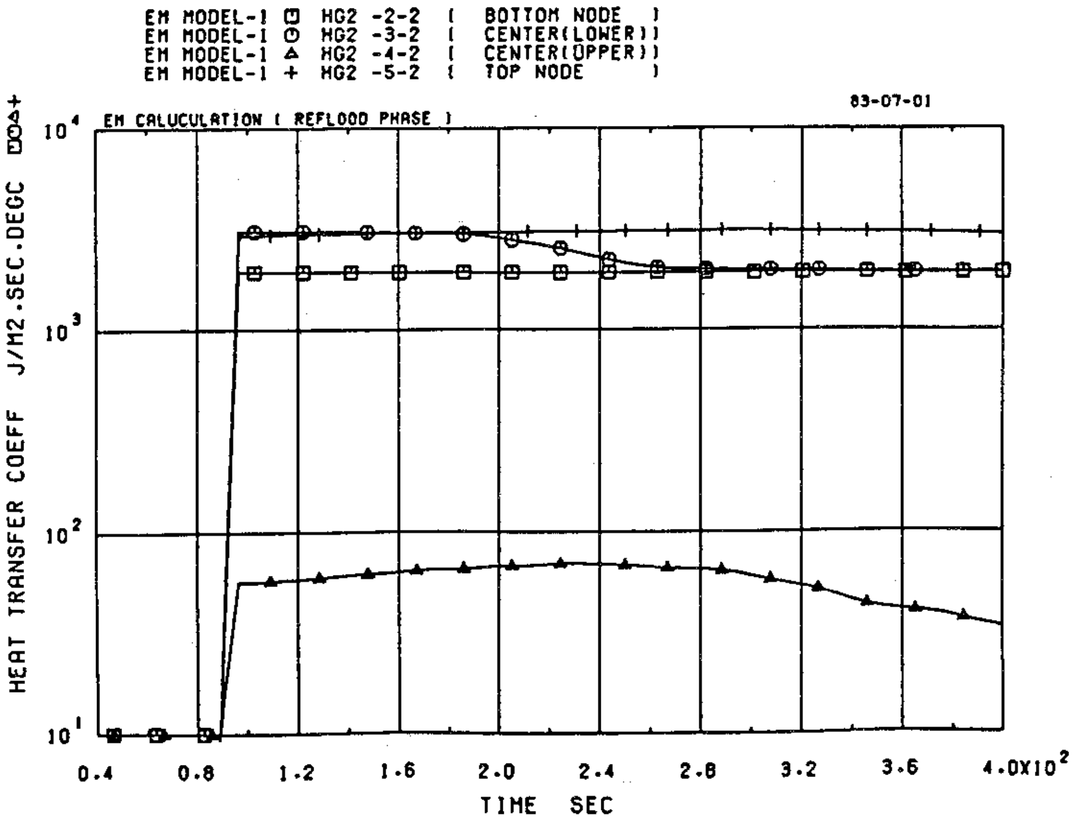

Fig. 4-54 Gap conductance (hot,burst)

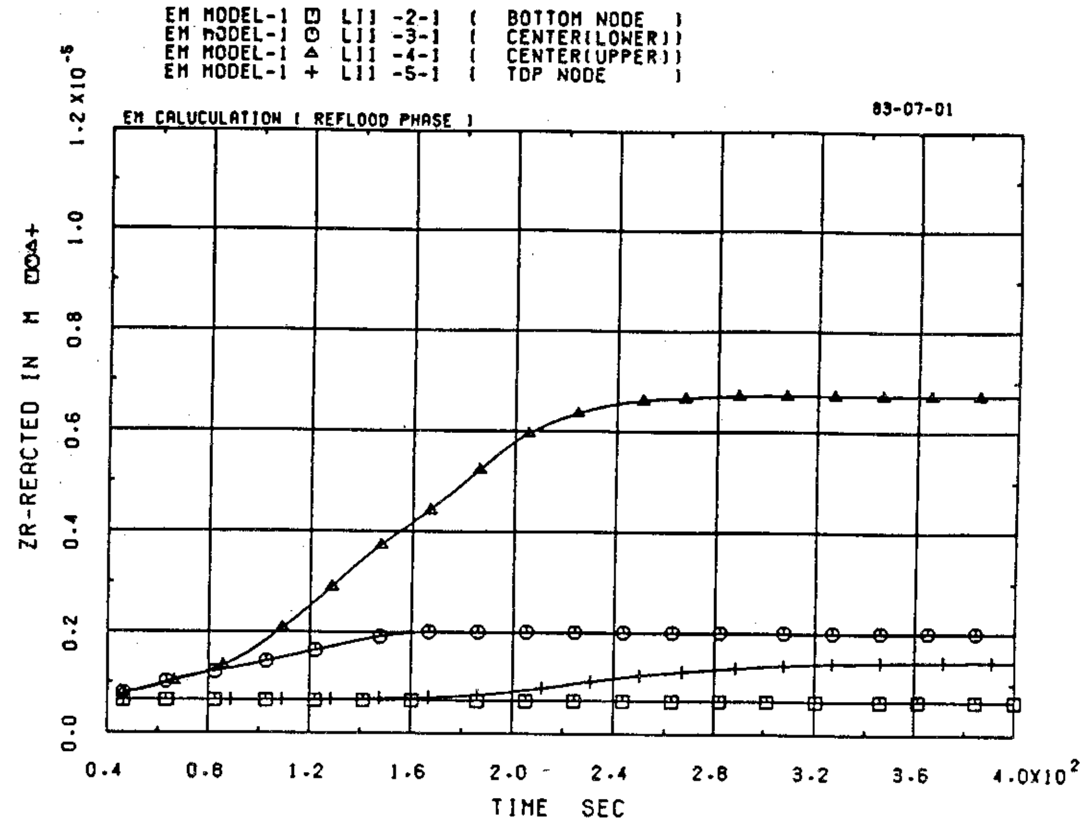

Fig. 4-55 Oxide thickness (ave,non-burst,outer)

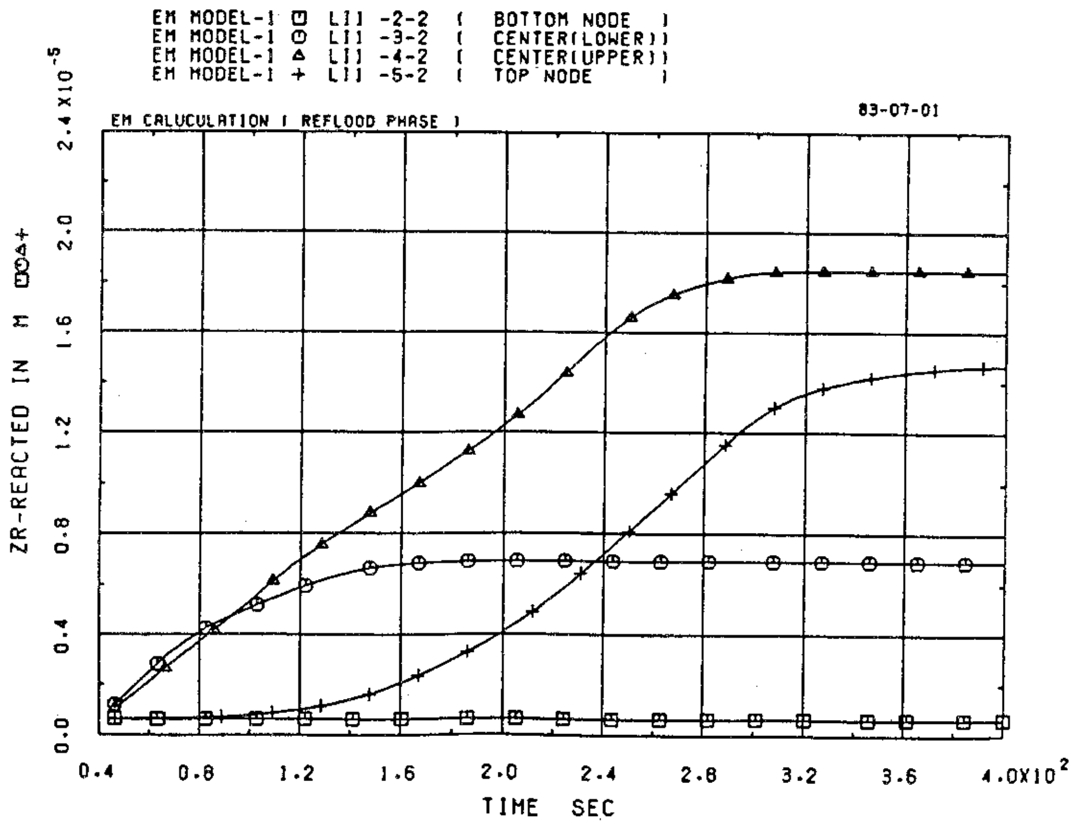

Fig. 4-56 Oxide thickness (hot,non-burst,outer)

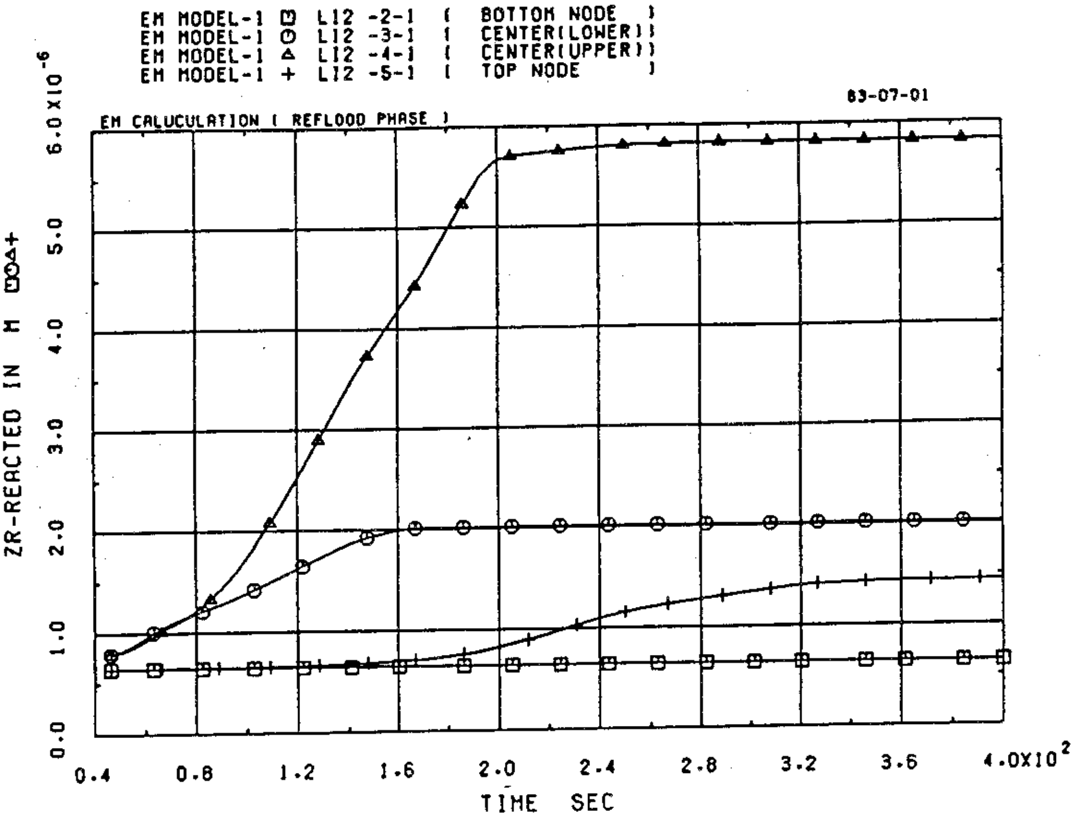

Fig. 4-57 Oxide thickness (ave,burst,outer)

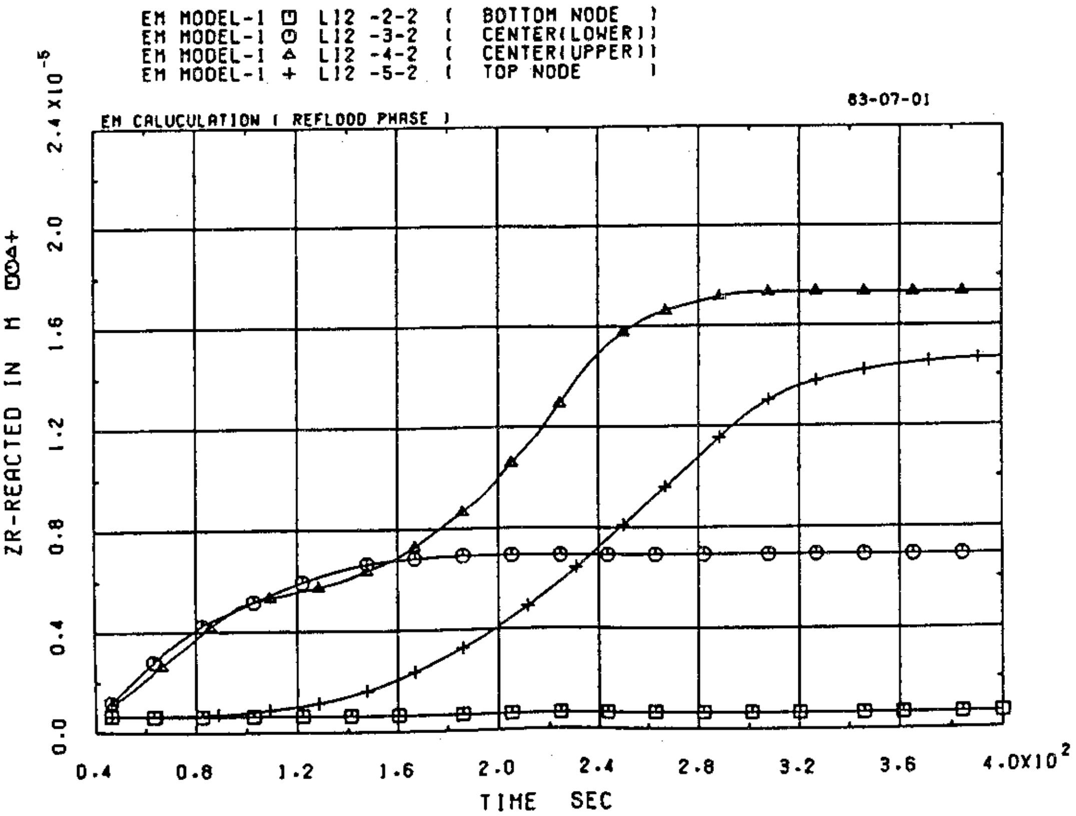

Fig. 4-58 Oxide thickness (hot,burst,outer)

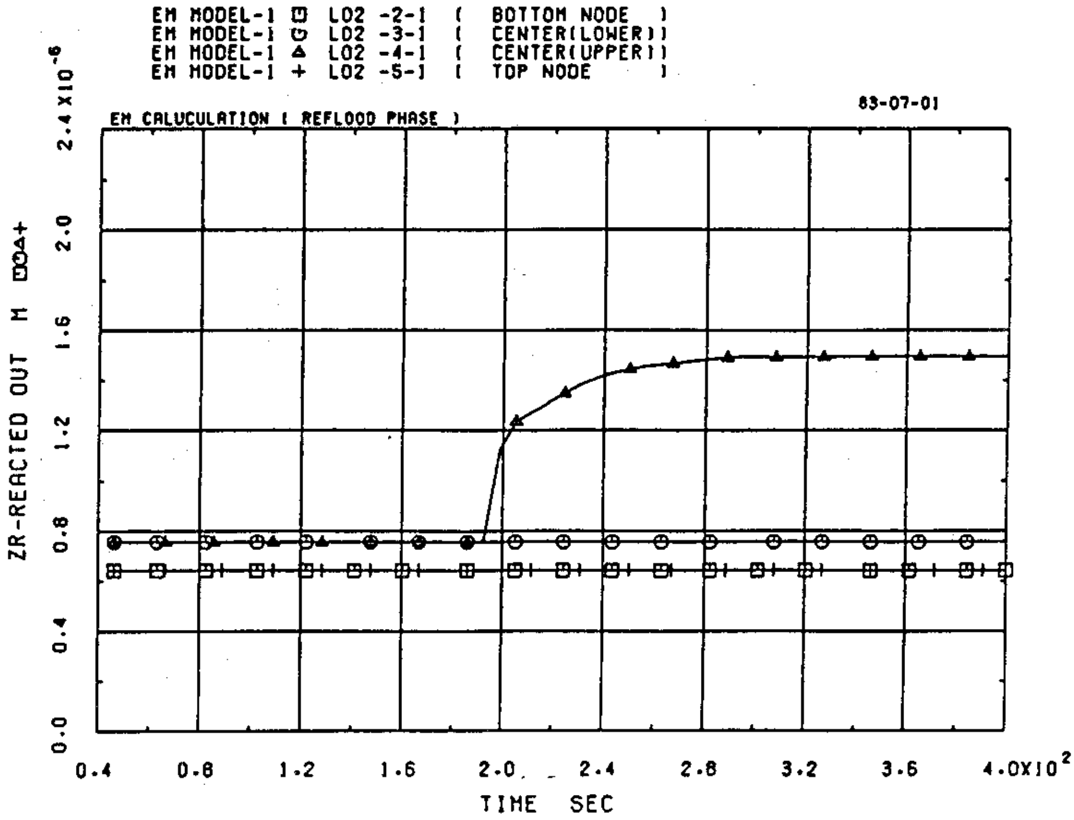

Fig. 4-59 Oxide thickness (ave,burst,inner)

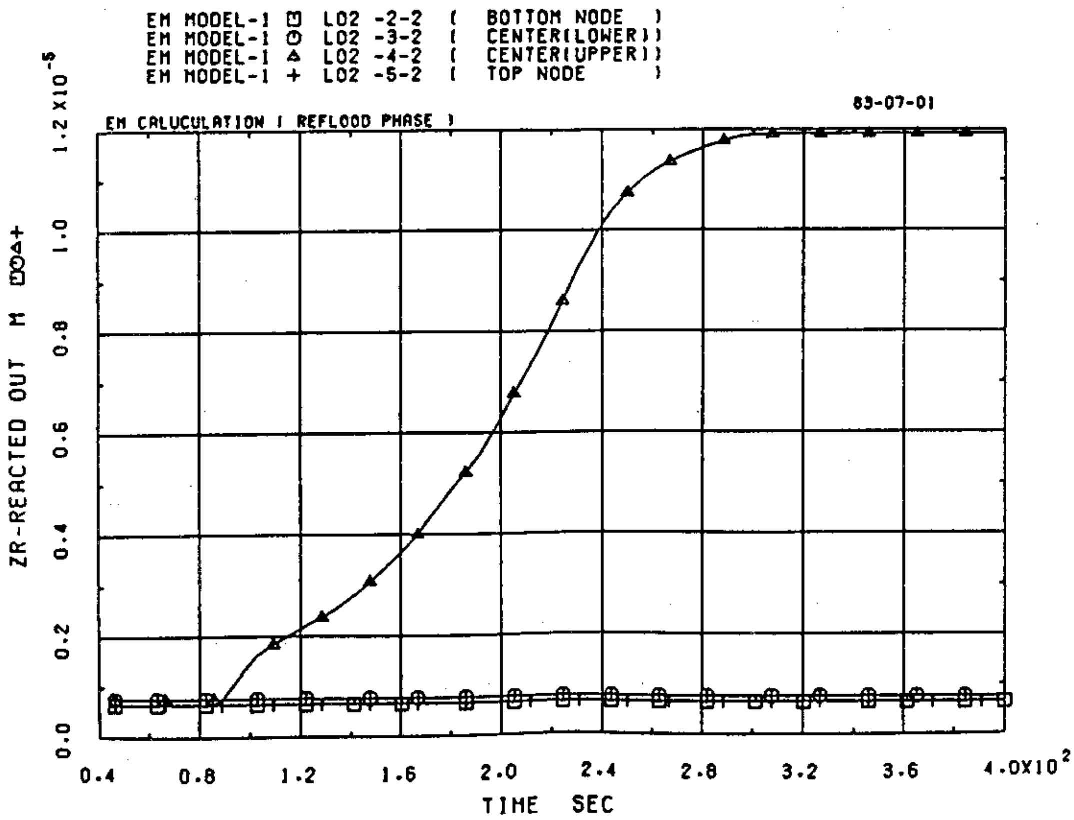

Fig. 4-60 Oxide thickness (hot,burst,inner)

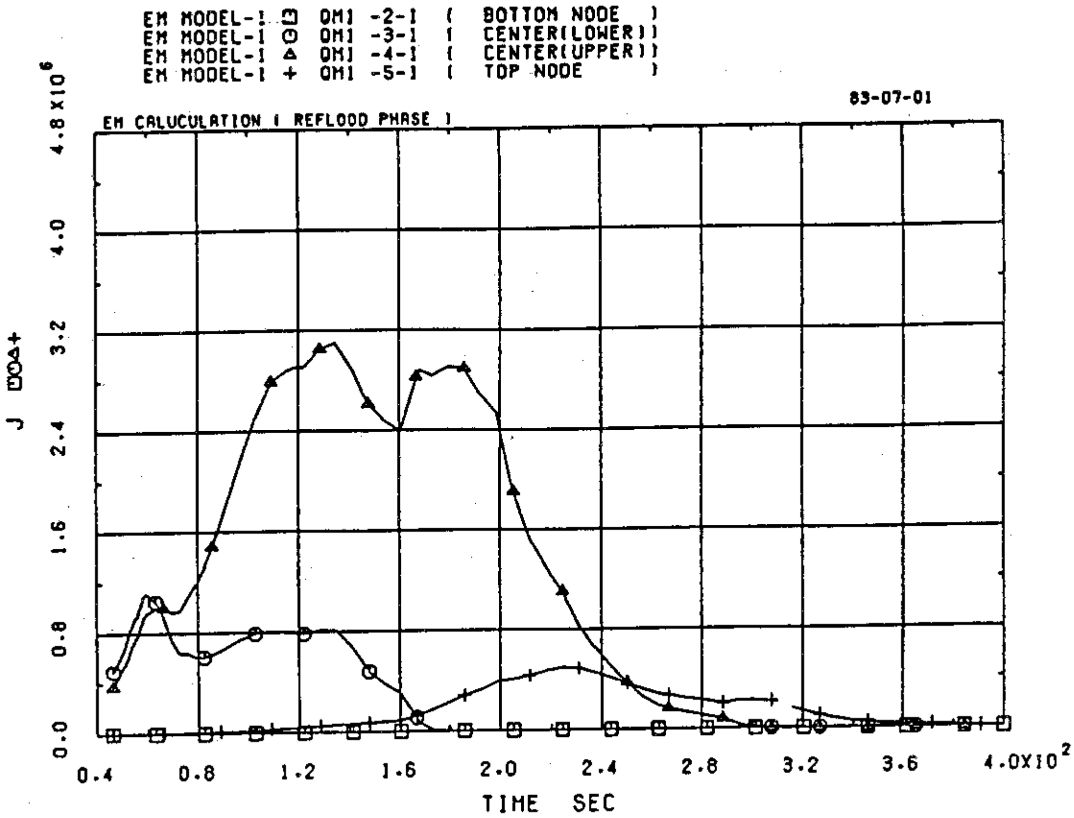

Fig. 4-61 M-W reaction heat generation rate (ave,non-burst)

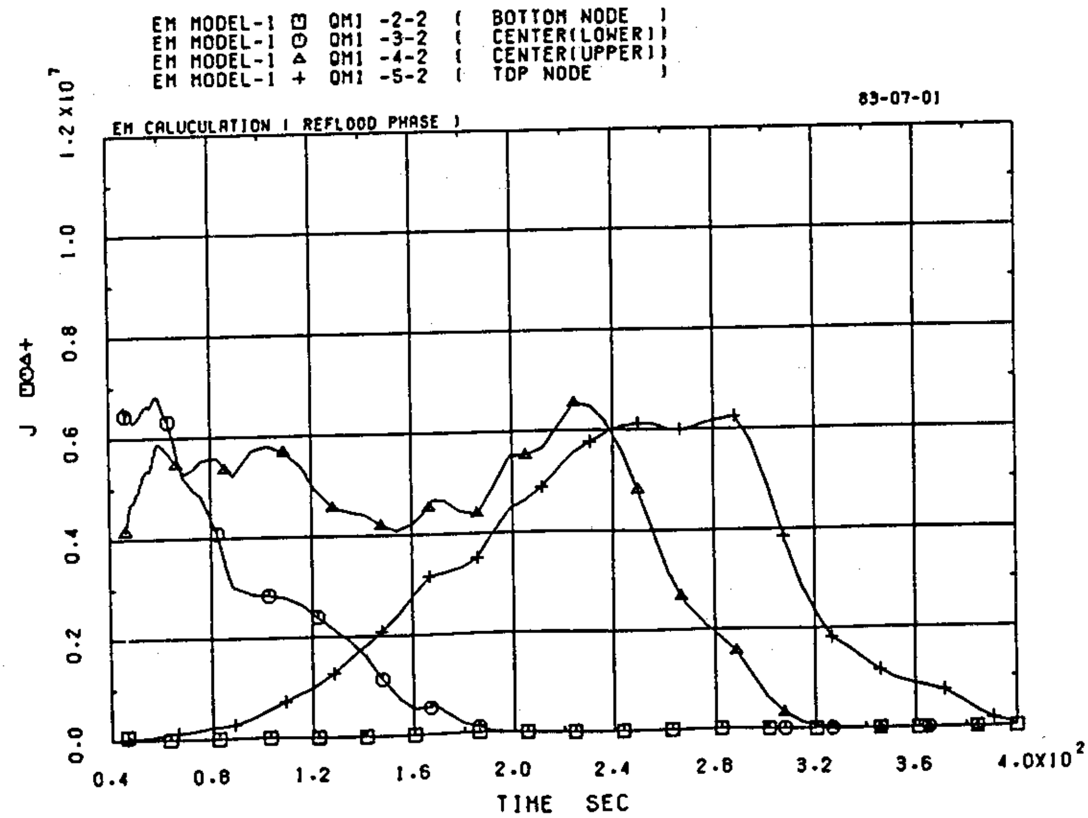

Fig. 4-62 M-W reaction heat generation rate (hot,non-burst)

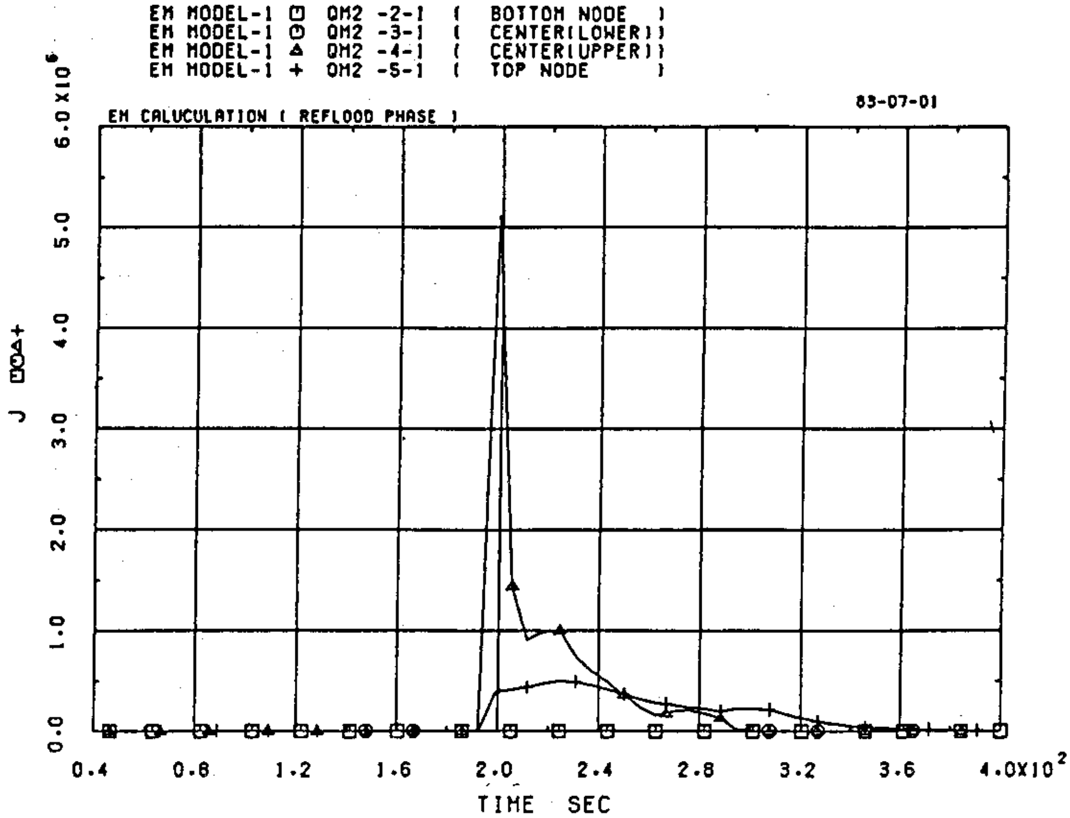

Fig. 4-63 M-W reaction heat generation rate (ave,burst)

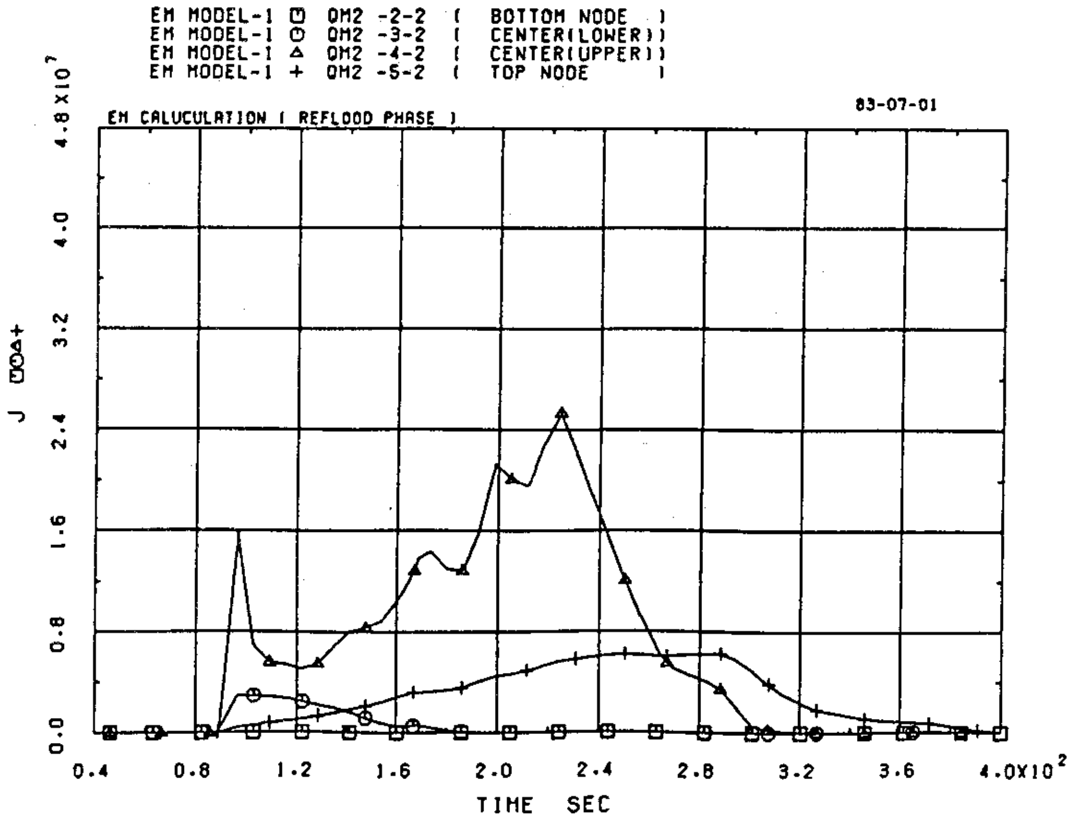

Fig. 4-64 M-W reaction heat generation rate (hot,burst)

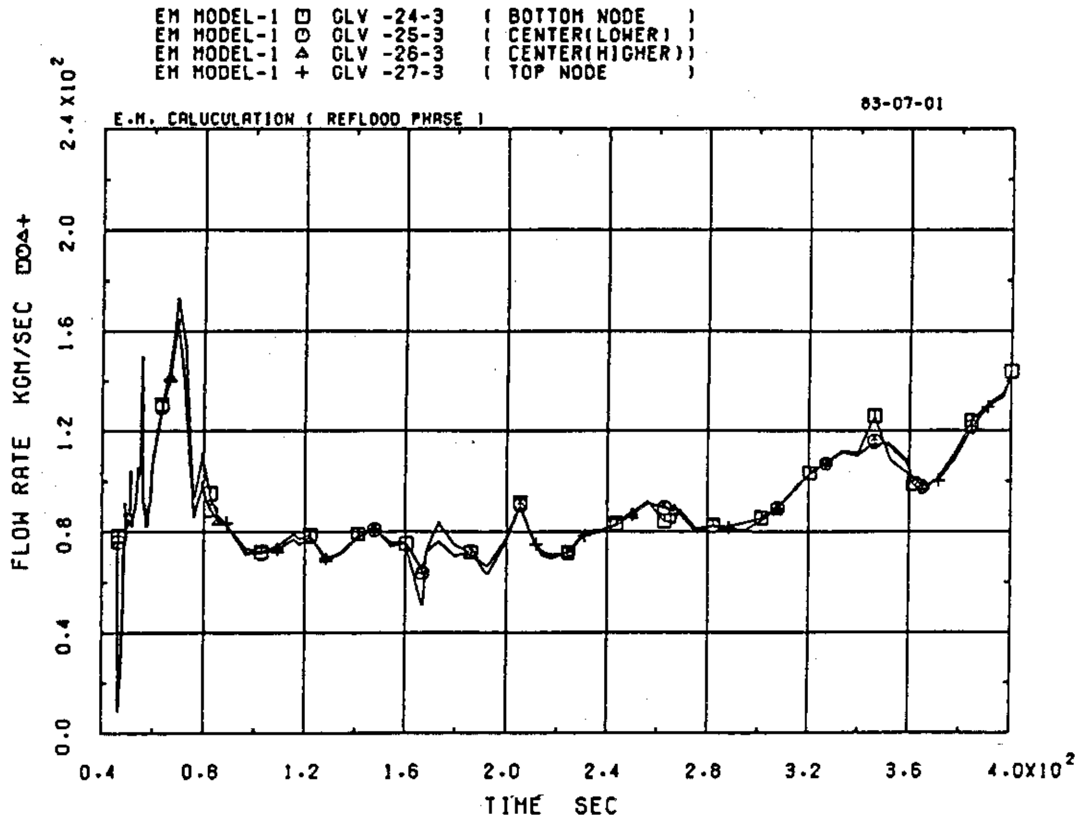

Fig. 4-65 Mass flow rate in core (average channel)

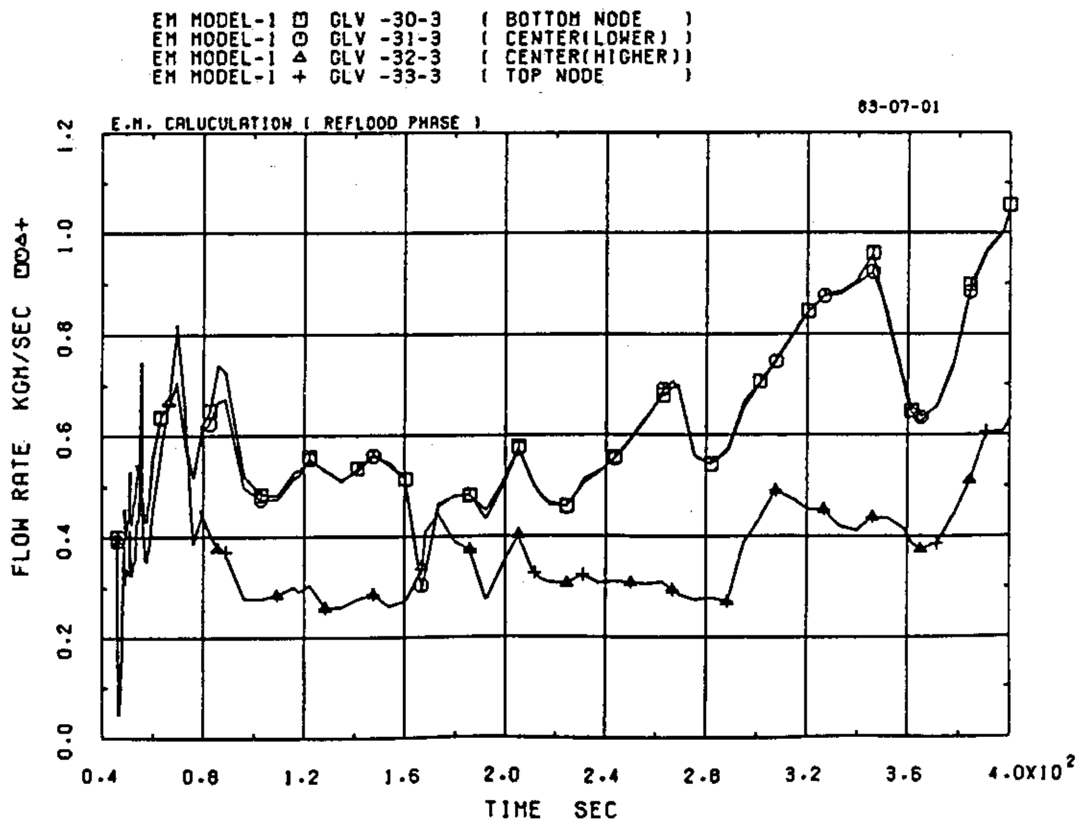

Fig. 4-66 Mass flow rate in core (hot channel)

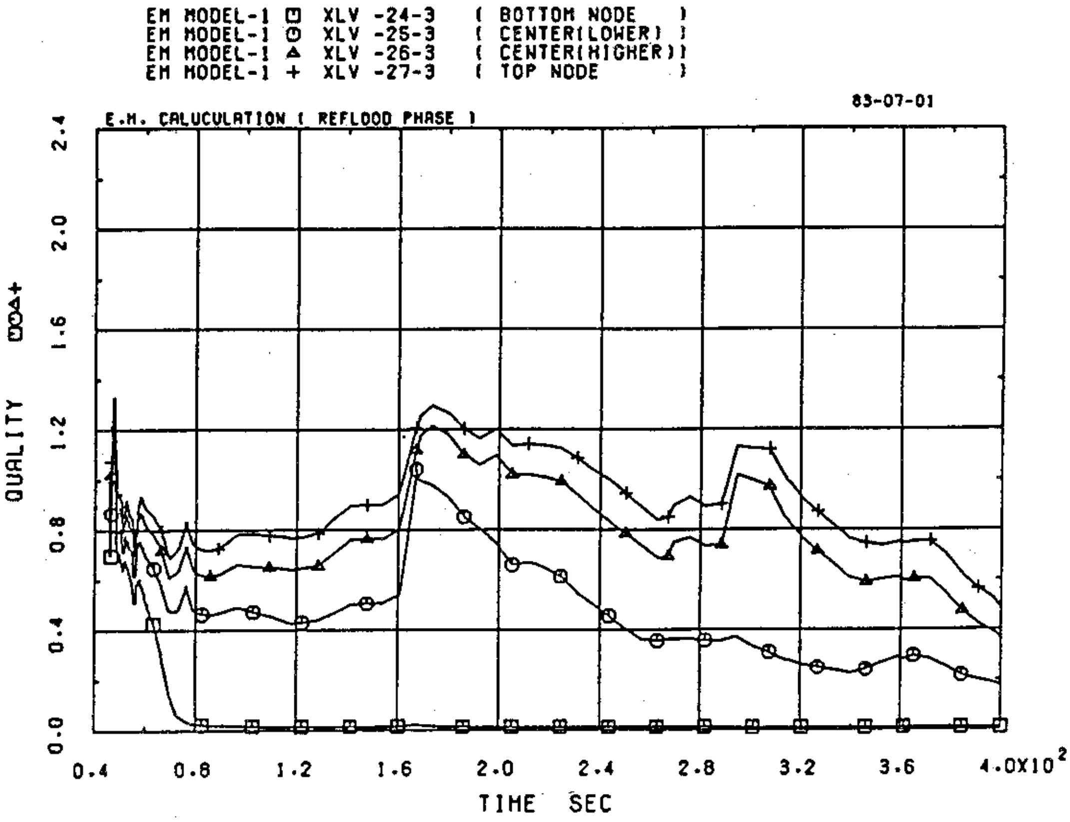

Fig. 4-67 Coolant quality in core (average channel)

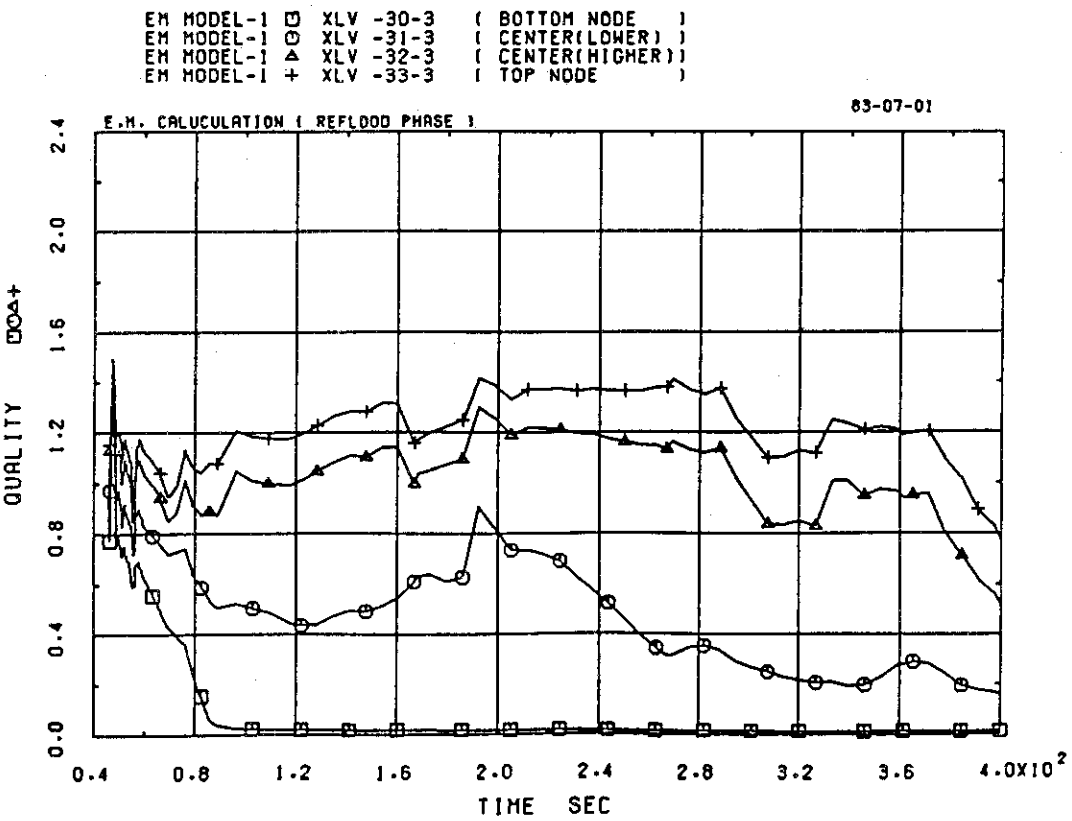

Fig. 4-68 Coolant quality in core (hot channel)

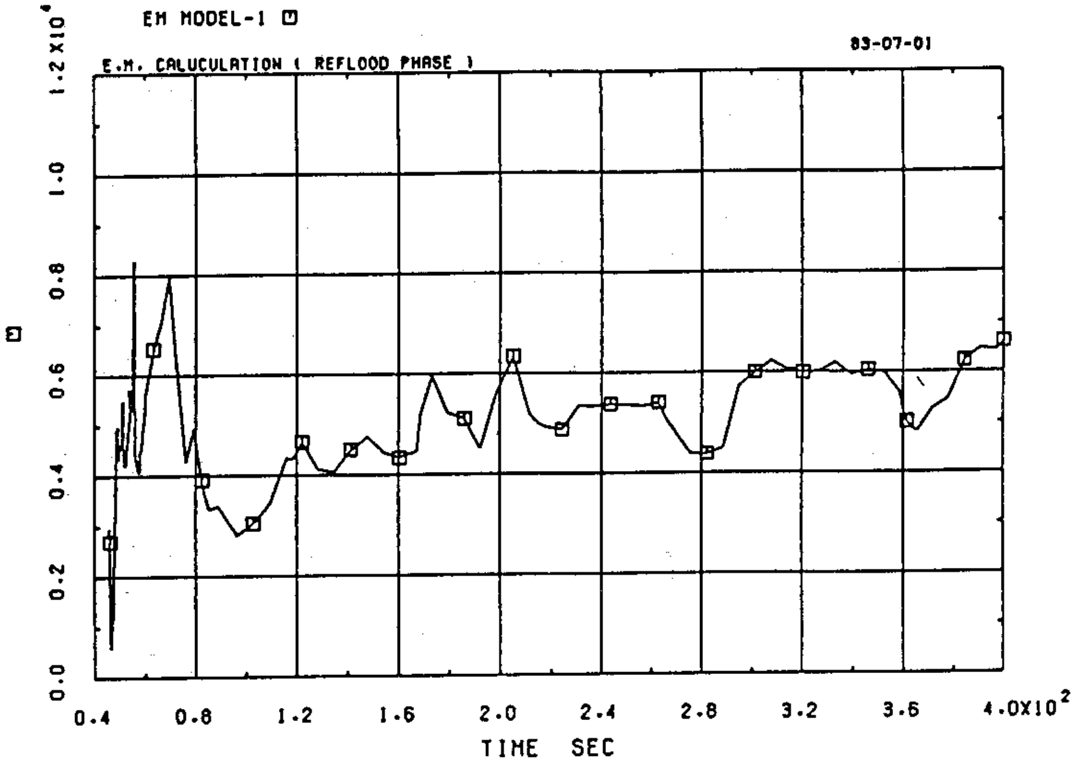

Fig. 4-69 Differential pressure across core (average channel)

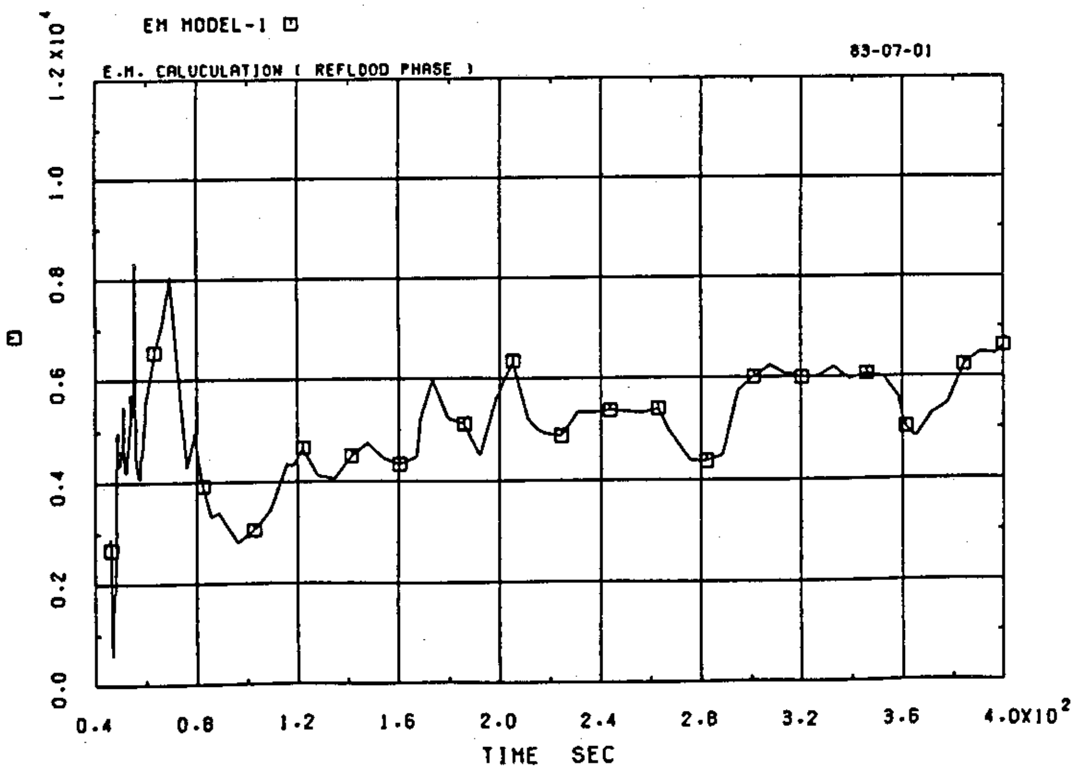

Fig. 4-70 Differential pressure across core (hot channel)

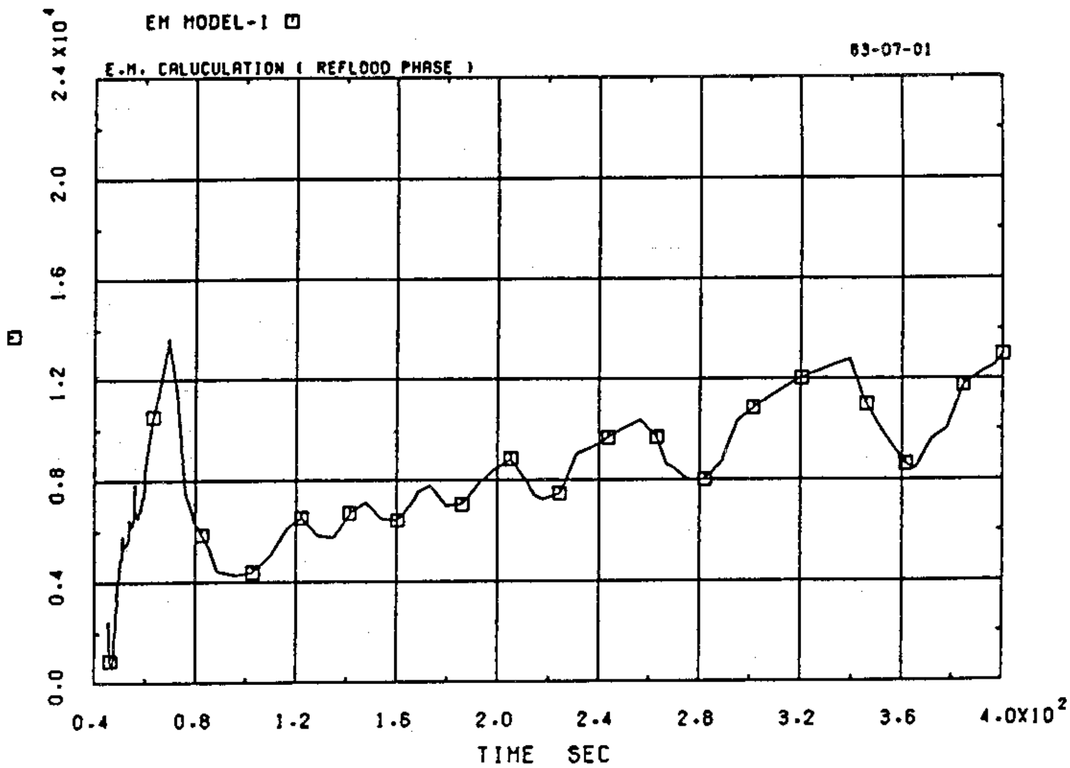

Fig. 4-71 Differential pressure across downcomer

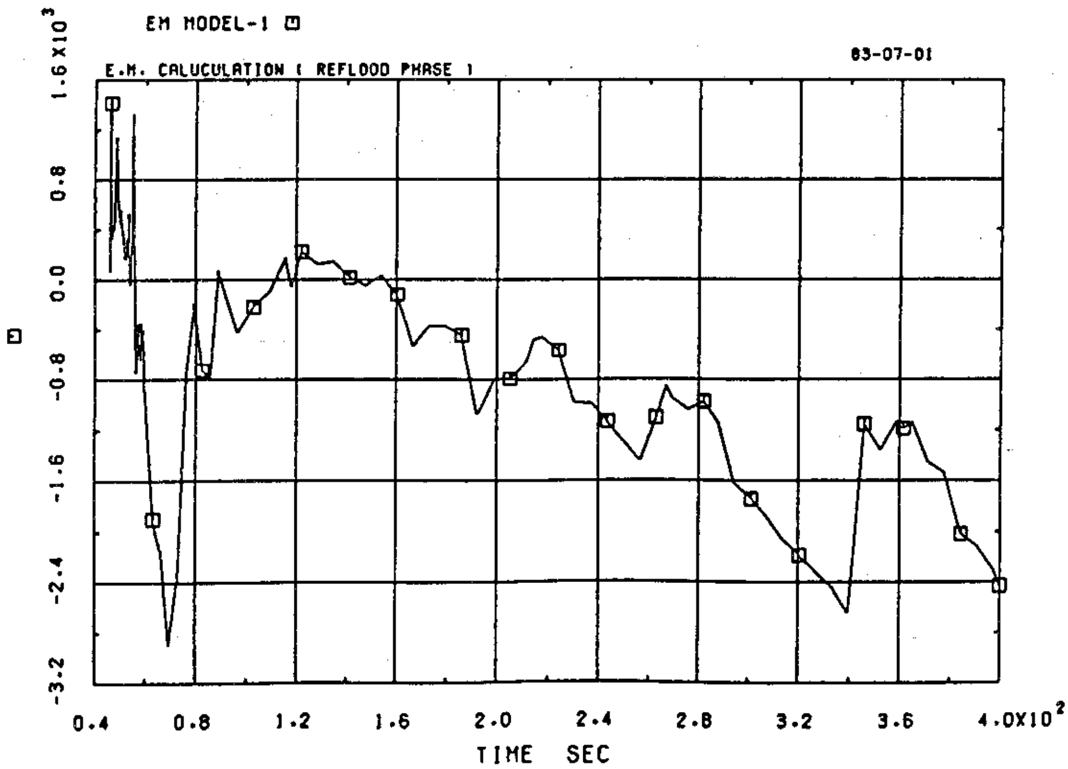

Fig. 4-72 Differential pressure between core and downcomer

5. Conclusion

In this report, the results of the first through EM calculation executed by THYDE-P1-EM have been presented. The main purpose of the present work is to establish EM logic equivalent to that in use for WREM/J2 with respect to ECCS analysis.

The code modifications were done so that the calculation would comply with the "Safety Evaluation Guideline for the performance of ECCS of LWRs" [11] which is equivalent to those used in WREM/J2.

As shown in the preceding sections, we got the satisfying results especially for the BLOWDOWN and REFILL phases.

The problems which have been pointed out in the course of the present calculation are summarized as follows :

(1) The discharge coefficient for the break flow model seems to have a large effect on the overall system states in the BLOWDOWN phase. So a sensitivity analysis should be made.

(2) The gravitational force term at the upper plenum mixing junction may have a considerable effect on the reverse flow in core at the early stage of the BLOWDOWN phase.

(3) The gravitational force term at the downcomer top mixing junction plays a very important role to terminate the ECCS water downcomer bypassing.

(4) The model to decide the quenching node and the expression of the HTC at the quenching node should be improved.

(5) There may be room for improvement in M-W reaction model of THYDE-P1-EM.

(6) The adaptation of the FLECHT correlation should be improved in THYDE-P1-EM.

Acknowledgment

The authors would like to express their sincere thanks to the members of Reactor Safety Evaluation Laboratory, especially to Mr. A. Kohsaka, Mr. M. Akimoto and Mr. F. Tanabe for their valuable discussions in the course of this work.

References

(1) Asahi, Y., "Description of THYDE-P Code (Preliminary Report of Methods and Models)", JAERI-M7751, 1978.

(2) Asahi, Y., "User's Manual for THYDE-P1", JAERI-M 82-38, 1982.

(3) Asahi, Y. and Hirano, M., "Verification study of LOCA Analysis Code THYDE-P (Sample Calculation Run 10)", JAERI-M8560, 1979.

(4) Hirano, M. and Asahi, Y., "Through Analysis of LOFT-L2-2 by THYDE-P Code 1 (Sample Calculation Run 30)", JAERI-M9535, 1981.

(5) Hirano, M., "Through Analysis of LOFT L2-3 by THYDE-P Code (Sample calculation Run 40)", JAERI-M9765, 1981.

(6) Shimizu, T. and Asahi, Y., "Through Calculation of 1,100 MWe PWR Large Break LOCA by THYDE-P (Sample Calculation Run 20)", JAERI-M9819, 1981.

(7) Hirano, M., "Analysis of LOFT Small Break Experiment L3-1 with THYDE-P Code (CSNI International Standard Probrem No.9 and THYDE-P Sample Calculation Run 50)", JAERI-M 82-008, 1982.

(8) Hirano, M., "Analysis of LOFT L3-6/L8-1 with THYDE-P (CSNI International Standard Probrem No.11 and THYDE-P Sample Calculation Run 60)", JAERI-M 82-028, 1982.

(9) Kosugi, S. and Asahi, Y., "Analasis of PKL K9 by THYDE-P Code (CSNI ISP No.10 and THYDE-P Sample Calculation Run 70)", JAERI-M 82-115, 1982.

(10) Hirano, M. and Kosugi S., "Base Input for Large Break LOCA Analysis of Commrecial PWR with Published Version of THYDE-P1 (THYDE-P1 Sample Calculation Run 21)", JAERI-M 83-002, 1983.

(11) Nuclear Safety Commission : "Safety Evaluation Guideline for the Performance of Emergency Cooling System of Light Water Reactors (in Japanese)", July 1981.

(12) Cadek, F. F. et al., "PWR FLECHT (Full Length Emergency Cooling Heat Transfer) Final Report", WCAP-7665, April 1971.

(13) Cadek, F. F. et al., "PWR FLECHT Final Report Supplement", WCAP-7931, October 1972.

(14) Chalton, et al., "RELAP4/MOD5 User's Manual Volume 3 (Checkout Applications)", ANCR-NUREG-1335(Vol. 3), 1976.

(15) Heney, R. E., "A Correlation for a Minimum Film Boiling Temperature", AIChE Symposium series 138, 81-90, 1974.

(16) Zaloudek, F. R., "Steam-Water Critical Flow from High Pressure Systems", HW-68936, Hanford works, 1963.

(17) Moody, F. J., "Maximum Flow Rate of a Single Component, Two-Phase Mixture", J. of Heat Transfer, Trans. ASME, Series C, Vol. 87, No.1, February 1965, pp. 134-142.

(18) Thom J. R. S., "Prediction of Pressure Drop During Forced Circulation Boiling of Water", Int. J. of Heat & Mass Transfer, 7, 1964, pp. 709-724.

(19) Martinelli, R. C. and Nelson, D. B., "Prediction of Pressure Drop During Forced Circulation Boiling of Water", Trans. ASME, Vol. 71, 1948, pp. 695-702.

(20) "WREM : Water Reactor Evaluation Model Revision 1," NUREG-75/056, U.S. Nuclear Reguratory Commision (May 1975)

(21) Tanabe, F. et al., "WREM-J2 : A JAERI Improved Version of WREM Code System", JAERI-M 9285, 1980.

(22) Tanabe, F. et al., Private comunication.

Appendix A-1 Input data for an initial job

```
 -- 1000 MWE PWR BLOWDOWN ANALYSIS ( WITH HOT CHANNEL) 82.07.09 --
/
/  **** DIMENSION DATA ****
BB01
  0  0  9  4  16  49  40  9 2  2  2  2  3  6  5  3 0 2 0 13 2 14
/
/  **** MINOR EDIT DATA ****
BB02
PRE-08  PRA-12  GLA-23  GLA-29  GLE-35  GLE-36  GLA-37  GLA-38  PRA-26
/
/  **** TIME STEP CONTROL DATA ****
BB03
SB0301
    0.2  0.2  100.
SB0302
    20   3  50   0  1.0E-3  1.0E-6  0.3  0.1
SB0303
    100  3  50   0  8.0E-3  1.0E-6  60.0  0.1
SB0304
    200  3  50   0  16.0E-3  1.0E-6  90.0  0.1
SB0305
    200  3  50   0  32.0E-3  1.0E-6  2000.0  0.1
/
/  **** TRIP CONTROLL DATA ****
BB04
SB0480
  1  0   1  0   1000.0       0.0
SB0481
  5 46   1  0      0.4       0.0
SB0482
  5 47   1  0      0.4       0.0
SB0483
  2  8   1  0      0.01      0.0
SB0484
  2  19  1  0      0.01      0.0
SB0485
  3  0   1  0      0.01      0.0
SB0486
  4  1   1  0     25.01      0.0
SB0487
 -4  1   1  0   1000.0       0.
SB0488
  4  2   1  0     25.01      0.0
SB0489
 -4  2   1  0   1000.0       0.
SB0492
  6  1 -3   1    240.0       0.005
SB0493
  6  2 -3   1    250.0       0.0
SB0494
```

Appendix A-1 (continued)

```
----*----1----*----2----*----3----*----4----*----5----*----6----*----7-R--*----8
  6  3 -3  1    360.0       0.0                                                  00005100
SB0495                                                                           00005200
 -6  1  3  1    350.0       0.0                                                  00005300
SB0496                                                                           00005400
 -6  2  3  1    305.0       0.0                                                  00005500
SB0497                                                                           00005600
 -6  3  3  1    380.0       0.00                                                 00005700
/                                                                                00005800
/  **** FLOW AJUST DATA ****                                                     00005900
BB05                                                                             00006000
  1  9000.0  360.0                                                               00006100
/                                                                                00006200
/  **** NODE DATA ****                                                           00006300
BB06                                                                             00006400
SB0601                                                                           00006500
 1  1 26  1  0  1     158.4538  0.737 0.  5.24  0.0                              00006600
                      0.043 0.084  0.0  0.0  0.0                                 00006700
SB0602                                                                           00006800
 2  1  1  2  0  1     158.9708  1.92  0.  1.665 1.665                            00006900
                      3.73  1.97  0.0  0.0  0.0                                  00007000
SB0603                                                                           00007100
 3  7  2  3  1 3265   158.7624  0.0197 0. 5.0   5.0                              00007200
                      0.033 0.048  0.0  0.0  0.0                                 00007300
SB0604                                                                           00007400
 4  7  3  4  1 3265   158.1581   0.0197 0. 5.46  5.46                            00007500
                      0.0   0.0    0.0   0.0  0.0                                00007600
SB0605                                                                           00007700
 5  7  4  5  1 3265   157.4898  0.0197 0. 10.46 -10.46                           00007800
                      0.0   0.0  0.033   0.048  0.0                              00007900
SB0606                                                                           00008000
 6  1  5  6  0  1     157.7862  1.92  0.  1.665 -1.665                           00008100
                      0.0   0.0   3.73   1.97  0.0                               00008200
SB0607                                                                           00008300
 7  1  6  7  0  1     157.4466  0.787 0.  7.34 -3.54                             00008400
                      0.042 0.077   -1.   -1.  0.0                               00008500
SB0608                                                                           00008600
 8  8  7 34  0  1     157.5243  0.737 0.  5.57635  3.54                          00008700
                      -1.   -1.   0.2029  0.2027  0.0                            00008800
SB0609                                                                           00008900
 9  1 34  8  0  1     162.0607  0.699 0.  2.825  0.0                             00009000
                      0.0   0.0   0.0   0.0  0.0                                 00009100
SB0610                                                                           00009200
10  1  8 29  0 1      162.0332   0.699 0.  3.13  0.0                             00009300
                      0.0   0.0   0.0   0.0  0.0                                 00009400
SB0611                                                                           00009500
11  1 26 27  0 3      158.4538  0.737  0.  2.0 0.                                00009600
                      0.043 0.083  0.0   0.0  0.0                                00009700
SB0612                                                                           00009800
12  1 27  9  0 3      158.4334   0.737  0.  3.24 0.                              00009900
                      0.0   0.0   0.0   0.0  0.0                                 00010000
SB0613                                                                           00010100
13  1  9 10  0 3      158.9528  1.92  0.  1.665  1.665                           00010200
                      3.73  1.97  0.0   0.0  0.0                                 00010300
SB0614                                                                           00010400
14  7 10 11  1 9795   158.7445  0.0197 0. 5.0  5.0                               00010500
                      0.033 0.048  0.0   0.0  0.0                                00010600
SB0615                                                                           00010700
15  7 11 12  1 9795   158.1387   0.0197 0. 5.46 5.46                             00010800
                      0.0   0.0   0.0   0.0  0.0                                 00010900
```

Appendix A-1 (continued)

```
----*----1----*----2----*----3----*----4----*----5----*----6----*----7-R--*----8
SB0616                                                                  00011000
16  7 12 13   1 9795   157.4691  0.0197 0. 10.46 -10.46                 00011100
                       0.0   0.0   0.033  0.048  0.0                    00011200
SB0617                                                                  00011300
17  1 13 14   0  3     157.7645   1.92  0.  1.665  -1.665               00011400
                       0.0   0.0    3.73  1.97  0.0                     00011500
SB0618                                                                  00011600
18  1 14 15   0  3     157.4249  0.787 0.   7.34 -3.54                  00011700
                       0.042  0.077  -1.    -1.   0.0                   00011800
SB0619                                                                  00011900
19  8 15 28   0  3     157.5027  0.737 0.   5.57635  3.54               00012000
                       -1.   -1.     0.2029  0.2027  0.0                00012100
SB0620                                                                  00012200
20  1 28 29   0 3      162.0373  0.699 0. 5.955   0.                    00012300
                       0.0   0.0     0.0    0.0    0.0                  00012400
SB0621                                                                  00012500
21  4 29 16   0 1      162.4638   1.869 0. 7.248 -7.248                 00012600
                       0.0   0.0     0.0    0.0    0.0                  00012700
SB0622                                                                  00012800
22  5 16 30   0 1      162.9140  2.487 0. 6.075 1.948                   00012900
                       0.0   0.0     0.0    0.0    0.0                  00013000
SB0623                                                                  00013100
23  2 30 17   0 39170 162.6047  1.0    0. 0.23   0.23                   00013200
                       0.74  0.74    0.0    0.0    0.0                  00013300
SB0624                                                                  00013400
24  2 17 18   1 39170 162.1173  1.0    0. 0.80   0.80                   00013500
                       0.0   0.0     0.0    0.0    0.0                  00013600
SB0625                                                                  00013700
25  2 18 31   1 39170 161.5410  1.0    0. 0.80   0.80                   00013800
                       0.0   0.0     0.0    0.0    0.0                  00013900
SB0626                                                                  00014000
26  2 31 19   1 39170 160.9517  1.0    0. 0.80   0.80                   00014100
                       0.0   0.0     0.0    0.0    0.0                  00014200
SB0627                                                                  00014300
27  2 19 20   1 39170 160.3296  1.0    0. 0.80   0.80                   00014400
                       0.0   0.0     0.0    0.0    0.0                  00014500
SB0628                                                                  00014600
28  2 20 33   0 39170 159.7062  1.0    0. 0.23   0.23                   00014700
                       0.0   0.0     0.0    0.0    0.0                  00014800
SB0629                                                                  00014900
29  2 30 21   0 200    162.6047  1.0    0. 0.23   0.23                  00015000
                       1.284  2.482  0.0  0.0    0.0                    00015100
SB0630                                                                  00015200
30  2 21 22   1 200    162.1173  1.0    0.   0.80  0.80                 00015300
                       0.0   0.0     0.0    0.0    0.0                  00015400
SB0631                                                                  00015500
31  2 22 32   1 200    161.5410  1.0    0.   0.80  0.80                 00015600
                       0.0   0.0     0.0    0.0    0.0                  00015700
SB0632                                                                  00015800
32  2 32 23   1 200    160.946155  1.0  0.   0.80  0.80                 00015900
                       0.0   0.0     0.0    0.0    0.0                  00016000
SB0633                                                                  00016100
33  2 23 24   1 200    160.3296  1.0    0.   0.80  0.80                 00016200
                       0.0   0.0     0.0    0.0    0.0                  00016300
SB0634                                                                  00016400
34  2 24 33   0 200    159.7062  1.0    0.   0.23  0.23                 00016500
                       0.76  0.34    0.0    0.0    0.0                  00016600
SB0635                                                                  00016700
35  3 30 33   0  1     162.6047  0.555 0.   3.66   3.66                 00016800
```

Appendix A-1 (continued)

```
----*----1----*----2----*----3----*----4----*----5----*----6----*----7-R--*----8
                         0.77  0.83   0.87  0.78   0.0                         00016900
SB0636                                                                          00017000
36  1 32 31   0 200    161.029550  0.034 0.  0.1   0.                          00017100
                         0.0   0.0    0.0   0.0   0.0                          00017200
SB0637                                                                          00017300
37  1 33 26   0  1     159.17209  3.44  0.  4.341  1.64                        00017400
                         0.0   0.0    0.0   0.0   0.0                          00017500
SB0638                                                                          00017600
38 13 26 40   0  1       5.0   2.216 0.  3.658  2.073                          00017700
                        1.491E4  1.491E4  0.0   0.0   0.0                      00017800
SB0639                                                                          00017900
39 13 27 25   0  1       5.0   0.29  0.  15.0   1.7                            00018000
                         0.41  0.87   0.0   0.0   0.0                          00018100
SB0640                                                                          00018200
40 13 25 35   0  1       5.0   0.29  0.  14.3   1.6                            00018300
                         0.0   0.0    0.0   0.0   0.0                          00018400
SB0641                                                                          00018500
41 13 28 37   0  3      10.0   0.305 0.   12.0  0.0                            00018600
                         0.0   0.0    0.0   0.0   37.8                         00018700
SB0642                                                                          00018800
42 13 34 38   0  1      10.0   0.305 0.   12.0  0.0                            00018900
                         0.0   0.0    0.0   0.0   37.8                         00019000
SB0643                                                                          00019100
43 13 28 36   0  3      10.0   0.222 0.  120.0  0.0                            00019200
                         0.109  0.049  0.0  0.0   51.7                         00019300
SB0644                                                                          00019400
44 13 34 39   0  1      10.0   0.222 0.  120.0  0.0                            00019500
                         0.109  0.049  0.0  0.0   51.7                         00019600
/                                                                               00019700
/  **** JUNCTION DATA ****                                                      00019800
BB07                                                                            00019900
    1   1   0.0                                                                 00020000
    2   1   0.0                                                                 00020100
    3   1   0.0                                                                 00020200
    4   1   0.0                                                                 00020300
    5   1   0.0                                                                 00020400
    6   1   0.0                                                                 00020500
    7   1   0.0                                                                 00020600
    8   1   0.0                                                                 00020700
    9   1   0.0                                                                 00020800
   10   1   0.0                                                                 00020900
   11   1   0.                                                                  00021000
   12   1   0.0                                                                 00021100
   13   1   0.0                                                                 00021200
   14   1   0.0                                                                 00021300
   15   1   0.0                                                                 00021400
   16   1   0.0                                                                 00021500
   17   1   0.0                                                                 00021600
   18   1   0.0                                                                 00021700
   19   1   0.0                                                                 00021800
   20   1   0.0                                                                 00021900
   21   1   0.                                                                  00022000
   22   1   0.                                                                  00022100
   23   1   0.                                                                  00022200
   24   1   0.                                                                  00022300
   25   1   0.                                                                  00022400
   26   2   1.027                                                               00022500
   27   4   0.049                                                               00022600
   28   4   0.351                                                               00022700
```

Appendix A-1 (continued)

```
----*----1----*----2----*----3----*----4----*----5----*----6----*----7-R--*----8
                                                                          00022800
  29   3   0.531                                                          00022900
  30   4   0.1                                                            00023000
  31   4   0.01                                                           00023100
  32   4   0.01                                                           00023200
  33   4   0.05                                                           00023300
  34   4   0.117                                                          00023400
  35   6   0.                                                             00023500
  36   5   0.                                                             00023600
  37   7   0.                                                             00023700
  38   7   0.                                                             00023800
  39   5   0.                                                             00023900
  40   8   0.                                                             00024000
/                                                                         00024100
/  **** MIXING JUNCTION DATA ****                                         00024200
BB08                                                                      00024300
SB0801                                                                    00024400
  26   3    1  11  38   0   0.25    0.75    0.    0.                     00024500
SB0802                                                                    00024600
  27   2   12  39   0   0   1.0     0.0     0.    0.                     00024700
SB0803                                                                    00024800
  28   3   20. 41  43   0   1.0     0.0     0.0   0.0                    00024900
SB0804                                                                    00025000
  29   1   21   0   0   0   1.0     0.0     0.0   0.0                    00025100
SB0805                                                                    00025200
  30   3   23  29  35   0   0.945   0.005   0.05  0.0                    00025300
SB0806                                                                    00025400
  31   1   26   0   0   0   1.0     0.0     0.    0.                     00025500
SB0807                                                                    00025600
  32   2   32  36   0   0   0.99    0.01    0.    0.                     00025700
SB0808                                                                    00025800
  33   1   37   0   0   0   1.0     0.0     0.0   0.0                    00025900
SB0809                                                                    00026000
  34   3    9  42  44   0   1.0     0.0     0.0   0.0                    00026100
/                                                                         00026200
/  **** PUMPED INJECTION DATA ****                                       00026300
BB09                                                                      00026400
SB0901                                                                    00026500
   1   37     37.8                                                        00026600
  2  1                                                                    00026700
  0.0    666.0  1000.0   666.0                                            00026800
SB0902                                                                    00026900
   2   38     37.8                                                        00027000
  2  1                                                                    00027100
  0.0    222.0  1000.0   222.0                                            00027200
/                                                                         00027300
/  **** PUMP DATA ****                                                   00027400
BB10                                                                      00027500
SB1001                                                                    00027600
 8 1 1  1185.  5.583  43250.  97.54  747.6  1185.  3455.  0. 0. 0.05     00027700
SB1002                                                                    00027800
19 1 1  1185.  5.583  43250.  97.54  747.6  1185.  3455.  0. 0. 0.05     00027900
/                                                                         00028000
/**** PUMP DATA TABLE **** (RELAP4 BUILT-IN DATA) WESTINGHOUSE PUMP      00028100
BB11                                                                      00028200
SB1101                                                                    00028300
 1                                                                        00028400
13                                                                        00028500
-1.  3.55    -.6  2.73    -.32  2.20    -.18  2.00    .0  1.73    .2  1.50 00028600
 .46 1.24    .52 1.23     .6   1.24     .66  1.24     .8  1.17    .9  1.10
```

Appendix A-1 (continued)

```
----*----1----*----2----*----3----*----4----*----5----*----6----*----7-R--*----8
 1.  1.00                                                                00028700
12                                                                       00028800
-1.  0.00   -.01  0.00    .0  -0.16     .1  -0.12    .2 -0.06    .28 0.00  00028900
 .4  0.09    .6   0.31    .7   0.42     .8   0.50    .88 0.54    1.  0.59  00029000
11                                                                       00029100
-1.  0.00   -.01  0.00    .0  -0.96     .1  -0.90    .2  -0.81    .3  -0.70 00029200
 .4 -0.54    .53 -0.30    .65  0.00     .8   0.37    1.   1.00            00029300
14                                                                       00029400
-1.  3.55   -.89  3.20   -.74  2.80    -.6   2.47   -.46  2.20   -.2   1.73 00029500
 0.  1.40    .37  0.80    .43  0.74     .5   0.68    .58  0.64    .64  0.62 00029600
 .7  0.61    1.   0.59                                                   00029700
17                                                                       00029800
-1.  2.98   -.82  2.40   -.6   1.87    -.46  1.60   -.34  1.40   -.2   1.21 00029900
-.1  1.10    .0   1.01    .1   0.96     .2   0.92    .3   0.90    .4   0.89 00030000
 .5  0.91    .7   0.99    .8   1.02     .9   1.02    1.   1.00            00030100
 9                                                                       00030200
-1.  0.00   -.01  0.00    .0  -1.00     .25 -0.60    .4  -0.37    .5  -0.25 00030300
 .6 -0.16    .8  -0.01    1.   0.11                                      00030400
 9                                                                       00030500
-1.  0.00   -.01  0.00    .0  -0.87     .1  -0.76    .2  -0.63    .3  -0.48 00030600
 .4 -0.31    .74  0.40    1.   1.00                                      00030700
10                                                                       00030800
-1.  2.98   -.91  2.80   -.8   2.60    -.7   2.42   -.6   2.25   -.42  2.00 00030900
 .0  1.42    .6   0.61    .8   0.35     1.   0.11                        00031000
16                                                                       00031100
-1. -1.16   -.9  -1.24   -.8  -1.77    -.7  -2.36   -.6  -2.79   -.5  -2.91 00031200
-.4 -2.67   -.25 -1.69   -.1  -0.50     .0   0.00    .1   0.83    .2   1.09 00031300
 .5  1.02    .7   1.01    .9   0.94     1.  1.00                         00031400
 7                                                                       00031500
-1.  0.00    .0   0.00    .2  -0.34     .4  -0.65    .6  -0.93    .8  -1.19 00031600
 1. -1.47                                                                00031700
 9                                                                       00031800
-1.  0.00    .0   0.00    .1  -0.04     .2   0.00    .3   0.10    .4   0.21 00031900
 .8  0.67    .9   0.80    1.   1.00                                      00032000
19                                                                       00032100
-1. -1.16   -.9  -0.78   -.8  -0.50    -.7  -0.31   -.6  -0.17   -.5  -0.08 00032200
-.35 0.00   -.2   0.05   -.1   0.08     .0   0.11    .1   0.13    .25  0.15 00032300
 .4  0.13    .5   0.07    .6  -0.04     .7  -0.23    .8  -0.51    .9  -0.91 00032400
 1. -1.47                                                                00032500
 0                                                                       00032600
 0                                                                       00032700
 0                                                                       00032800
 0                                                                       00032900
11                                                                       00033000
  .0  0.00   .1  0.00     .15  0.05     .24  0.80     .3  0.96     .4  0.98 00033100
  .6  0.97   .8  0.90     .9   0.80     .96  0.50     1.  0.00             00033200
 2                                                                       00033300
 0.0  0.00   1.0  0.00                                                   00033400
  6  6                                                                   00033500
        0.0  0.2         0.4         0.6         0.8         1.0         00033600
  0.0   0.0  0.0         0.0         0.0         0.0         0.0         00033700
  0.2   0.0  3.065E-5    7.7239E-5   1.3263E-4   1.946E-4    2.6207E-4   00033800
  0.4   0.0  4.866E-5    1.2261E-4   2.1053E-4   3.0996E-4   4.1602E-4   00033900
  0.6   0.0  6.376E-5    1.6066E-4   2.7587E-4   4.0485E-4   5.4514E-4   00034000
  0.8   0.0  7.7239E-5   1.9463E-4   3.3419E-4   4.9044E-4   6.6037E-4   00034100
  1.0   0.0  8.9628E-5   2.2585E-4   3.878E-4    5.691E-4    7.6631E-4   00034200
/                                                                        00034300
/  **** ACCUMLATOR DATA ****                                             00034400
BB12                                                                     00034500
```

Appendix A-1 (continued)

```
----*----1----*----2----*----3----*----4----*----5----*----6----*----7-R--*----8
SB1201
   48   36   70.   30.   51.7   44.
  0.194  3.0
SB1202
   49   39   23.3  10.   51.7   44.
  0.194  1.0
/
/  **** BREAK POINT DATA ****
BB13
   8  0.01  0.4  0.8  0.6  0.6  0.8  0.6  0.6  0.0  0.0  0.0  0.0
   6
  0.0 1.0  7.5  2.7  15.  4.0  30.  4.0  60.  4.0  1000. 4.0
/
/  **** PRESSURIZER DATA ****
BB14
   45   35   11  3.58  15.56  9.0  0.99  0.1
        1.7  385.0
   50.0  1.0  0.1  0.0  0.0
   0.915  0.915  0.915  1.525  3.05  4.58
   0.564  0.67  0.619
      2
   0.  1.0  1.0  1.0  1000.  1.0  1.0  1.0
/
/  **** STEAM GENERATOR DATA ****
BB15
SB1501
 46 3265  3  5  3  1
 5.5   18.9  0.7  0.5    3.0E-2  1.0E-2    10.4  4.0  222.1  474.5
 0.1  0.95  62.0
       2.0  11.0
 -40.  -30.  -25.
      0.001    80.  0.5  0.5  0.5
   3
   0.0  1.0  1.0  1.0  1.0  1.0  1.0  1.0  1000.0  1.0  1.0  0.0
SB1502
  47    9795  14  16  3  1
  16.5  18.9   2.1   0.5     3.0E-2  1.0E-2    10.4  4.0  222.1 1423.5
 0.1  0.95  62.0
       2.0  11.0
  -40.0  -30.0  -25.0
      0.003    80.  0.5  0.5  0.5
   3
  0.0 1.0  1.0  1.0  1.0  1.0  1.0  1.0  1000.0  1.0  1.0  0.0
/
/  **** CORE DATA ****
BB16
/    --- AVERAGE  CHANNEL -----
SB1601
  1
 39170  23  28  1  3  1  2  2
  9000.0  5.3658E-3  0.6187E-3   4.6573E-3   1.42E-2      0.6    1.0E-4
  0.0124  0.0212E-02  0.0305  0.1402E-02
  0.111  0.1254E-02  0.301  0.2529E-02
  1.13  0.0736E-02  3.00 0.0269E-02
  5.0   0.6  4.91E-04  3.41E-06  1.2  1.54E03
  0.  156.  234.  234.  156.  0.
  1.6122E-07  6.42E-07  7.56E-07  7.56E-07  6.42E-07  1.622E-07
  1.6122E-07  6.42E-07  7.56E-07  7.56E-07  6.42E-07  1.622E-07
  1.6122E-07  6.42E-07  7.56E-07  7.56E-07  6.42E-07  1.622E-07
```

Appendix A-1 (continued)

```
----*----1----*----2----*----3----*----4----*----5----*----6----*----7-R--*----8
  1.6122E-07  6.42E-07  7.56E-07  7.56E-07  6.42E-07  1.622E-07               00040500
/      --- HOT CHANNEL ---                                                     00040600
SB1602                                                                         00040700
  2                                                                            00040800
  200     29  34  1  3  1  2  2                                                00040900
  9000.0  5.3665E-3  0.6187E-3   4.6682E-3    1.42E-2      0.6    1.0E-4      00041000
  0.  203.0  304.0  304.0  203.0  0.                                           00041100
  1.6122E-07  6.42E-07  7.56E-07  7.56E-07  6.42E-07  1.622E-07               00041200
  1.6122E-07  6.42E-07  7.56E-07  7.56E-07  6.42E-07  1.622E-07               00041300
  1.6122E-07  6.42E-07  7.56E-07  7.56E-07  6.42E-07  1.622E-07               00041400
  1.6122E-07  6.42E-07  7.56E-07  7.56E-07  6.42E-07  1.622E-07               00041500
/                                                                              00041600
/  **** REACTIVITY DATA ****                                                   00041700
BB17                                                                           00041800
    3                                                                          00041900
  0.  0.  0.5  -5.  1.  -25.                                                   00042000
    5                                                                          00042100
 18. 3.56E-3   538. 0.   1093. -3.08E-3   1649. -2.7E-3   2760. -2.44E-300042200
    5                                                                          00042300
  0.01  0.0  1.0  -0.1  1.5  -0.2  2.0  -3.0  1000. -8.0                       00042400
/                                                                              00042500
/   ****METAL WATER REACTION DATA ****                                         00042600
BB18                                                                           00042700
    1.54E03 0.775E-04 2.29E04                                                  00042800
/                                                                              00042900
/  **** FUEL GAP DATA ****                                                     00043000
BB19                                                                           00043100
 0.0301  0.0  1.235E-5  0.0  0.0  0.0  0.0  0.6  0.6  0.0                      00043200
 0.9495  0.0157  0.0028  0.0  0.032  0.0  0.0                                  00043300
/                                                                              00043400
/  **** BURST DATA   ****                                                      00043500
BB20                                                                           00043600
2  2  5.0E7  6.96E-08  2.87E4  2.86E-03  1.15E0  1.528E0                       00043700
1.49E-07  2.0E-08  1.25E-16  1.85E-01  8.0E09  3.3E-03                         00043800
       0.1                                                                     00043900
/                                                                              00044000
/**** CONTROL DATA FOR HEAT SLAB ****                                          00044100
BB21                                                                           00044200
 3 1                                                                           00044300
/                                                                              00044400
/**** HEAT SLAB DATA ****                                                      00044500
BB22                                                                           00044600
SB2201                                                                         00044700
 1 1 1 1  0 21 4.573 8.019   8.05456 0. 0. 0.                                  00044800
     1 2  7  0               0.03556 0.                                        00044900
SB2202                                                                         00045000
 2 2 1 2 21  0 7.303 2.197   2.4169  0. 0. 0.                                  00045100
     1 1  4  0               0.00397 0.                                        00045200
     2 3 10  0               0.21593 0.                                        00045300
SB2203                                                                         00045400
 3 2 1 2 22  0 2.871 2.195   2.3355  0. 0. 0.                                  00045500
     1 1  4  0               0.00397 0.                                        00045600
     2 3  8  0               0.13653 0.                                        00045700
SB2204                                                                         00045800
 4 2 3 2 11  0 2.00   0.3682 0.43171 0. 0. 0.                                  00045900
     1 1  5  0               0.01270 0.                                        00046000
     2 1  5  0               0.05081 0.                                        00046100
SB2205                                                                         00046200
 5 2 3 2 12  0 3.182 0.3682 0.43171 0. 0. 0.                                   00046300
```

Appendix A-1 (continued)

```
----*----1----*----2----*----3----*----4----*----5----*----6----*----7-R--*----8
     1 1  5  0                0.01270 0.                                        00046400
     2 1  5  0                0.05081 0.                                        00046500
SB2206                                                                          00046600
 6 2 1 2  1  0 5.182 0.3682 0.43171 0. 0. 0.                                    00046700
     1 1  5  0                0.01270 0.                                        00046800
     2 1  5  0                0.05081 0.                                        00046900
SB2207                                                                          00047000
 7 2 3 2 18  0 7.315 0.3938 0.46112 0. 0. 0.                                    00047100
     1 1  5  0                0.01270 0.                                        00047200
     2 1  5  0                0.05462 0.                                        00047300
SB2208                                                                          00047400
 8 2 1 2  7  0 7.315 0.3938 0.46112 0. 0. 0.                                    00047500
     1 1  5  0                0.01270 0.                                        00047600
     2 1  5  0                0.05462 0.                                        00047700
SB2209                                                                          00047800
 9 2 3 2 20  0 6.400 0.3493 0.40961 0. 0. 0.                                    00047900
     1 1  5  0                0.01270 0.                                        00048000
     2 1  5  0                0.04761 0.                                        00048100
SB2210                                                                          00048200
10 2 1 2  9  0 3.200 0.3493 0.40961 0. 0. 0.                                    00048300
     1 1  5  0                0.01270 0.                                        00048400
     2 1  5  0                0.04761 0.                                        00048500
SB2211                                                                          00048600
11 2 1 2 10  0 3.200 0.3493 0.40961 0. 0. 0.                                    00048700
     1 1  5  0                0.01270 0.                                        00048800
     2 1  5  0                0.04761 0.                                        00048900
SB2212                                                                          00049000
12 2 1 1 37 21 3.176 1.8797 1.93685 0. 0. 0.                                    00049100
     1 2  9  0                0.05715 0.                                        00049200
SB2213                                                                          00049300
13 2 1 1 35 21 4.267 1.8797 1.93685 0. 0. 0.                                    00049400
     1 2  9  0                0.05715 0.                                        00049500
/                                                                               00049600
/**** MATERIAL DATA ****                                                        00049700
BB23                                                                            00049800
SB2301                                                                          00049900
 1                                                                              00050000
 STAINLESS STEEL ( COMPOSITION UNKNOWN )                                        00050100
 2                                                                              00050200
 20.0 7850.    1000. 7850.                                                      00050300
 9                                                                              00050400
 93.3 0.1165  148.9 0.1206  204.4 0.1247  260.0 0.1288  315.6 0.1319            00050500
371.1 0.1349  426.7 0.1370  537.8 0.1411 1093.3 0.1636                          00050600
 2                                                                              00050700
 93.3 3.43E-3  537.8 4.88E-3                                                    00050800
SB2302                                                                          00050900
 2                                                                              00051000
 STAINLESS STEEL ( 18-CR , 8-NI )                                               00051100
 2                                                                              00051200
 20.0 7820.    1000. 7820.                                                      00051300
 9                                                                              00051400
 93.3 0.1170  148.9 0.1211  204.4 0.1252  260.0 0.1293  315.6 0.1324            00051500
371.1 0.1354  426.7 0.1375  537.8 0.1416 1093.3 0.1642                          00051600
 2                                                                              00051700
 93.3 3.94E-3  537.8 5.42E-3                                                    00051800
SB2303                                                                          00051900
 3                                                                              00052000
 MN-MO-NI-STEEL ( A533 ? : 1.5-MN , 0.5-MO , 1.0-NI )                           00052100
 2                                                                              00052200
```

Appendix A-1 (continued)

```
----*----1----*----2----*----3----*----4----*----5----*----6----*----7-R--*----8
 20.0 7800.    1000. 7800.                                                00052300
 5                                                                        00052400
 75.0 0.1249  225.0 0.1279  275.0 0.1340  325.0 0.1380  375.0 0.1441      00052500
 5                                                                        00052600
 0.0 1.24E-2  100. 4.88E-3  200. 1.17E-2  300. 1.10E-2  400. 1.02E-2      00052700
/                                                                         00052800
/**** RELATIVE POWER DATA FOR HEAT SLAB ****(DUMMY DATA)                   00052900
BB24                                                                      00053000
SB2401                                                                    00053100
 1                                                                        00053200
 2                                                                        00053300
 0.0 0.0  100.0 0.0                                                       00053400
/                                                                         00053500
/  **** OTHER DATA ****                                                   00053600
BB25                                                                      00053700
   0. 1.4  1.4  0.                                                        00053800
BEND                                                                      00053900
4                                                                         00054000
 0  0  0  0  0  15.                                                       00054100
  0. 1.0+10 0.  -1.0E+10   0.01      0.01                                 00054200
  0                                                                       00054300
  0  0.0                                                                  00054400
  0  0.0                                                                  00054500
```

Appendix A-2 Input data for a restart job

```
 -- 1000 MWE PWR BLOWDOWN ANALYSIS ( WITH HOT CHANNEL) 82.07.09 --
/
/  **** DIMENSION DATA ****
BB01
  0  2  9  4  16  49  40  9 2  2  2  2  3  6  5  3 0 2 0 13 2 14
/
/  **** MINOR EDIT DATA ****
BB02
PRE-08  PRA-12  GLA-23  GLA-29  GLE-35  GLE-36  GLA-37  GLA-38  PRA-26
/
/  **** TIME STEP CONTROL DATA ****
BB03
SB0301
    0.2  0.2  100.
SB0302
    20   3  50   0  1.0E-3  1.0E-6  0.3  0.1
SB0303
    100  3  50   0  8.0E-3  1.0E-6  60.0  0.1
SB0304
    200  3  50   0  16.0E-3  1.0E-6  90.0  0.1
SB0305
    200  3  50   0  32.0E-3  1.0E-6  2000.0  0.1
/
/  **** TRIP CONTROLL DATA ****
BB04
SB0480
  1  0   1  0  1000.0      0.0
SB0481
  5 46   1  0     0.4      0.0
SB0482
  5 47   1  0     0.4      0.0
SB0483
  2  8   1  0     0.01     0.0
SB0484
  2  19  1  0     0.01     0.0
SB0485
  3  0   1  0     0.01     0.0
SB0486
  4  1   1  0    25.01     0.0
SB0487
 -4  1   1  0  1000.0      0.
SB0488
  4  2   1  0    25.01     0.0
SB0489
 -4  2   1  0  1000.0      0.
SB0492
  6  1  -3  1   240.0      0.005
SB0493
  6  2  -3  1   250.0      0.0
SB0494
```

Appendix A-2 (continued)

```
----*----1----*----2----*----3----*----4----*----5----*----6----*----7-R--*----8
  6  3 -3  1   360.0       0.0                                         00005100
SB0495                                                                 00005200
 -6  1  3  1   350.0       0.0                                         00005300
SB0496                                                                 00005400
 -6  2  3  1   305.0       0.0                                         00005500
SB0497                                                                 00005600
 -6  3  3  1   380.0       0.00                                        00005700
/                                                                      00005800
BEND                                                                   00005900
10                                                                     00006000
 0  0  0  0  0  40.                                                    00006100
  0. 1.0+10 0.  -1.0E+10    0.01       0.01                            00006200
  0                                                                    00006300
  0  0.0                                                               00006400
  0  0.0                                                               00006500
```

Appendix B Nomenclature

A	Cross-sectional area of flow (m^2)
C	Adjusting factor used in eq. 2-1 (-)
C_d^{sat}	Discharge coefficient for saturated critical flow (-)
C_d^{sub}	Discharge coefficient for subcooled critical flow (-)
D	Hydraulic diameter (m)
f	Friction factor (-)
f_1	Jacobian equation value derived from mass equation
G^A	Mass flow rate at the upstream point of node ($kg/m^2 \cdot sec$)
G^E	Mass flow rate at the downstream point of node ($kg/m^2 \cdot sec$)
G_M	Critical mass flow rate at the break point ($kg/m^2 \cdot sec$)
g_M	Critical mass flow rate by Moody ($kg/m^2 \cdot sec$)
h_{fs}	Saturated fluid enthalpy (Kcal/kg)
k	Loss coefficient
L	Length of the node (m)
P_{ACC}	Pressure at accumulator (kgw/m^2)
P_{CL}	Pressure at cold-leg (kgw/m^2)
P_{fric}	Frictional pressure drop (kgw/m^2)
T_{EOBP}	Time of End-of-Bypass (sec)
T_{LPinj}	Time of L.P. injection start (sec)
ΔT	Time step width (sec)
W	Volumetric flow rate (m^3/sec)
W_{ACC}	Volumetric flow rate from accumulator (m^3/sec)
x	Quality (-)
η	Coefficient used in the eq. 2-6 (-)
ρ	Density (kg/m^3)
$\bar{\rho}$	Node average density (kg/m^3)
$\bar{\rho}_{old}$	Node average density at one time step before (kg/m^3)
ρ_{fs}	Saturated fluid density (kg/m^3)
τ_D	Delay time constant for density change (sec)
Φ^2	Two phase multiplier (-)

Appendix B Nomenclature

A	Cross-sectional area of flow (m^2)
C	Adjusting factor used in eq. 2-1 (-)
C_d^{sat}	Discharge coefficient for saturated critical flow (-)
C_d^{sub}	Discharge coefficient for subcooled critical flow (-)
D	Hydraulic diameter (m)
f	Friction factor (-)
f_1	Jacobian equation value derived from mass equation
G^A	Mass flow rate at the upstream point of node ($kg/m^2 \cdot sec$)
G^E	Mass flow rate at the downstream point of node ($kg/m^2 \cdot sec$)
G_M	Critical mass flow rate at the break point ($kg/m^2 \cdot sec$)
g_M	Critical mass flow rate by Moody ($kg/m^2 \cdot sec$)
h_{fs}	Saturated fluid enthalpy (Kcal/kg)
k	Loss coefficient
L	Length of the node (m)
P_{ACC}	Pressure at accumulator (kgw/m^2)
P_{CL}	Pressure at cold-leg (kgw/m^2)
P_{fric}	Frictional pressure drop (kgw/m^2)
T_{EOBP}	Time of End-of-Bypass (sec)
T_{LPinj}	Time of L.P. injection start (sec)
ΔT	Time step width (sec)
W	Volumetric flow rate (m^3/sec)
W_{ACC}	Volumetric flow rate from accumulator (m^3/sec)
x	Quality (-)
η	Coefficient used in the eq. 2-6 (-)
ρ	Density (kg/m^3)
$\bar{\rho}$	Node average density (kg/m^3)
$\bar{\rho}_{old}$	Node average density at one time step before (kg/m^3)
ρ_{fs}	Saturated fluid density (kg/m^3)
τ_D	Delay time constant for density change (sec)
Φ^2	Two phase multiplier (-)